Title

STIM2 contributes to enhanced store-operated Ca^{2+} entry in pulmonary artery smooth muscle cells from patients with idiopathic pulmonary arterial hypertension

Author

Song, Michael Y.

Publication Date

2011

Peer reviewed|Thesis/dissertation

UNIVERSITY OF CALIFORNIA, SAN DIEGO

STIM2 Contributes to Enhanced Store-operated Ca^{2+} Entry in Pulmonary Artery Smooth Muscle Cells from Patients with Idiopathic Pulmonary Arterial Hypertension

A Dissertation submitted in partial satisfaction of the
requirements for the degree Doctor of Philosophy

in

Biomedical Sciences

by

Michael Y. Song

Committee in charge:

Professor Frank Powell, Chair
Professor Kim Barrett
Professor Joan Heller Brown
Professor Michael Hogan
Professor Geert Schmid-Schönbein
Professor Jason Yuan

2011

The dissertation of Michael Y. Song is approved, and it is acceptable in quality and form for publication on microfilm and electronically:

Chair

University of California, San Diego

2011

Epigraph

What the superior man seeks is in himself; what the small man seeks is in others.

Confucius

Table of Contents

List of Abbreviations

aa	amino acid
Ca^{2+}	Ca^{2+} ion
$[Ca^{2+}]_{cyt}$	cytosolic Ca^{2+} concentration
$[Ca^{2+}]_{SR}$	sarcoplasmic reticulum Ca^{2+} concentration
CCE	capacitative Ca^{2+} entry
CH	chronic hypoxia
CO	cardiac output
Co-IP	co-immunoprecipitation
COPD	chronic obstructive pulmonary disease
CTEPH	chronic thromboembolic pulmonary hypertension
DMEM	Dulbecco's Modified Eagle's Medium
EGFP	enhanced green fluorescent protein
E_K	K^+ equilibrium potential
E_m	resting membrane potential
ER	endoplasmic reticulum
hPASMC	human pulmonary artery smooth muscle cell
IPAH	idiopathic pulmonary arterial hypertension
K^+	potassium ion
$[K^+]_i$	intracellular K^+ concentration
$[K^+]_e$	extracellular K^+ concentration
K_V channel	voltage gated K^+ channel

$K_V1.5$	voltage-gated K^+ channel 1.5
Na^+	sodium ion
Na^+/K^+-ATPase	sodium potassium ATPase
NPH	non-pulmonary hypertensive
NPH-PASMC	non-pulmonary hypertensive patient pulmonary artery smooth muscle cells
Orai	Orai1 and Orai2 and Orai3
Orai1//2/3	Orai1 and Orai2 and Orai3
PA	pulmonary artery
PAEC	pulmonary artery endothelial cell
PAH	pulmonary arterial hypertension
PAP	pulmonary arterial pressure
PASMC	pulmonary artery smooth muscle cell
PH	pulmonary hypertension
PTE	pulmonary thromboendarterectomy
PVR	pulmonary vascular resistance
ROC	receptor-operated channel
ROCE	receptor-operated Ca^{2+} entry
rPASMC	rat pulmonary artery smooth muscle cell
RV	right ventricle
RVH	right ventricular hypertrophy
Ryr	ryanadine receptor
SERCA	sarcoplasmic endoplasmic reticulum Ca^{2+} ATPase

SOC	store-operated channel
SOCE	store-operated Ca^{2+} entry
SPH	secondary pulmonary hypertension
SR	sarcoplasmic reticulum
STIM	STIM1 and STIM2
STIM1	stromal interacting molecule 1
STIM1/2	STIM1 and STIM2
STIM2	stromal interacting molecule 2
TRP	transient receptor potential
TRPC	canonical transient receptor potential
VSMC	vascular smooth muscle cell

List of Figures

Acknowledgments

I would like to thank my family and friends who have always supported me. Without their support, I would not have been successful in many of my endeavors.

Chapter 5 and 7, in part, has been submitted for publication of the material as it may appear in Pulmonary Circulation, 2011, Song, MY; Makino, A, Yuan JX or in Antioxidants and Redox Signaling, 2011, Song, MY; Makino, A, Yuan JX. The dissertation author was the primary investigator and author of these papers.

Curriculum Vitae

Education:

Sept. 2006 – June 2011	Doctor of Philosophy, Department of Medicine, Biomedical Sciences Graduate Program, University of California, San Diego, CA
Sept. 2002 – April 2006	Bachelor of Science, Department of Biochemistry, Literature Science and the Arts Program, University of Michigan, Ann Arbor, MI

Memberships and Honors:

2006 – 2009	Director of Sponsorship for UCSD Entrepreneurship Competition
2006	University Honors, University of Michigan, Ann Arbor
2004	Regents Merit Scholarship, University of Michigan, Ann Arbor
2003	UROP Summer Research Fellowship, University of Michigan, Ann Arbor
2002	Michigan Merit Award
2002	National Merit Scholarship

Research and Teaching:

September 2007 – Present

Thesis research with Professor Jason Yuan studying the role of STIM and Orai in chronic hypoxia and idiopathic pulmonary arterial hypertension associated increase in store-operated Ca^{2+} entry in pulmonary artery smooth muscle cells.

September 2008 – December 2008

Graduate teaching assistant for Professor Immo Scheffler's second semester biochemistry.

May 2007 – July 2007

Research rotation with Professor Marc Montminy studying the biochemical interaction between cAMP Response Element Binding protein and TORC2 at the Salk Institute for Biological Studies.

April 2007 – May 2007

Research rotation with Professor Jerold Chun studying Lysophospholipid signaling and aneuploidy in the mammalian brain at The Scripps Reseach Institute in La Jolla, CA.

January 2007 – April 2007

University of California, San Diego research rotation with Professor Don Cleveland studying the physiological mechanism of neurofilament post-translational modification and polymerization.

September 2006 – December 2006

University of California, San Diego research rotation with Professor Binhai Zheng. Made a genetic construct to label human embryonic stem cells with mCherry or dtTomato. Gained experience in cloning.

July 2006 – September 2006

University of California, San Diego research rotation with Professor Jason Yuan. Studied the differing effects of thrombin on pulmonary artery smooth muscle and endothelial cells. Gained experience with tissue culture, Ca^{2+} florescence imaging, and patch clamp.

September 2002 – April 2006

Undergraduate research at the University of Michigan with Professor Louis D'Alecy and Professor Charles Zwemer. Studied the mechanisms of hypoxic conditioning in mice. Gained experience working with mice, hypoxia, and high performance liquid chromatography.

Publications:

Song MY, Makino A, Yuan JX. STIM2 Contributes to Enhanced Store-operated Ca^{2+} Entry in Pulmonary Artery Smooth Muscle Cells from Patients with Idiopathic Pulmonary Arterial Hypertension**.** Pulm Circ. 2011; 1: 84-94.

Song MY, Makino A, Yuan JX. Role of Reactive Oxygen Species and Redox in Regulating the Function of Transient Receptor Potential Channels. Antioxid Redox Signal. 2011 Apr 11. [Epub ahead of print]

Song MY, Yuan JX. Introduction to TRP Channels: Structure, Function, and Regulation. In: Membrane Receptors, Channels and Transporters in Pulmonary Circulation, edited by Yuan JX, and Ward JP. New York, NY: Humana Press, 2010, pp. 99-108.

Song MY*, Zwemer CF*, Whitsaw SE, D'Alecy, LG. Effect of Nitric Oxide Synthase Inhibition on Hypoxic Tolerance in Mice. J Appl Physiol. 2007; 102(2): 610-5. *Co-first authors.

Zwemer CF*, **Song MY***, Carello KA, D'Alecy LG. Strain Differences in Response to Acute Hypoxia: CD-1 versus C57BL/6J Mice. J Appl Physiol 2007; 102: 286-93. *Co-first authors.

Research Support:

UC San Diego Gastroenterology Training Grant (T32 DK07202)
HHMI Med-Into-Grad Training Grant
University of Michigan UROP Summer Research Fellowship

Abstract of the Dissertation

STIM2 Contributes to Enhanced Store-operated Ca^{2+} Entry in Pulmonary Artery Smooth Muscle Cells from Patients with Idiopathic Pulmonary Arterial Hypertension

by

Michael Y. Song

Doctor of Philosophy in Biomedical Sciences

University of California, San Diego, 2011

Professor Frank Powell, Chair

Prolonged pulmonary vasoconstriction and vascular remodeling cause idiopathic pulmonary arterial hypertension (IPAH). Pulmonary vasoconstriction is caused by pulmonary artery smooth muscle cell (PASMC) contraction, and enhanced proliferation of PASMC contributes to vascular remodeling. An increase in cytosolic Ca^{2+} concentration ($[Ca^{2+}]_{cyt}$) in PASMC triggers both contraction and proliferation. Inhibition of Ca^{2+} influx completely inhibits prolonged pulmonary vasoconstriction and stops PASMC proliferation. Store-operated Ca^{2+} entry (SOCE) is an important mechanism that mediates Ca^{2+} influx in PASMC and most other cell types. We

previously reported that SOCE was significantly enhanced in PASMC exposed to hypoxia and in PASMC from IPAH patients. Stromal interaction molecule (STIM1/2) and Orai proteins (Orai1/2/3) were identified recently as essential components that mediate SOCE. We aim to examine whether the expression levels of STIM and Orai are altered in IPAH-PASMC compared to control PASMC, and whether these putative changes in expression level are responsible for the enhanced SOCE and proliferation observed in IPAH-PASMC.

The protein expression level of STIM2 was increased in IPAH-PASMC, whereas STIM1 protein expression was decreased. Hypoxia (4% O_2, 5% CO_2, balance N_2) enhanced the protein expression level of STIM2, but not STIM1, in rat PASMC after 48 hours. In IPAH-PASMC knockdown of STIM2 decreased SOCE and proliferation, while knockdown of STIM2 in control PASMC had no effect on either SOCE or proliferation. Overexpression of STIM2 in control PASMC failed to enhance SOCE or proliferation. These data indicate that enhanced protein expression of STIM2 is necessary, but not sufficient, for enhanced SOCE and proliferation of IPAH-PASMC.

Orai2 protein expression level was increased in IPAH-PASMC. Orai1 and Orai3 protein expression levels were not statistically significantly altered. Furthermore, 48 hours of hypoxia significantly increased protein expression of Orai1 and Orai2, but not Orai3. Overexpression of Orai2 alone in PASMC did not enhance SOCE. Co-overexpression of both STIM2 and Orai2, however, did augment SOCE in PASMC. In conclusion, upregulated protein expression of STIM2 is necessary, but insufficient, for

augmented SOCE and enhanced proliferation in PASMC from IPAH patients. Increased expression of both STIM2 and Orai2 is sufficient to enhance SOCE in normal PASMC.

Chapter 1. Physiology of the Pulmonary Circulation

1.1 Change in Arterial Radius is Important in Changing Pulmonary Artery Pressure

The pulmonary circulation is a high flow, low resistance system that relies on arterial distension and recruitment to keep pressures relatively stable and adapt to changing cardiac output. Normal mean pulmonary arterial pressure (PAP) is ~12-14 mmHg. Pulmonary hypertension is defined as PAP > 25 mmHg at rest or > 30 mmHg during exercise, but can exceed 90 mmHg in some cases. In PAH patients, recruitment and distension cannot compensate for increased arterial pressures so the right heart adapts by hypertrophying to overcome the increased pressures of the pulmonary arterial tree. Eventually, however, right ventricular hypertrophy (RVH) becomes pathogenic and leads to right heart failure. As such, PAH is also accompanied by elevated right heart pressures and decreased cardiac output[1].

PA tone, largely determined by the contractile activity of PASMC in resistance arterioles, is the primary determinant of PAP. PAP is the product of pulmonary vascular resistance (PVR) and cardiac output (CO):

$$PAP = PVR \times CO$$

PVR is inversely proportional to the fourth power of the radius, *r*, of the arterial lumen according to Poiseuille's equation, which describes viscous fluid flow through a tube of radius r.

$$PVR = (8 \times L \times \eta) / (\pi \times r^4)$$

L is the total length of the blood vessels and η is the coefficient of blood viscosity. Since the radius is raised to the fourth power, both PVR and PAP are exceptionally sensitive to changes in arterial lumen diameter. Therefore, a small decrease in radius can cause a large increase in PVR and PAP.

1.2 Hypoxic Pulmonary Vasoconstriction and Chronic Hypoxia

Hypoxic pulmonary vasoconstriction (HPV) is a physiological mechanism that causes localized vasoconstriction of pulmonary arteries in response to low oxygen[2]. HPV is a response to alveolar hypoxia that distributes pulmonary capillary blood flow away from alveoli with low oxygen content to areas of high oxygen availability. This principle, also known as the von Euler–Liljestrand mechanism, optimizes gas exchange at the blood–air interface. HPV imparts an advantage in respiration where ventilation is matched to perfusion such that the gas exchange is maximized. Impairment of this mechanism during pathological situations may result in insufficient oxygenation of arterial blood and poor oxygen supply to the body.

Chronic hypoxia, as it occurs at high altitude or during respiratory diseases (including chronic obstructive pulmonary disease, sleep apnea, fibrosis, failure of ventilation due to neurological diseases) leads to general vasoconstriction of the pulmonary vasculature inducing vascular remodeling processes with subsequent right heart hypertrophy. Due to the opposite functions of lung vessels and systemic vessels, collecting and distributing oxygen, respectively, different reactions to hypoxia have developed. Whereas most systemic vessels of adult organisms dilate during hypoxia, pulmonary vessels constrict. During embryonic development lung vessels exhibit pronounced vasoconstriction, in order to minimize blood flow through the noninflated lungs, and to preserve the fetal circulation. After birth, pulmonary oxygenation in concert with lung inflation, leads to vasodilation and perfusion of the lung[3,4].

In the isolated, buffer-perfused lung, HPV is activated at a partial pressure of oxygen (P_{O2}) of 100 mmHg (13.3 kPa)[2]. Pulmonary arterial smooth muscle cells (PASMC) contract in response to hypoxia at a P_{O2} of 25–50 mmHg (3.33–6.66 kPa), particularly in resistance arteries[5,6]. The pulmonary vasculature responds to changes in P_{O2} within seconds[7]. In response to similar changes in P_{O2}, smooth muscle cells from the systemic circulation, such as isolated cerebral arteries, dilate. Pulmonary artery smooth muscle cells can sense low oxygen and cause vasoconstriction of arteries, therefore they are of critical importance in the normal function of the pulmonary circulation and are important in pulmonary disease that involve vasoconstricton[2].

1.2 Smooth Muscle Cells in the Pulmonary Circulation

Muscle is specialized tissue that can both contract and conduct electrical impulses[8,9]. Muscle is classified functionally as either voluntary or involuntary and structurally as either striated or smooth. From this system of classification there emerge three types of muscles: smooth involuntary muscle, striated voluntary (skeletal) muscle and striated involuntary (cardiac) muscle. The fibers of skeletal muscle and cardiac muscle exhibit cross striations and are referred to as striated muscle. Skeletal muscle fibers are formed by the fusion of individual small muscle cells or my oblasts, during development and are filled with longitudinally arrayed subunits called myofibrils. The myofibrils are made up of the myofilaments myosin (thick filaments) and actin (thin filaments). The striations reflect the arrangement of actin and myosin filaments and support structures. The individual contractile units are called sarcomeres. A myofibril consists of many sarcomeres arranged end to end. The most obvious feature in longitudinal sections of skeletal muscle is the alternating pattern of dark and light bands, called respectively the anisotropic (A) and isotropic (I) band. The I band is bisected by a dense zone called the Z line, to which the thin filaments of the I band are attached.

Cardiac muscle is the type of muscle found in the heart and at the base of the venae cavae as they enter into the heart[10]. Cardiac muscle is intrinsically contractile but is regulated by autonomic and hormonal stimuli. Cardiac muscle exhibits striations because it also has actin and myosin filaments arranged into sarcomeres. Generally these

striations do not appear as well defined as in skeletal muscle. Also compared to skeletal muscle, cardiac muscle has a greater number of mitochondria in its cytoplasm. At the light microscope level, a number of features distinguish cardiac from skeletal muscle. Cardiac muscle cells have only one or two nuclei, which are centrally located. The myofibrils separate to pass around the nucleus, leaving a perinuclear clear area. As in skeletal muscle, individual muscle fibers are surrounded by connective tissue. Numerous capillaries are found in the connective tissue around cardiac muscle fibers. Cardiac muscle cells are joined to one another in a linear array. The boundary between two cells is called an intercalated disc. Intercalated discs consist of several types of cell junctions whose purpose is to facilitate the passage of an electrical impulse from cell to cell and to keep the cells bound together during constant contractile activity. Unlike skeletal muscle fibers, cardiac muscle fibers branch and anastomose with one another. Specialized cardiac muscle fibers, called Purkinje fibers, arise from the atrioventricular node and travel along the interventricular septum toward the apex of the heart, sending branches into the ventricular tissue. Purkinje fibers are of larger diameter than ordinary cardiac fibers, with fewer myofibrils and an extensive, well-defined clear area around the nucleus. They conduct impulses at a rate about four times faster than that of ordinary cardiac fibers and serve to coordinate the contraction of the atria and ventricles[11].

Smooth muscle cells line the walls of hollow organs such as blood vessels and the walls of the gastrointestinal tract[12]. Smooth muscle cells are normally organized in 2-3 layers with one layer running circularly around the lumen and another layer running longitudinally along the length of the organ. Smooth muscle cells are spindle shaped

with one central nucleus per cell and are usually organized in small clusters of cells. Fine collagenous, reticular connective tissue connects the cell bundles. One way to distinguish smooth muscle from striated muscle is the absence of the regular pattern of sarcomeres (no A or I bands or Z lines). Smooth muscle cells can be distinguished from connective tissue by their organized appearance. They are usually in a homogeneous bundle or sheet of cells rather than scattered single cells. Fibroblasts, on the other hand, are scattered throughout the connective tissue in isolated groups.

The region around the nucleus of smooth muscle cells are filled with sarcoplasmic reticulum (SR) and mitochondria. These mitochondria provide the ATP needed for contraction and the SR functions as the main Ca^{2+} store. The cytoplasm of smooth muscle cells contains contractile filaments broken up by focal densities. Focal densities are organizational sites where the thick and thin filaments (actin and myosin) interact and are held together. Desmin and vimentin filaments bind at these sites to help hold the thick and thin filaments together. Desmin and vimentin intermediate filaments are necessary to relay the contraction and help to shorten the cell. The focal densities also contain α-actinin, an α-actin binding protein. The thin filaments are composed of actin with tropomyosin but no troponin is present in the smooth muscle cells[13].

Smooth muscle cells are interconnected by gap junctions, which link the cytoplasm of multiple cells and allow for direct cell-to-cell communication. Gap junctions are composed of connexon proteins that form molecular pores or channels between cells[14]. Gap junctions allow small molecules or ions to pass from cell to cell and

thereby allow the entire bundle of smooth muscle to act in concert. Smooth muscle cells are surrounded by an external lamina. The external lamina is similar to the basal lamina, which is secreted by endothelial cells, and surrounds the sarcolemma of smooth muscle cells. The external lamina is secreted by smooth muscle cells and is composed of collagen type IV, laminin and perlecan (heparan sulfate proteoglycan). Functionally the external lamina anchors smooth muscle cells together and serves as a conduit for contraction by transmitting the force to other cells and thus allowing the bundle to function as one unit[14].

Chapter 2. Ion Channels in PASMC

2.1 Regulation of Cytosolic Ca^{2+} Concentration

The presence and regulation of the divalent cation Ca^{2+} (Ca^{2+}) is fundamentally important to the functions of that constitute life at the cellular level[15]. Much energy is expended in extruding Ca^{2+} from the cytoplasm and sequestering Ca^{2+} into the sarcoplasmic (or endoplasmic) reticulum, mitochondria, and extracellular space (in order to maintain a low concentration of Ca^{2+} in the cytosol). Ca^{2+} gradients across the plasma membranes allow for the function of metabolism, nerve propagation, muscle contraction, and other important processes. Ca^{2+} is also fundamentally important in the regulation of transcription, translation, cellular division, and apoptosis[16,17]. It is then unsurprising that the regulation of intracellular Ca^{2+} levels in the cytosol and organelles is fundamentally involved in many forms of pathophysiology including diseases involving the vasculature[16,18,19].

The concentration of Ca^{2+} in different intracellular compartments and the flux of Ca^{2+} between compartments are of great importance in the function of smooth muscle cells and endothelial cells. Since smooth muscle and endothelial cells are the principle cells in determining vascular tone and blood vessel diameter, the regulation of cytosolic Ca^{2+} is of great importance to the physiological function of the vasculature. Abnormalities in intracellular Ca^{2+} regulation and chronic elevation of resting $[Ca^{2+}]_{cyt}$

have been linked to pulmonary and systemic arterial hypertension[20]. Therefore it is of critical importance to understand the function and regulation of the ion channels and pumps, which mediate Ca^{2+} transportation across the plasma membrane and intracellular organelle membranes.

The lipid membrane is impermeable to Ca^{2+}. Transportation of Ca^{2+} across the plasma membrane (and the SR/ER membrane) takes place through various Ca^{2+} channels, pumps, and exchangers. Ca^{2+}-permeable channels allow Ca^{2+} to flow across membranes based on electrochemical gradients. Ca^{2+} pumps (*e.g.*, Ca^{2+}/Mg^{2+} ATPase or Ca^{2+} pump) transport Ca^{2+} against its concentration gradient using energy produced by ATP. And, Ca^{2+} exchangers (*e.g.*, Na^{+}/Ca^{2+} exchanger or NCX) can transport Ca^{2+} across the membrane using the transmembrane electrochemical gradient of other ions (Figure 1).

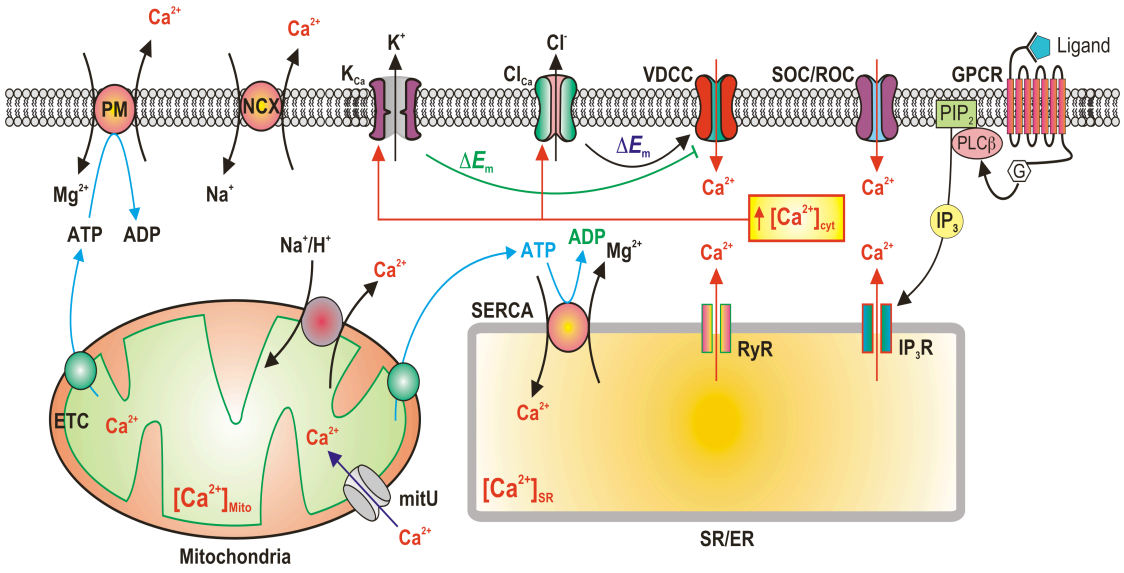

Figure 1: The concentration of cytosolic Ca^{2+} ($[Ca^{2+}]_{cyt}$) is tightly regulated by various Ca^{2+} channels and transporters. Activation of membrane receptors, such as G protein-coupled receptors (GPCR) stimulates IP_3 synthesis, induces Ca^{2+} release from the SR/ER through IP_3 receptors (IP_3R), and increases $[Ca^{2+}]_{cyt}$. The IP_3-induced store depletion opens store-operated Ca^{2+} channels, which leads to store-operated Ca^{2+} entry (SOCE), and further increases $[Ca^{2+}]_{cyt}$ and allows for prolonged ER/SR Ca^{2+} release. Membrane depolarization (induced by decreased activity or number of K^+ channels and Na^+/K^+ ATPase) opens voltage-dependent Ca^{2+} channels (VDCC), increases Ca^{2+} influx, and increases $[Ca^{2+}]_{cyt}$. Ca^{2+} influx through VDCC can activate ryanodine receptors (RyR), which are Ca^{2+} sensitive, and induce Ca^{2+} release from the SR/ER in a mechanism termed Ca^{2+} induced Ca^{2+} release. $[Ca^{2+}]_{cyt}$ can be decreased by Ca^{2+} sequestration into the SR/ER and mitochondria by SERCA and the mitochondrial Ca^{2+} uniporter (mitU), respectively, and by Ca^{2+} extrusion via the Ca^{2+}/Mg^{2+} ATPase (PMCA) on the plasma membrane. $[Ca^{2+}]_{cyt}$ can be increased not only by Ca^{2+} release from the SR/ER through RyR/IP_3R, but also from the mitochondria Na^+/Ca^{2+} exchanger. A rise in $[Ca^{2+}]_{cyt}$ can *i*) open Ca^{2+}-activated K^+ (K_{Ca}) channels and cause membrane hyperpolarization or repolarization, which closes VDCC, and *ii*) open Ca^{2+}-activated Cl^- (Cl_{Ca}) channels and cause membrane depolarization, which activates VDCC and causes further increase in $[Ca^{2+}]_{cyt}$.

The extracellular Ca^{2+} concentration is 1.6-1.8 mM, while the cytosolic Ca^{2+} concentration ($[Ca^{2+}]_{cyt}$) is approximately 100 nM. Various Ca^{2+} transporters are functionally involved in maintaining the concentration gradient of Ca^{2+} across membranes and the low resting $[Ca^{2+}]_{cyt}$ [21]. The Ca^{2+} concentration in the intracellular stores, such as SR/ER, can be as high as 1 mM because of Ca^{2+} pumps on the SR/ER membrane (*i.e.*, SERCA), which uses the energy produced by ATP to constantly transport (or uptake) Ca^{2+} from the cytosol to the SR/ER (Figure 1). In addition, intracellular Ca^{2+} level is also regulated by many other Ca^{2+} transporters, such as Na^{+}/Ca^{2+} exchangers (NCX) and H^{+}/Ca^{2+} exchangers on the plasma membrane and SR/ER membrane and Ca^{2+} uniporters on the mitochondrial membrane[21].

$[Ca^{2+}]_{cyt}$ can be increased by Ca^{2+} release from the SR/ER through inositol-1,4,5 phosphate (IP_3) receptors (IP_3R) and ryanodine receptors (RyR) on the SR/ER membrane, and Ca^{2+} influx through different Ca^{2+} channels on the plasma membrane[22]. There are three major classes of Ca^{2+}-permeable channels on the plasma membrane that are functionally expressed in vascular smooth muscle cells: *a*) voltage-dependent Ca^{2+} channels (VDCC) which are opened by membrane depolarization, *b*) receptor-operated Ca^{2+} channels (ROC) which are opened by diacylglycerol synthesized via PIP_2 when membrane receptors are activated by ligands, and *c*) store-operated Ca^{2+} channels (SOC) which are opened when Ca^{2+} in the intracellular Ca^{2+} store (*i.e.*, SR/ER) is depleted by either activation of IP_3R/RyR or inhibition of SERCA (Figure 1)[23].

While the concentration of Ca^{2+} and proportion of Ca^{2+} bound to calmodulin (CaM) in the nucleus are important in regulating various transcription factors involved in VSMC physiology and pathophysiology, the concentration of Ca^{2+} in the nuclear compartment is unregulated and roughly equal to the cytosolic compartment due to free flow though large nuclear pores[24]. By sequestering Ca^{2+} into the SR/ER and, to a lesser extent, into mitochondria, and by extruding Ca^{2+} from the cytosol to the extracellular space, the concentration of Ca^{2+} in the cytoplasm is maintained at a low level such that influx of Ca^{2+} from outside the cell or release of Ca^{2+} from intracellular stores requires no energy and functions as a signaling event for cell contraction, migration, and proliferation. In smooth muscle cells, a rise in $[Ca^{2+}]_{cyt}$ leads to cell contraction, increases cell migration, and stimulates cell proliferation[25]. An acute rise in $[Ca^{2+}]_{cyt}$ can cause vasoconstriction, and chronically elevated $[Ca^{2+}]_{cyt}$ leads to thickening of the vessel wall (due to its stimulating effect on cell proliferation and migration), thus decreasing the luminal volume of the vessel and the ability of the vessel to expand to meet increased flow.

2.2 Ca^{2+} as a Trigger for Contraction and Proliferation in PASMC

An increase in $[Ca^{2+}]_{cyt}$ is necessary for contraction in PASMC[4,25]. Both Ca^{2+} influx through plasma membrane Ca^{2+} channels and Ca^{2+} release from intracellular stores (*e.g.*, the sarcoplasmic reticulum) contribute to a rise in $[Ca^{2+}]_{cyt}$. In rat pulmonary arterial rings, removal of extracellular Ca^{2+} prevents pharmacologically induced contraction[26], indicating that Ca^{2+} influx through channels situated on the plasma membrane is necessary for contraction. When $[Ca^{2+}]_{cyt}$ increases, it binds to calmodulin which then activates myosin light chain kinase (MLCK). Activated MLCK phosphorylates the regulatory light chain of myosin, allowing for the activation of myosin ATPase. The ensuing hydrolysis of ATP provides the energy source needed for the cross-bridging cycles between myosin and actin filaments. These cross-bridging interactions constitute cellular contraction[27], and in the case of concerted contraction of VSMC, vasoconstriction. Chronic PASMC contraction is responsible for the elevated pulmonary arterial pressures observed in some instances of IPAH.

In addition to causing contraction, increased $[Ca^{2+}]_{cyt}$ is also a major stimulus for cellular proliferation. Increases in $[Ca^{2+}]_{cyt}$ and nuclear Ca^{2+} trigger Ca^{2+}-dependent gene transcription in vascular smooth muscle cells[28,29]. Both nuclear and cytosolic Ca^{2+} pools promote proliferation by activating Ca^{2+} dependent kinases (*e.g.*, CaMK), immediate early genes and other transcription factors (*e.g.*, c-fos, NFAT, CREB) which are necessary for cell growth[28,29]. Ca^{2+} can also affect gene expression through its interaction with PKC and calmodulin or by activation of cell cycle proteins (cyclins and cyclin

dependent kinases). In addition to stimulating quiescent cells to enter the cell cycle (G_0 to G_1 transition), Ca^{2+} is also required for progression through the G_1 to S and G_2 to mitosis checkpoints, as well as mitosis itself[30,31]. In PASMC specifically, both increased $[Ca^{2+}]_{cyt}$ and intracellularly stored Ca^{2+} are thought to play a role in proliferation[32]. In the presence of serum and growth factors, Ca^{2+} depletion inhibits growth of PASMC[33] (Figure 2).

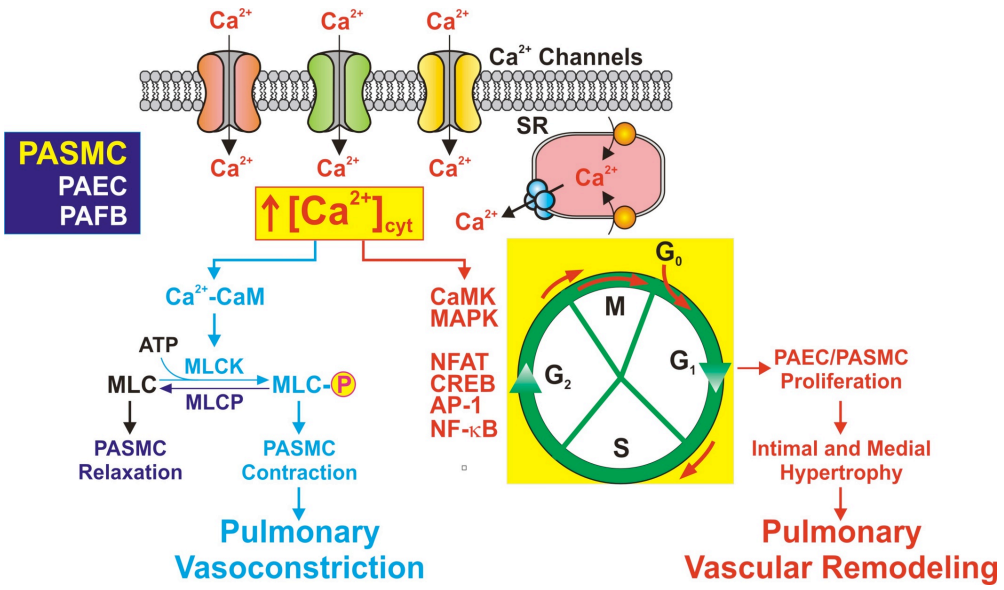

Figure 2: An increase in $[Ca^{2+}]_{cyt}$ in PASMC leads to pulmonary vasoconstriction and pulmonary vascular remodeling. $[Ca^{2+}]_{cyt}$ is increased by release of Ca^{2+} from the SR and by influx of Ca^{2+} across the plasma membrane. Cytosolic free Ca^{2+} is bound by calmodulin (CaM) to form the Ca^{2+}-calmodulin complex (Ca^{2+}-CaM), which activates myosin light chain kinase (MLCK). MLCK utilizes ATP to phosphorylate myosin light chain (MLC), which causes contraction in PASMC and leads to pulmonary vasoconstriction. An increase in $[Ca^{2+}]_{cyt}$ can also activate various Ca^{2+} sensitive proteins such as CaMK and MAPK and can activate Ca^{2+} sensitive transcription factors such as NFAT, CREB, AP-1, and NF-κB. These proteins and transcription factors can then lead to increase proliferation of PASMC. Furthermore, an increase in $[Ca^{2+}]_{cyt}$ is necessary for progression though several cell cycle checkpoints during mitosis. Therefore, an increase in $[Ca^{2+}]_{cyt}$ leads to PASMC proliferation, as well as PAEC proliferation, which causes intimal and medial hypertrophy and pulmonary vascular remodeling.

2.3 Ca^{2+} Channels on the Plasma Membrane

Ca^{2+} channels on the cell surface are classified into three groups based on how they are activated. Receptor-operated Channels (ROC) (Figure 3), Store-operated Channels (SOC) (Figure 4), and Voltage-dependent Ca^{2+} Channels (VDCC) all mediate the influx of Ca^{2+} into the cytosol. ROC are activated by stimulation of receptors such as G protein-coupled receptors (GPCR) or receptor tyrosine kinase (RTK). Serotonin (5-HT) activates serotonin receptor, which is a GPCR, on the plasma membrane to produce diacylglycerol (DAG) and inositol triphosphate (IP_3). Endothelin-1 (ET-1) also stimulates the production of IP_3 and DAG through GPCR dependent mechanism. PDGF or EGF activates RTK class of receptors and leads to the downstream production of DAG and IP_3. DAG activates ROC, which are located on the plasma membrane. IP_3 stimulates IP_3 receptor (IP_3R), which is a Ca^{2+} channel on the ER/SR membrane, to release Ca^{2+} from the ER/SR store. This leads to depletion of the ER/SR store, which signals to activate SOC on the plasma membrane. Both ROC and SOC, when activated, allow Ca^{2+} to flow into the cytosol. In fact, an established treatment of PAH is the ET-1 receptor antagonist Bosantan. VDCC are activated by membrane depolarization and will be explore in later sections.

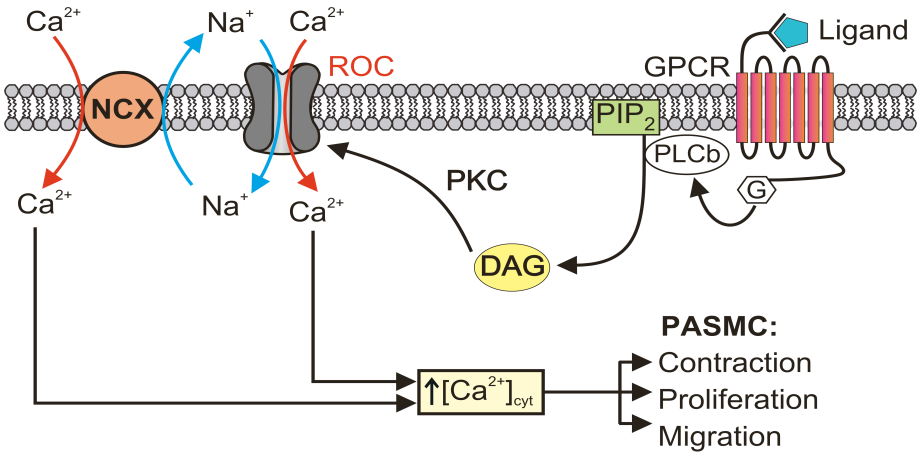

Figure 3: Receptor-operated (ROCE) Ca^{2+} entry occurs through receptor-operated (ROC) Ca^{2+} channels. G protein-coupled receptors (GPCR) signal though second messenger diacylglycerol (DAG) which opens ROC on the plasma membrane. Ca^{2+} influx though ROC (termed ROCE) increases $[Ca^{2+}]_{cyt}$ and leads to smooth muscle cell contraction, proliferation, and migration. Furthermore, increased cytosolic $[Na^{+}]$ due to Na^{+} influx through and ROC can activate the reverse mode of Na^{+}/Ca^{2+} exchange and cause inward transportation of Ca^{2+}.

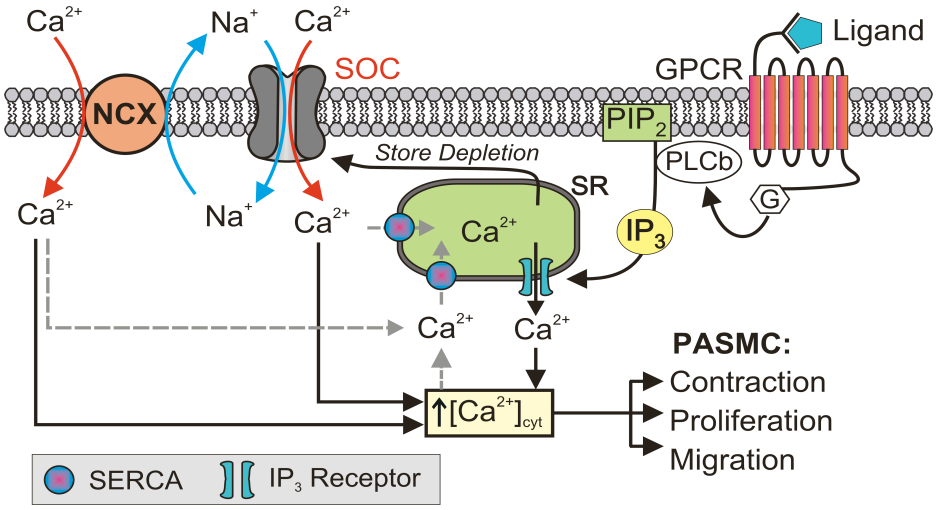

Figure 4: Store-operated (SOCE) Ca^{2+} entry occurs through store-operated (SOC) Ca^{2+} channels. Second messenger IP_3 activates IP_3R on the SR/ER membrane and causes Ca^{2+} release or mobilization from the SR/ER to the cytosol. The subsequent depletion of Ca^{2+} from the stores opens SOC on the plasma membrane and leads to SOCE. Ca^{2+} influx though SOC increases $[Ca^{2+}]_{cyt}$ and leads to smooth muscle cell contraction, proliferation, and migration. Furthermore, increased cytosolic $[Na^{+}]$ due to Na^{+} influx through and SOC can activate the reverse mode of Na^{+}/Ca^{2+} exchange and cause inward transportation of Ca^{2+}.

2.3.1 Receptor-operated Channels

Transient receptor potential (TRP) channels function as receptor-operated channels in PASMC. TRP channels are cation channels that mainly mediate the influx of Na^+ and Ca^{2+} across the plasma membrane and into the cytoplasm[15]. TRP channels were first discovered due to a mutation in *Drosophila* photoreceptor, which resulted in inhibited Ca^{2+} permeability and sensitivity to light[34]. The influx of cations into the cytoplasm depolarizes cells and is necessary for action potentials in excitable cells such as neurons[35]. In non-excitable cells, membrane depolarization by TRP channels stimulates voltage-dependent channels (Ca^{2+}, K^+, Cl^-) and influences many cellular events such as transcription and translation[36], while increased Ca^{2+} entry through TRP channels is involved in ligand-mediated cell contraction, migration and proliferation. TRP channels and their regulation are thus fundamentally important in cellular function and disease[15].

TRP genes are expressed in organisms from archaea to plants to animals[37,38]. In animals, TRP is expressed in brain, heart, lung, and other tissues[38]. Mammalian TRP channels possess a high degree of sequence homology particularly in the putative functional domains[39]. The TRP superfamily of genes is categorized into two groups based on sequence and topological similarities[40]. Group 1 includes TRPC, TRPV, TRPM, TRPA, and TRPN. And, group 2 includes TRPP and TRPML.

Structure, Function and Regulation of TRP Channels

TRP proteins form cation channels with varying selectivity to different cations[41,42]. TRP proteins are transmembrane proteins with six transmembrane domains with a pore domain wedged between the fifth and sixth transmembrane domains (Figure 5). The N- and C-terminal domains are intracellular and believed to be involved in regulation of TRP channel function and in channel assembly. It is believed that TRP channels are homo or hetero- tetramers of TRP proteins with each subunit contributing to selectivity of the ion-conducting pore[43]. Allosteric interactions between subunits contribute to gating of TRP channels; however, the location and structure of these gates are unknown[44]. Amino acid sequences flanking the pore forming regions of TRP proteins are strongly conserved across the various TRP channel families highlighting their importance in pore formation and/or pore gating[45].

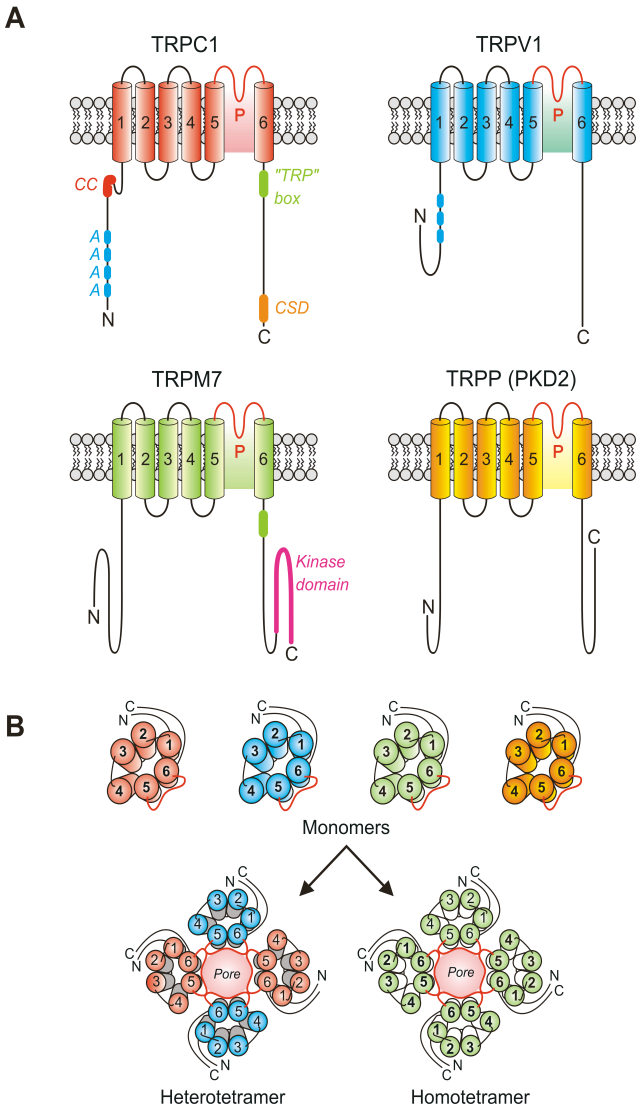

Figure 5: Structure and topology of TRP channels. A. TRPC, TRPV, TRPM, and TRPP classes of TRP channels are six transmembrane domain ion channels in the plasma membrane. The pore forming domain (P) lies between the S5 and S6 transmembrane domains. TRPC1 contains a coiled-coil domain and many ankyrin repeats near its N-terminus. Near the C-terminal domain of TRPC1 is a "TRP" box domain, which is a conserved region following the last transmembrane domain, and a caveolin-1 scaffolding domain (CSD). TRPV1 also contains several ankyrin repeats. TRPM7 contains a kinase domain near its C-terminus. **B.** Functional TRP channels are hetero or homo-tetramers formed by various TRP monomers.

TRP channel function is regulated by four basic mechanisms: *a*) plasma membrane receptor activation, *b*) ligand activation, *c*) direct activation, and *d*) indirect activation[46]. G protein-coupled receptors (GPCR) and receptor tyrosine kinases (RTK) act through diacylglycerol (as well as IP_3-mediated store depletion) to activate TRP channels on the plasma membrane[44,47]. Furthermore, activation of GPCR and RTK also increase synthesis of IP_3, depletes Ca^{2+} from the intracellular Ca^{2+} stores (*i.e.*, SR/ER) and leads to SOCE through TRP channels on the plasma membrane[48]. The TRP channels that are activated by diacylglycerol are termed ROC, while the TRP channels that are activated by store depletion are termed SOC. Most of TRP channel subunits can form both ROC and SOC in many cell types including vascular smooth muscle and endothelial cells.

Various ligands can activate TRP channels. Ligand activation includes activation by *a*) exogenous small molecules such as capsaicin, icilin, 2-APB; *b*) endogenous lipids such as DAG, phosphoinositides, eicosanoids, purine nucleotides; *c*) ions such as Ca^{2+}, Mg^{2+}, and *d*) the Ca^{2+}/CaM complex[49-51]. TRP channel activity can be stimulated through direct activation as well. Examples of direct activation of TRP channels include temperature change[37], mechanical stimulation[52], and conformational coupling with other proteins such as STIM1 or IP_3R. Indirect activation refers to transcriptional control or insertion of vesicles containing TRP proteins into the plasma membrane.

Over ten TRP isoforms are expressed in the vasculature. Expression of mRNA, protein, or both of TRPC1-7, TRPV1-4, TRPP2, TRPM2-4, -7, -8 has been implicated in different vascular smooth muscle and endothelial cells.

TRPC

TRPC1-7 are categorized into three categories based on sequence and functional characteristics[37]. TRPC1, 4, and 5 form one group. TRPC1 was the first mammalian TRP protein discovered. It is widely expressed in many tissues and thought to form heteromeric channels with TRPC4 and TRPC5[53]. TRPC4 and TRPC5 are believed to form homomeric channels. When expressed together, TRPC1, 4, and 5 form non-selective cation channels that are activated by G_q signaling through a PLCß1 pathway[54]. Growth factor stimulates rapid translocation of TRPC5 into the plasma membrane from vesicles located near the plasma membrane [54].

TRPC3, 6, and 7 have roughly 75% sequence homology and when co-expressed reconstitute non-selective, inward and outward rectifying, cation channels[46]. These channels are activated by receptor mediated pathway involving DAG and are believed to be important in vascular and airway smooth muscle[55]. Channels formed by TRPC3 or TRPC6 are also regulated by N-linked glycosylation and Ca^{2+}/CaM[56]. TRPC3 is activated by phosphorylation by PKG[57], while TRPC6 can be phosphorylated by the Src family of tyrosine kinases[58]. TRPC2 shares roughly 30% sequence homology with TRPC3/6/7[59].

TRPC2 full length mRNA is expressed in mouse and rat tissues[60]. However, TRPC2 is a pseudogene in humans[46].

TRPC1 is expressed in the vasculature and is linked to Ca^{2+} entry as a ROC and a SOC. Expression and knockdown data support the theory that TRPC1 forms heteromultimeric channels with TRPC3-5 and TRPP2 in the vasculature[53,61]. Furthermore TRPC1 may play an important role in mediating SOCE. Our lab has previously demonstrated that overexpression of TRPC1 in endothelium denuded rat pulmonary arteries enhances CPA induced pulmonary vasoconstriction, which is mediated by SOCE[62].

TRPC3 and 6 are expressed in vascular tissues and are believed to function primarily as ROC, although TRPC6 may also form heterotetrameric channels with other TRP isoforms that can be activated by store depletion in pulmonary vascular smooth muscle and endothelial cells[63]. TRPC6 is expressed in SMC in the systemic and pulmonary vasculature. Knockout of TRPC6 abrogates the hypoxic pulmonary vasoconstriction and hypoxia-induced cation influx[64]. TRPC4 is predominantly expressed in the endothelium and it is important in regulating lung microvascular permeablilty, agonist-dependent vasorelaxation, and gene transcription[65]. While TRPC4 is expressed at a lower level in VSMC, it may play a role in regulating contraction and proliferation in both store- and receptor- mediated manners[54,66]. TRPC5 expression in VSMC is unclear. Some researchers describe TRPC5 protein and transcript expression in

PASMC and PAEC while other researchers show conflicting data[67,68]. TRPC7 is thought to contribute to both ROC and SOC formation[69].

TRPC Channels and Contraction and Proliferation of SMC

TRPC channels are important in the regulation of vascular tone since they mediate the Ca^{2+} influx that mediates agonist-induced vasoconstriction and mitogen-mediated smooth muscle cell proliferation[44,47]. And, the ability of TRPC channels to alter $[Ca^{2+}]_{cyt}$ without any change in membrane potential lends them the ability to modulate vasoconstriction and vasorelaxation through a voltage-independent mechanism. Agonist- and hypoxia-induced pulmonary vasoconstriction is believed to be, at least in part, mediated though Ca^{2+} influx through TRPC1 and TRPC6 channels[70,71]. Upregulated TRPC channel expression, enhanced SOCE, and increased $[Ca^{2+}]_{cyt}$ are associated with enhanced proliferation in PASMC isolated from patients with IPAH[72,73].

TRPC and ROS

TRPC3 and TRPC4 expressed in HEK293 cells formed redox sensitive cation channels that were activated by hydrogen peroxide [74]. It is, however, unknown if the activation of TRPC3 and TRPC4 is mediated through the oxidation-reduction of cysteine thiol groups. It has been suggested that hydrogen peroxide may indirectly activate TRPC3 and TRPC4 channels though activation of phospholipase C (PLC). In endothelial cells, TRPC3 and TRPC4 are believed to form heteromeric channels that are redox

sensitive. In these cells, tert-butylhydroperoxide (tBHP) leads to membrane depolarization with currents that resemble TRP currents in terms of cation selectivity, La^{3+} sensitivity, and a lack of voltage dependence. Furthermore, expression of the N-terminal fragment of human TRPC3, but not the C-terminal fragment, abolished the oxidant-induced cation current. These data suggest that TRPC3 forms channels that are activated by ROS in porcine aortic endothelial cells[75]. Later, the same group of investigators showed that TRPC3 and TRPC4 associate to form heteromeric channels in porcine aortic endothelial cells and HEK293 cells[76]. These TRPC3/4 heterometic channels were activated by cholesterol oxidase suggesting that they are regulated by redox state. However, no direct evidence links TRPC4 itself to redox regulation. TRPC5 homotetrameric channels and TRPC5/TRPC1 heterotetrameric channels, expressed in HEK293 cells, are activated by extracellular thioredoxin. Reduced thioredoxin breaks a disulfide bond in the extracellular loop adjacent to the ion selectivity filter of TRPC5 and increase the ion conductivity of the channel[77,78].

TRPC and NO

NO is a cell signaling molecule involved in a number of physiological and pathophysiological processes. In the nervous system, NO is a neural transmitter, while in the vascular system, NO is mainly an endothelium-derived relaxing and hyperpolarizing factor. NO is synthesized by NO synthases (NOS), which includes three isoforms: endothelial NOS (eNOS), inducible NOS (iNOS), and neuronal NOS (nNOS). Each of the enzymes is a homodimer requiring three co-substrates (L-arginine, NADPH and O_2)

and five cofactors (FAD, FMN, Ca^{2+}-calmodulin, heme, and tetrahydrobiopterin) for activity. The redox biochemistry of NO involves the action of three redox species: NO^+ (nitrosonium), NO^- (nitroxyl anion) and $NO^\bullet$ (the free radical gas). NO can react with oxygen (O_2), superoxide anion ($O_2^{\bullet-}$), redox metals, and other radical species. The effects of NO can be mediated through the formation of reactive nitrogen oxide species from reactions of NO with either oxygen or superoxide anion. There are several mechanisms by which NO affects the function of living cells: *a*) oxidation of iron-containing proteins, *b*) ADP ribosylation of proteins, *c*) nitrosylation of protein sulfhydryl group, *d*) activation of iron regulatory factors, *e*) nitration of amino acid residues in proteins, and *f*) activation of soluble guanylate cyclase (sGC). In other words, NO can directly cause nitrosative reaction by adding the equivalent of NO^+ to an amino, thiol, or hydroxyl aromatic group, oxidative reaction by removal of 1 or 2 electrons from a substrate, or nitration reactions by adding an equivalent of an NO^{2+} to an aromatic group.

In vascular smooth muscle cells, NO mainly acts through the stimulation of the soluble guanylate cyclase, which is a heterodimeric enzyme with subsequent formation of cyclic GMP (cGMP). cGMP activates protein kinase G (PKG), which causes phosphorylation of myosin light chain phosphatase (MLCP) and therefore inactivation of myosin light chain kinase (MLCK) and leads ultimately to the dephosphorylation of the myosin light chair, causing smooth muscle relaxation. In addition to phosphorylation of MLCP, cGMP/PKG also causes phosphorylation of other proteins, such as TRPC6 channels[79]. Indeed, NO/cGMP/PKG-mediated phosphorylation of threonine (Thr69) in the N-terminal of TRPC6 protein significantly attenuates receptor-mediated Ca^{2+} entry

through TRPC6 channels[79]. These observations imply that PKG-mediated phosphorylation of specific amino acid residues (*e.g.*, threonine and serine residues) in the TRPC6 protein causes inhibition of the channel activity. In contrast, NO-mediated cGMP-independent S-nitrosylation of certain cysteine residues in the TRPC1/4/5 and TRPV1/3/4 proteins significantly enhances Ca^{2+} influx through these channels[80,81]. Specifically, for example, Cys553 and Cys558 of TRPC5 are localized in the cytoplasm and mediate the channel's sensitivity to NO/S-nitrosylation in endothelial cells[80,81]. Nitrosylation of TRPC5 in endothelial cells upon G protein coupled ATP receptor stimulation elicits Ca^{2+} entry. These observations imply that cGMP/PKG-dependent phosphorylation and cGMP/PKG-independent S-nitrosylation are two different pathways for NO-mediated effect on TRP channels. Whether NO-mediated effect is to activate or inhibit the channels depends on *a*) which pathway (PGK-dependent phosphorylation vs. PKG-independent S-nitrosylation) occurs faster to reach the target protein (or which pathway is predominant in a given cell), *b*) which TRP channel subtype (*e.g.*, TRPC5 vs. TRPC6) is predominantly expressed in a given cell as the target, and *c*) whether the target amino acids (*e.g.*, threonine and serine for phosphorylation, and cysteine residues for S-nitrosylation) for phosphorylation or S-nitrosylation are present in the predominant TRP channels in a given cell.

2.3.2 Store-operated Channels

Strong evidence suggests that Orai1 functions as a SOC. Orai1 was discovered through genome wide RNAi screening. A mutation in Orai1 in patients with severe combined immuno deficiency eliminates the Ca^{2+} release-activated Ca^{2+} currents (I_{CRAC}), which can then be reconstituted by expressing wild-type Orai1[82,83]. Orai1 spans the plasma membrane four times with both the C- and N- terminus in the cytoplasm. Co-expression of STIM1 with Orai1 in HEK293 cells resulted in a large increase in SOCE and I_{CRAC} compared to vector control cells[84-86]. Co-immunoprecipitation data show that STIM1 and Orai1 interact, and store depletion significantly increases the amount to interaction[87]. Furthermore, other isoforms of Orai (*e.g.*, Orai2 and Orai3) are also thought to play a role in SOCE[83]. It is unclear, however, what role these Orai isoforms have in the function of smooth muscle cells.

2.3.3 Voltage-dependent Channels

Ca^{2+} entry involves a variety of Ca^{2+} channels that can be classified into voltage-dependent L- and T-type Ca^{2+} channels (VDCC) and voltage independent Ca^{2+} channels. The VDCC "L-type" are considered "high voltage-activated" currents and the "T-type" are "low voltage-activated." Both types are thought to exist in three states consisting of resting, open and inactivated conformations. Switching conformations is dependent on membrane depolarization[88,89]. T-type channel mediated Ca^{2+} entry is linked to cell proliferation with the channel activity associated with G1-S boundary of cell cycle progression in aortic myocytes[90]. It has been reported that T-type channels are needed in the early stages of skeletal muscle and cardiac development and expression is lost as SMC differentiate and lose their ability to proliferate. However, they reappear in pathological cell proliferation in cancer cells and in cultured VSMC[91]. The L-type channel can be targeted indirectly through G protein-coupled receptors by a host of cellular second messenger systems that are activated by various agonists including but not limited to, norepinephrine, endothelin, angiotensin II, 5-HT and nitric oxide. Stimulation by protein kinases such as protein kinase G can inhibit L-type current while protein kinase C has been shown to potentiate L-type currents[92]. Also, there is evidence that nonreceptor tyrosine kinases such as c-Src enhance L-type currents [93].

Dysfunctional K_v channels have been shown to impact Ca^{2+} signaling in PAH patients. For example, PASMC isolated from IPAH patients have a depolarized resting membrane potential with higher $[Ca^{2+}]_{cyt}$ that display a blunted response to K_v channel

blockers[94,95]. Another consequence of dysfunctional K_v channels is a decrease in apoptosis. Increased K^+ and Cl^- efflux is a requirement for cell shrinkage as H_2O follows the ions out of the cell. This leads to apoptotic volume decrease, with decreased cell volume being one of the earliest indicators of apoptosis[96]. For example, K^+ channel-associated protein/protein inhibitor of activated STAT (KChAP) induces apoptosis in prostate cancer cells by increasing K^+ efflux and apoptotic volume decrease[97].

The membrane potential of vascular smooth muscle cells is critical in controlling $[Ca^{2+}]_{cyt}$. L-type voltage-dependent Ca^{2+} channels on the plasma membrane are opened by membrane depolarization and allow the influx of Ca^{2+} to the cytoplasm. This increase of $[Ca^{2+}]_{cyt}$ activates Ca^{2+}/calmodulin-dependent myosin light chain kinase (MLCK) and ultimately causes smooth muscle contraction. In isolated arteries, high K^+ solution causes a sustained contraction that is mainly due to membrane depolarization and opening of VDCC in VSMC. In addition to activating MLCK and causing contraction, a localized rise in cytosolic $[Ca^{2+}]$ due to Ca^{2+} release through RyR on the SR/ER membrane leads to Ca^{2+} sparks, which subsequently opens Ca^{2+}-activated K^+ (K_{Ca}) channels in the plasma membrane, induces membrane hyperpolarization, and causes relaxation of VSMCs. Furthermore, extrusion of Ca^{2+} by the PMCA or reuptake of Ca^{2+} by SERCA can also decrease $[Ca^{2+}]_{cyt}$ and lead to vasorelaxation.

Excitable and contractile cells, such as neurons and PASMC, have voltage-dependent Ca^{2+} channels VDCC. Diminished $I_{K(V)}$ causes membrane depolarization which triggers VDCC opening, thus promoting Ca^{2+} influx and raising $[Ca^{2+}]_{cyt}$ (Figure

6)[98]. K_V channel blockers can depolarize E_m sufficiently to allow for $[Ca^{2+}]_{cyt}$ increase. For example, application of 4-AP, a K_V channel blocker, to primary culture rat PASMC depolarized E_m and increased $[Ca^{2+}]_{cyt}$, whereas sodium nitroprusside (which generates NO) opened K_V channels and hyperpolarized the membrane, thus preventing the 4-AP induced rise in $[Ca^{2+}]_{cyt}$[99]. In PASMC, increased $[Ca^{2+}]_{cyt}$ triggers proliferation and contraction[100,101]. Conversely, membrane hyperpolarization occurs when more K^+ channels open than were so at rest, making it more difficult to open VDCC and thus less likely that the cell will contract. Overexpression of $K_V1.5$, but not $K_V1.4$, hyperpolarizes mouse fibroblasts[102], indicating that $K_V1.5$ specifically may be important in regulating E_m.

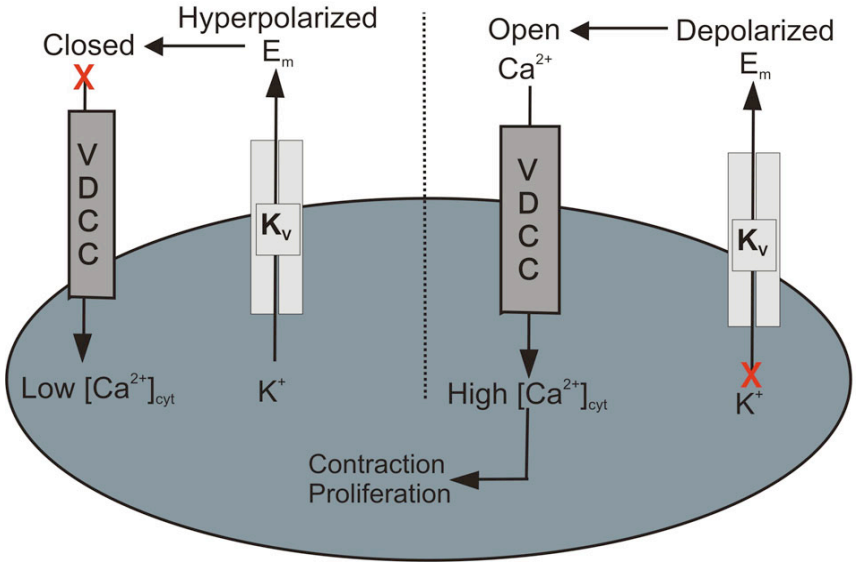

Figure 6: Role of K_V Channels in the Regulation of E_m in PASMC. When K_V channels are open, E_m is maintained at relatively hyperpolarized potentials and voltage-dependent Ca^{2+} channels (VDCC) are closed (left). However, with K_V channel block or current inhibition, E_m is depolarized, leading to VDCC opening and an increase in $[Ca^{2+}]_{cyt}$ (right).

In some cases, a 3-mV depolarization would lead to a two-fold increase in Ca^{2+} influx[103,104]. As VDCC open at potentials more positive than -30 mV, depolarizations over a small voltage range near E_m (around -40 mV for PASMC) opens L-type Ca^{2+} channels and can lead to a sustained elevation of $[Ca^{2+}]_{cyt}$[105-107]. Because of its rapid and ubiquitous role in cell signaling, resting $[Ca^{2+}]_{cyt}$ is kept low, ~100 nM, by various mechanisms including Ca^{2+} extrusion, sequestration into the endoplasmic or sarcoplasmic reticulum and intracellular buffering. Therefore, most increases in cellular Ca^{2+}, even local events, trigger a cellular response.

Although all K^+ channels are capable of exquisite selectivity for K^+ ions, they are gated by different stimuli and have different structures. K^+ channels are classified into 4 subgroups based on their structure and physiological activators and inhibitors: voltage-dependent (K_V), Ca^{2+} activated (K_{Ca}), inward rectifier (K_{IR}), and two pore domain channels (K_{2P}). K^+ channels are the most diverse group of ion channels, encoded for by at least 70 mammalian genes and expressed as more than 100 principal pore forming α subunits[108,109].

K_V channels are found in a wide variety of cell types including vascular smooth muscle cells, neurons, lymphocytes, and cardiac cells where they play a role in cardiac and neuronal repolarization, apoptosis, volume regulation and proliferation. The Drosophila voltage-dependent *Shaker* channel, the first K^+ channel cloned, was isolated on the basis of flies' shaking leg response to ether anesthesia[110]. The mammalian Shaker-

related channels comprise the K_V1 subfamily. K_V1 channels activate rapidly at potentials close to the resting membrane potential and are sensitive to pharmacological block by 4-AP. Three *Drosophila* related K_V channel genes, *Shab*, *Shaw* and *Shal*, which correlate with mammalian K_V2, K_V3 and K_V4 subfamilies, respectively, were identified by homology screening with *Shaker* cDNA probes, and human homologues of all 4 subfamilies have been found[111].

2.4 Store-operated Ca^{2+} Entry

Store-operated Ca^{2+} entry (SOCE) is the phenomenon through which depletion of intracellular Ca^{2+} stores opens SOC on the plasma membrane. Upon depletion of Ca^{2+} in the SR/ER, this Ca^{2+} deficiency is sensed and transmitted to channels on the plasma membrane to allow Ca^{2+} to flow into the cytoplasm where it is then sequestered into the SR/ER by SERCA thus replenishing Ca^{2+} stores (Figure 7). Store-operated Ca^{2+} entry is necessary for the continued presence of Ca^{2+} signaling. Without SOCE, SR/ER Ca^{2+} stores would quickly become depleted in a matter of minutes. Under physiological conditions, activation of IP3R will lead to ER/SR store depletion. SR/ER Ca^{2+} release and then re-uptake, by SERCA, form measureable cytosolic Ca^{2+} oscillations, which are important for many cellular mechanisms such as contraction, proliferation, gene expression, etc. However, due to the PMCA constantly pumping Ca^{2+} out of the cytosol the amplitude of Ca^{2+} oscillations will progressively decrease and eventually the SR/ER Ca^{2+} store will become totally depleted. However before the SR/ER store is significantly diminished, SOCE is activated to allow extracellular Ca^{2+} to flow into the cytosol where it can be used to replenish the SR/ER Ca^{2+}.

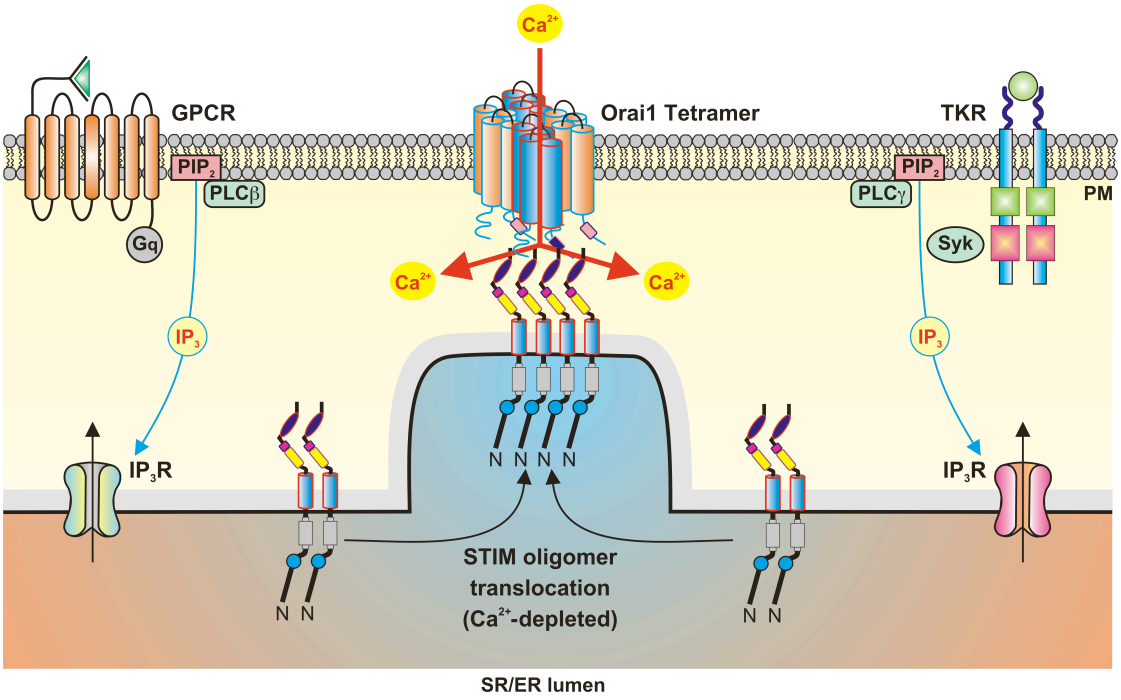

Figure 7: Mechanism of store-operated Ca^{2+} entry (SOCE). Stimulation of GPCR or tyrosine kinase receptors (TKR) on the plasma membrane increases IP_3 synthesis, activates IP_3 receptors on the SR/ER membrane, induces Ca^{2+} mobilization from the SR/ER to the cytosol, and leads to depletion of the SR/ER Ca^{2+} stores. The store depletion activates STIM causing them to oligomerize and translocate to regions of the SR/ER membrane near the plasma membrane (or SR/ER-plasma membrane junction). The N-terminal region of STIM is located in the SR/ER lumen and contains a Ca^{2+} binding EF-hand domain. Depletion of Ca^{2+} in the SR/ER leads to uncoupling of Ca^{2+} with the ER-hand domain leading to activation of STIM. Translocated STIM oligomers can then activate Orai1, which forms SOC as tetramers, and trigger Ca^{2+} influx (or SOCE).

2.4.1 STIM1 and STIM2

The molecular components of SOCE were largely unknown until 2005 when Roos *et al*. and Liou *et al*. used large scale RNA interference (RNAi) screens to reveal an important role for stromal interacting molecule 1 (STIM1) in SOCE (Figure 7)[112]. They found that knockdown of STIM1 dramatically reduces SOCE in various cell types including *Drosophila* S2, Jurkat T cells, HEK 293, neuroblastoma SH-SY5Y, and HeLa cells[113]. STIM1 is a sensor of $[Ca^{2+}]$ in the SR/ER ($[Ca^{2+}]_{SR/ER}$)[114]. STIM1 is a 685 amino acid long single transmembrane protein that is expressed on the SR/ER membrane and plasma membrane. Near the N-terminus of STIM1 is an EF-hand domain that senses $[Ca^{2+}]_{SR/ER}$ (which is in the range of 0.5-2 mM). When the Ca^{2+} store is diminished, Ca^{2+} is not bound to the EF-hand domain and STIM1 undergoes a conformational change, which allows it to multimerize, translocate to the SR/ER-plasma membrane junction (or puncta), bind with Orai1 tetramers on the plasma membrane and activate SOC and induce SOCE[112]. Mutagenesis of the EF-hand domain (mimicking low Ca^{2+}) leads to STIM1 multimerizing in distinct regions near the plasma membrane, called puncta, in the absence of store depletion and activate SOC. Examination by TIRF microscopy shows that store depletion induces ER-PM junctions (puncta). At these ER-PM, or SR-PM in the case of SMC, junctions STIM1 is localized roughly 10-20 nm from SOC on the plasma membrane[115].

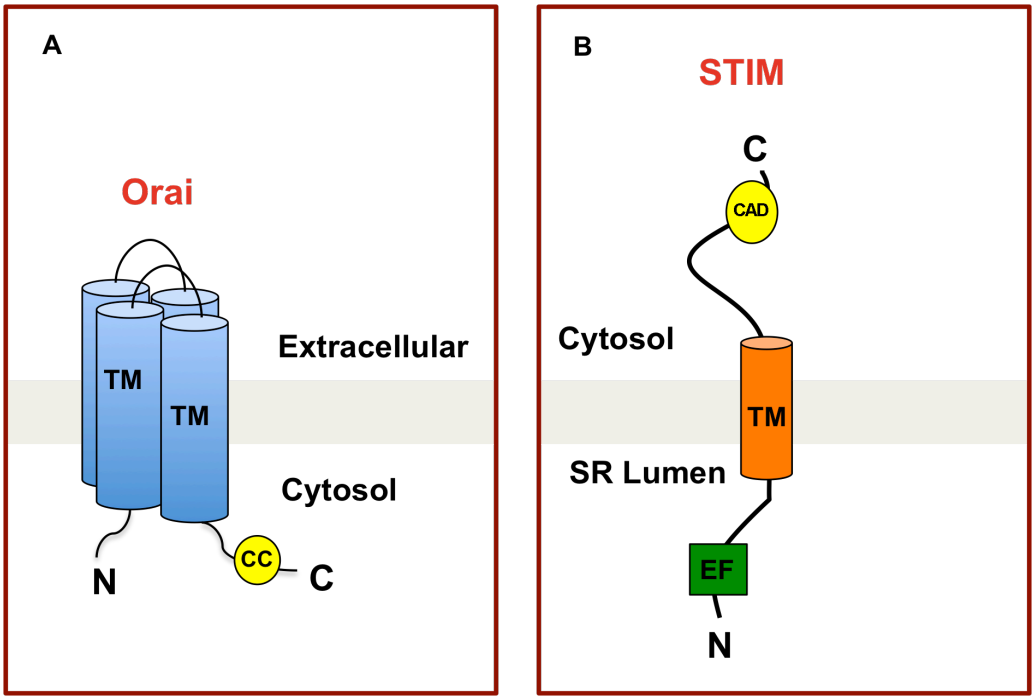

Figure 8: Structure and function of Orai and STIM. A. The isoforms of Orai, Orai1, Orai2 and Orai3, are four transmembrane domain proteins expressed on the plasma membrane. Both the N and C-termini are cytosolic, and a coiled-coiled domain near the C-terminus interacts with STIM. Recruitment and formation of tetramers of Orai, by STIM, form functional store-operated channels. The first and third transmembrane domains of Orai form the pore of the channel, which is selective to Ca^{2+}. **B.** STIM1 and STIM2 are single transmembrane domain proteins, which are expressed on the ER/SR membrane. The N-terminus is in the ER/SR lumen while the C-terminus is located in the cytosol. The N-terminus EF-hand domain binds Ca^{2+} and senses store depletion. Store depletion leads to unbinding of Ca^{2+} from the EF-hand domain followed by STIM oligeramerization and translocation to plasma membrane ER/SR membrane junctions, which leads to recruitment of Orai by the C-terminus Ca^{2+} activating domain (CAD) of STIM.

STIM1 (also known as GOK) is found on chromosome 11p15.5. STIM1 was originally described in human tumor cell lines and shown to induce growth inhibition and cell degeneration. Dziadek *et al*. used cell surface biotinylation to show STIM1 expression on the plasma membrane. These investigators then showed by western blot that STIM1 undergoes N-linked glycosylation and is phosphorylated mainly on serine and threonine residues on its C-terminal domain[116]. Later studies showed that STIM1 is also expressed on the ER membrane[112]. STIM1 contains an ER luminal EF-hand and a sterile-α motif (SAM) including two N-linked glycosylation sites near its N-terminus. C-terminal to the SAM domain is a transmembrane domain. The STIM1 C-terminus is located in the cytosol, containing two coiled-coil regions overlapping with an ezrin-radixin-moesin (ERM)-like domain, followed by a serine/proline and a lysine-rich region. The ERM domain of STIM1 contains the crucial Orai-activating domain, named CRAC-activating domain CAD (CAD), Orai-activating small fragment (OASF), or STIM–Orai-activating region (SOAR). These domains include the second coiled-coil domain and the following approximately 55 amino acids[117].

STIM1 senses Ca^{2+} concentrations in the ER lumen via its EF-hand, which is required for coupling store depletion to Ca^{2+} influx. Under normal circumstances when the Ca^{2+} concentration in the ER is high, STIM1 is uniformly distributed within the ER membrane and Ca^{2+} is bound to the EF-hand domain. The STIM1 EF-hand senses a decrease in the ER Ca^{2+} level from 300–500 μM under resting cell conditions down to approximately 200 μM. Upon store depletion, STIM1 translocates along the ER/SR

membrane to ER-PM junctions called puncta and recruits and activates SOC[118]. This culminates in the activation of so called store-operated Ca^{2+} entry roughly six to ten seconds following STIM1 translocation.

Several groups reported an insertion of STIM1 into the plasma membrane, rather than a translocation along the ER membrane, after store depletion. Spassova *et al*. have observed STIM1 plasma membrane expression independent of store depletion, proposing that plasma membrane- and ER-resident STIM1 interact. Further studies have demonstrated that N-terminal tagged STIM1 is not exposed extracellularly. Hauser *et al*. have compared the distribution of either N-terminally or C-terminally tagged STIM1 upon store depletion and have identified that both forms redistribute after store depletion. However, STIM1 tagged N-terminal with fluorescent proteins does not insert into the plasma membrane in contrast to its C-terminally tagged form. Thus, protein tags may affect STIM1 trafficking and insertion into the plasma membrane. Antibodies against the N-terminal sequence of STIM1 were observed to partially suppress SOCE but was not confirmed in another study. Therefore, the theory that STIM1 traffics and inserts into the plasma membrane is unsubstantiated at best. Furthermore, many researchers have shown that translocation of STIM to puncta is sufficient to activate SOCE.

The C-terminal cytosolic part of STIM1 is necessary for Orai activation. When the C-terminal portion alone was co-expressed with Orai1 in HEK293 cells, the STIM1 C-terminus localized close to the plasma membrane and co-localized with Orai1. By contrast, a STIM1 deletion mutant lacking the C-terminus is no longer able to co-localize

with overexpressed Orai1 upon store depletion and is diffusely distributed throughout the ER membrane. Disruption of the ERM domain also impairs STIM1 distribution and function. STIM1 domains following the ERM domain have been reported to be less important for CRAC activation, as the deletion of the serine/proline-rich region has no significant effect on SOCE. The very end of STIM1 C-terminus contains a lysine-rich domain, the deletion of which eliminates puncta formation despite preserved STIM1 homomerization. This mutant is still able to activate Orai1 channels upon store depletion, yet with a somewhat delayed response.

STIM2

STIM2 shares 47% sequence homology as STIM1 and activates SOC in the same manner involving Ca^{2+} dissociation from the EF-hand domain, then oligeramerization, and then translocation to ER-PM junctions and recruitment of SOC. The role of STIM2 in SOCE is less clear as most studies have focused on STIM1. Initial evidence regarding STIM2's role was contradictory as high levels of STIM2 expression inhibitied SOCE. Brandman et al later found that at physiological expression levels STIM2 activated SOCE. And, importantly these researchers used a siRNA screen of the human signaling proteome to show that STIM2 is the strongest regulator of basal $[Ca^{2+}]_{cyt}$ (calmodulin 1 was the next strongest regulator) and that STIM2 can activate Ca^{2+} influx following smaller decrease in ER Ca^{2+} compared to STIM1. They used ionomyocin, which stimulates ER Ca^{2+} release and EGTA, which chelates extracellular Ca^{2+}, to demonstrate that siRNA mediated knockdown of STIM2 decreases $[Ca^{2+}]_{ER}$

compared to STIM1 knockdown. These researchers then overexpressed the either YFP-STIM2 or YFP-STIM1. They quantified the fluorescence of YFP-STIM1 and YFP-STIM2 to ensure the same protein expression level of STIM1 and STIM2. Then they measured the effect of overexpression of the same amount of STIM1 or STIM2 on basal $[Ca^{2+}]_{cyt}$. They found that STIM2 had a much larger effect of basal $[Ca^{2+}]_{cyt}$ compared to the same to amount of STIM1. They then verified this finding using the ER targeted Ca^{2+} sensor D1ER. STIM2 translocated to ER-PM junctions three times faster than STIM1 in response to low levels of store depletion, suggesting that STIM2 is more sensitive to low levels of store depletion and plays a more important role in physiological amounts of store depletion. This difference in STIM1 and STIM2 is often overlooked as fast and severe depletion of ER Ca^{2+} using thapsigargin quickly activates both STIM1 and STIM2 within one minute. They used YFP tagged STIM2 to observe translocation of STIM2 to ER-PM junctions following store depletion. These researchers suggest a paradigm shift placing STIM2, rather than STIM1, as the central protein that tightly regulates cytosolic and ER $[Ca^{2+}]$.

STIM1 and STIM2 have been shown to be able to form heteromultimers in addition to homomultimers. However, STIM2 can function independent from STIM1. Brandman *et al*. showed that overexpression of STIM2 and knockdown of STIM1 in the same cell had no effect on Ca^{2+} regulation compared to STIM2 overexpression alone. And, that both STIM2 alone or STIM1 alone can mediate SOCE by activating Orai1.

Neurons express very little STIM1 and Orai1, but still exhibit strong SOCE. Berna-Erro *et al*. showed that STIM2, and perhaps Orai2 and Orai3, are the predominant

isoforms for SOCE in neurons. STIM2 mRNA and protein levels, as measured by western blot and immunocytochemistry, are high in neurons compared to that of STIM1. Complete knockout of of STIM2 in mice was embryonic lethal in some strains but viable for 4-5 weeks after birth in another strain of mice. Cortical neurons isolated from these STIM2$^{-/-}$ mice demonstrated significantly weaker SOCE compared to WT mice. STIM2$^{-/-}$ mouse cortical neurons also demonstrated significantly lower basal cytosolic and ER [Ca^{2+}] compared to cortical neurons isolated from WT, STIM1$^{-/-}$, and Orai1$^{-/-}$ mice. This finding corroborates the report by Bradmann *et al*. regarding the important role of STIM2 in regulating basal cytosolic and ER [Ca^{2+}]. However, these data were obtained using cortical neurons, which naturally express very little STIM1 and Orai1. It would be interesting to examine different cell type, such as PASMC, in STIM2$^{-/-}$ mice.

2.4.2 Store-operated Ca^{2+} Channel - Orai1, Orai2 and Orai3

In Greek mythology, Orai are the keepers of the gates of heaven. ORAI is now also used to describe the plasma membrane Ca^{2+} influx proteins categorized as SOC. Feske *et al*. identified Orai1 as the protein responsible for the entry of Ca^{2+} following Ca^{2+} store depletion using two different approaches. One approach involved genotyping and using linkage analysis in individuals that have a defect in store-operated Ca^{2+} entry. These individuals have a specific form of human hereditary severe combined immunodeficiency (SCID). SCID patients are homozygous for a single missense mutation in Orai1, *i.e*. Orai1 R91W, leading to the loss of SOCE. The second approach used a *Drosophila* RNA interference screen based on the assessment of store depletion-mediated Ca^{2+} entry and nuclear factor of activated T-cells (NFAT) nuclear translocation. Around the same time, two other groups independently identified the same gene in *Drosophila* using genome-wide RNA interference screens and its human orthologs.

Many early studies of ORAI genes use the nomenclature "CRACM", however, the majority of current studies use *ORAI* to describe the genes (ORAI1, ORAI2, and ORAI3), which encode proteins Orai1, Orai2, and Orai3 28–33 kDa Orai proteins are located on the plasma membrane and appear to function as tetramers. Orai tetramers are teardrop shaped, with each protein capable of high levels of glycosylation (up to 8 kDa per protein).

Orai1

Strong evidence suggests that Orai1 interacts with STIM1 and functions as a SOC. Orai1 was discovered through genome wide RNAi screening. A mutation in Orai1 in patients with severe combined immunodeficiency eliminates the Ca^{2+} release-activated Ca^{2+} currents (I_{CRAC}), which can then be reconstituted by expressing wild-type Orai1[82,83]. Orai1 spans the plasma membrane four times with both the C- and N- terminus in the cytoplasm. The extracellular loop between the third and fourth transmembrane segments contains an N-glycosylation site. The first and third transmembrane regions together with the extracellular loop following the first transmembrane domain of each of four Orai1 monomers form the channel pore. Co-expression of STIM1 with Orai1 in HEK293 cells resulted in large increases in SOCE and I_{CRAC} compared to vector control cells[84]. Co-immunoprecipitation data show that STIM1 and Orai1 interact, and store depletion significantly increases the amount of interaction[119].

Orai2 and Orai3

The Orai family consists further of Orai2 and Orai3. Both Orai2 and Orai3 when co-expressed with STIM1 in HEK cells show a similar but reduced, compared to co-expression with Orai1, store-operated Ca^{2+} current. The overall domain structure of Orai2 and Orai3 is similar to that of Orai1, with a coiled-coil domain in the C-terminus that interacts with STIM. However, Orai2 and Orai3 are missing the proline-rich region near the N-terminus. The respective Orai channels exhibit distinct inactivation profiles,

permeability properties, and 2-aminoethoxydiphenyl borate (2-APB) sensitivity. However all three Orai channels can be activated following store depletion via a coupling to STIM1 or STIM2. Orai proteins are able to heteromultimerize in all possible combinations to form functional channels.

Orai Channel Selectivity

All three Orai proteins can assemble to form a tetrameric channel with a unique structure that is unrelated to any other known ion-channel family. A hallmark of Orai channels is their high Ca^{2+} selectivity over Ba^{2+} or Sr^{2+}. Furthermore, omission of Ca^{2+} in the presence of Mg^{2+} and Na^{+} on the extracellular side fully abolishes current influx, suggesting that Orai channels are also selective of these ions. However, in a divalent-free bath solution, a prominent Na^{+} influx is induced, while Cs^{+} permeability is unusually low with a permeability ratio of $P_{Cs}/P_{Na} = 0.15$ for Orai1. Taken together these data show that Orai channels are extremely selective for Ca^{2+}, however not totally inpermiable to monovalent cations such as Na^{+}. This is contrary to voltage-gated L-type Ca^{2+} channels that exhibit a P_{Cs}/P_{Na} ratio of 0.6. The low Cs^{+} permeability of Orai channel pores is likely accomplished by their minimum pore dimensions with an estimated diameter of 3.8 Å, which is based on the permeability of different methylammonium derivatives. For comparison, pores of voltage-gated L-type and TRP channels are much larger, with diameters of 6.2 Å and 5.4 Å, respectively.

Orai Channel Formation

While the Orai1 C-terminus, especially its putative coiled-coil domain, has been elucidated as the main interaction domain for store-dependent STIM1–Orai1 coupling, the role of the N-terminus in the STIM1/Orai1 signaling machinery is less clear. Orai1 N-terminus contains a proline- and arginine-rich region, which is lacking in Orai2 and Orai3. At the end of the N-terminal cytosolic region, all Orai proteins include a highly conserved amino acid stretch. The proline- and arginine-rich N-terminal cytosolic sequences have been suggested to play an essential role in Orai1 channel assembly. An Orai2 chimera containing the Orai1 N-terminus exhibits a marked increase in store-operated currents, while Orai1 with a shortened N-terminal tail similar to that of Orai2 and Orai3 displays significantly reduced Ca^{2+} entry in comparison to wild type Orai1. Deletion of the whole N-terminus of Orai1 abolishes SOCE, while its partial truncation up to amino acid 73 retains Orai1 channel activity. This observation suggests the highly conserved region between amino acid 74 and 90 in the Orai1 N-terminus as a domain indispensable for Orai1 activation.

The exact architecture of the Orai pore is unknown; however, part of the first and third transmembrane (TM) segment and the first extracellular loop contribute to the pore-forming domain. Within these domains, negatively charged key residues have been identified as essential for the Ca^{2+} selectivity. The first extracellular loop represents

another important site of the selectivity filter. By contrast to the conserved glutamates in the TM domains of all three Orai proteins, key residues within the loop consist either of glutamates, glutamines, aspartates, or asparagines (D110/112/114 for Orai1; E84/Q86/Q88 for Orai2; E85/D87/E89 for Orai3; D182/D184/N186 for *Drosophila* Orai). While a single point mutation of one of these aspartates in Orai1 to an alanine does not affect Ca^{2+} currents, inhibition by 5 nM gadolinium is substantially reduced for the first acidic residue, moderately for the second, and slightly diminished for the third negatively charged residue in comparison to wild type Orai1. Based on such structure/permeation studies, a model has been proposed for the Orai selectivity filter with two negatively charged rings of amino acids: one within TM1 and TM3, consisting of eight acidic residues in a tetrameric channel, and the other composed by the first extracellular loops including 12 negatively charged or polar amino-acids. According to the model one Ca^{2+} ion coordinately binds to the outer mouth of the Orai channel represented by the extracellular loops and a second one to the acidic membrane ring embedded within the TM domains. These multiple Ca^{2+} binding sites are suggested to strengthen Ca^{2+} selectivity.

TRPC

Before the discovery of Orai genes and their gene products, the seven TRPC proteins were the only candidates for SOC. Cloned TRPCs enhance store-depletion activated Ca^{2+} entry and injection of specific anti-TRPC antibodies or genetic ablation of

TRPC genes reduces SOCE. Moreover, Zagranichnaya *et al*. showed partial reduction of SOCE in response to siRNAs that targeted TRPC1, TRPC3, or TRPC7, which, when combined, were partially additive. Our lab has also demonstrated that siRNA mediated knockdown of TRPC1 in PASMC decreases SOCE. Furthermore, TRPC4 knockout mice lack SOCE and there is an 80% loss of SOCE found in submaxillary acinar cells from TRPC1 knockout mice.

Chapter 3. Pulmonary Hypertension

3.1 What is Pulmonary Hypertension?

Pulmonary arterial hypertension (PAH), a rare but devastating disease which, if left untreated, leads to right heart failure and death. PAH affects people of all ages, including newborns. 2-5 people per million per year are diagnosed with idiopathic pulmonary arterial hypertension (IPAH). Patients present with a range of nonspecific symptoms, including exertional dyspnea, chest pain, fatigue, syncope, cyanosis, and peripheral edema. The generality of these symptoms and the rarity of the disease make diagnosis a difficult task, and the mean time from onset of symptoms to diagnosis is two years, although up until recently it was as much as five years[120].

Under normal physiologic conditions the pulmonary circulation is maintained in a high-flow, low pressure and low resistance state. Under pathophysiological conditions restriction of blood flow by pulmonary arteries increases the pulmonary vascular resistance, which causes pulmonary arterial hypertension. Increased PVR burdens the right heart and over time results in right ventricular hypertrophy and eventually right heart failure and death. The main symptoms of PH are dyspnea, low exercise tolerance and in severe cases syncopy. Dyspnea is a result of inadequate gas exchange and an inability of the heart to further increase cardiac in response to cerebral hypoxia. A patient may also experience fatigue, weakness and syncope. A syncope

episode may initially appear upon exertion but can eventually happen at rest. PAH is defined clinically as a resting mean pulmonary arterial pressure (mPAP) that is ≥ 25 mmHg or a mPAP ≥ 30 mmHg during exercise[120,121].

The true incidence of PAH is difficult to gauge due to its heterogeneity and that it may be secondary in nature to an underlying disease. A german doctor, Dr. Romberg is credited with reporting the first case in 1891. He published his findings from an autopsy that showed thickening of the pulmonary artery from a patient with no other apparent lung or heart disease. It was not until 1951 that an American physician Dr. Dresdale used the term primary pulmonary hypertension (PPH) to define a condition in which an elevated pulmonary artery pressure exists without demonstrable cause[122]. In the United States there is an incidence of roughly 2-3 cases per million. And, there is a female bias with a ratio of 2.3:1 with a median age of diagnosis of 36 years with a mean survival from diagnosis of 2.8 years[1,122].

Classification

An increase in pulmonary arterial hypertension in healthy young adults coinciding with an epidemic of anorexigenic-associated PPH during the 1950's and 1960's led to the first World Health Organization (WHO) meeting on PH in 1973 as an effort to better understand the condition. The initial classification utilized two categories: primary PH and secondary PH depending on certain risk factors[123]. As a result of the conference, international efforts intensified to more clearly define and diagnose PH. For example, the

National Heart, Lung and Blood Institute's (NHLBI) Division of Lung Disease in 1981-85 started a national patient registry to identify demographics and characteristics consisting of three components: a statistical-epidemiological core, a pathology core and 32 clinical centers. At the time the registry compiled the best epidemiological data and contributed to a better understanding of PH because the conclusions were comparable to retrospective reports published later from France, Israel and Japan in terms of mean age onset (36.4 years), female-to-male ratio (1.7:1.0) with no racial predisposition. Twenty-five years later, the 2nd World Symposium on Pulmonary Hypertension was held in Evian, France. This meeting broadened the definition into 5 categories or clinical classifications later to be known as the "Evian classification." Assigning categories based on shared underlying pathologies allowed investigators to focus treatments on a well-defined group of patients. Multiple clinical trials ensued and resulted in 8 different medications for the treatment of PAH worldwide. The Third World Symposium on Pulmonary Arterial Hypertension (PAH) was held in Venice, Italy in 2003. The gathering provided an opportunity to assess the usefulness of the Evian classification and propose alterations if needed. The most distinctive change was dropping the term PPH and replacing it with Idiopathic Pulmonary Arterial Hypertension (IPAH). This first category included two subgroups, the first had both familial and sporadic forms of the disease and the second subgroup was comprised of a number of conditions or diseases of known causes with a common localization of lesions in the small pulmonary arterioles[123]. The most recent WHO conference convened in 2008 in Dana Point, California. The group of international experts generally agreed to maintain the philosophy and organization of the Evian and Venice classifications. However, it was also agreed upon that modifications should be

made in order to reflect relevant data published in the previous 5 years[124]. With regard to the classification of PH, PAH has been the focus since the first WHO meeting in 1973. The subgroup of PAH can be distinguished clinically from PH by in addition to a resting mPAP > 25 mm Hg that pulmonary arterial wedge pressure must be ≤ 15 mm Hg which is determined by right heart catheterization[125].

Pathology and pathophysiology of PAH

PH is a disease that is rarely diagnosed during routine medical examinations. The diagnosis is typically made out of exclusion of other disorders such as congenital heart disease, emphysema or pulmonary thromboemboli. As mentioned above, PH is defined as a mean pulmonary arterial pressure > 25 mmHg and >30 mmHg during exercise. This definition is based on right heart catheterization and provides a more conclusive diagnosis than an estimated PAP that is derived from estimating the systolic PAP through echocardiography[126].

Genetic variations in several genes have been linked to familial PAH (fPAH) patients. These genes include transforming growth factor-β (TGF-β), bone morphogenic protein receptor 2 (BMPR2) and serotonin. Although these mutations are prevalent in the familial PAH patients only 20% of the population with the BMPR2 mutations exhibits disease progression. There are two BMPRs, BMP-R1a (type 1) and BMP-R1b (type 2). Binding of BMP ligand to BMPR activates downstream signaling components such as Smad proteins that translocate to the nucleus and regulate expression of genes important

for proapoptotic and anti-proliferative pathways[127]. Having an abberant BMPR genetic profile predisposes them to elevated risk factors in developing PAH. The association between PAH and BMPR2 was first reported in 2000[128]. Shortly after, heterologous mice were engineered to investigate the mechanisms of BMPR2 in PAH. Surprisingly, the mice showed normal PAP at rest and actually required a trigger to elevate PAP such interleukin (IL-1β) or serotonin[47,129,130]. The phenotype did display increased smooth muscle proliferation with expansion of collagen and matrix proteins. A plausible explanation to defective BMPR2 signaling was provided by Fantozzi *et al*. in a study that demonstrated that bone morphogenetic protein-2 stimulation of PASMC upregulated the expression of voltage-gated K^+ channels[131]. The increase in K_v channel expression and activity may be an important component in proapoptotic and antiproliferative effects of BMP-2 signaling that is lacking in PAH patients with BMPR2 mutations.

Although there is no single genetic cause of IPAH, heterogeneous mutations in the bone morphogenetic protein (BMP) receptor type II (BMPR2) gene (which encodes the BMPR-II protein) have been linked to both familial and sporadic PAH[128,132]. BMPR-II is a cell surface receptor of the TGF-β superfamily of signaling molecules that is needed for recognition of BMP ligands. BMPR-Ia is another receptor molecule involved in this pathway. BMP ligand binding triggers receptor oligomerization, stimulating transcription factors of the Smad family, which activate genes involved in cell growth arrest and induction of apoptosis through Bcl-2 downregulation[133-135].

BMP signaling in PASMC induces apoptosis[136]. In PASMC, BMPs promote apoptosis by activating caspases, releasing cytochrome c, and downregulating antiapoptotic Bcl-2[136]. BMPR-II mutations found in IPAH patients diminish the antiproliferative and proapoptotic effects of BMP signaling[137-139]. Mutations in the BMPR-II receptor identified in IPAH patients renders normal PASMC resistant to BMP-induced apoptosis[136], indicating that a loss of pro-apoptotic BMP signaling, which would result in an overall increase in PASMC in the pulmonary vasculature and thus remodeling and arterial lumen obstruction, lies at the core of many cases of IPAH. In PASMC, BMP-2 (a ligand for the BMP receptor) treatment increases whole cell $I_{K(V)}$ and $K_V1.5$ mRNA and protein[131,140]. However, PASMC from IPAH patients are more resistant to apoptosis induced by BMP than cells from normotensive control or SPH patients[141]. Similarly, while BMP ligand (BMP-2, -4 and -7) inhibits serum-stimulated DNA synthesis and proliferation in PASMC from normal subject or SPH patients, BMPs fail to inhibit the same in PASMC from IPAH patients[142]. These data suggest an overall resistance to apoptosis in PASMC from IPAH patients and that PASMC from IPAH patients react abnormally to endogenous proliferation and antiproliferation signals in the vasculature.

Although *BMPR2* mutations are the single most prevalent genetic factor associated with IPAH known at this time, they do not account for all instances of the disease: ~70% of familial PAH cases have *BMPR2* mutations; the prevalence of the mutations is 10-40% in sporadic IPAH and the penetrance is incomplete, as only ~20-30% of BMPRII mutant carriers develop the disease. Indeed, a large study of ten IPAH

families identified another locus for PAH, and there is emerging evidence that a polymorphism in the serotonin transporter is linked to PAH susceptibility[143]. Environmental factors, such as amphetamine use and HIV infection, have been correlated to PAH as well. Even in the background of known PAH risk factors such as fenfluramine use, mutations such as one found in the serotonin 5-HT receptor may predispose individuals to PAH[144]. Thus, there are likely several genetic modifiers that influence disease pathogenesis.

How is it that some fPAH patients have heterozygous germline mutations of TGF-β and/or BMPR2 but the majority of them do not develop PAH? One explanation is that a "second hit" or unidentified trigger may be required. A "serotonin hypothesis" has been discussed for many years dating back to the use of diet pills such as dexfenfluramine (Dfen). Serotonin has a complicated pharmacology so the effects on PAH are still debated. The intended use of Dfen was to increase blood serotonin by inhibiting the neuronal serotonin transporter (SERT) thereby preventing its reuptake and causing enhanced 5-HT_{2B} receptor stimulation[145]. Serotonin has been shown to promote PASMC proliferation, pulmonary arterial constriction, local microthrombosis and inactivate K^+ channels[146]. The effects of serotonin can be augmented in more than one way. For example, polymorphisms in SERT have been described that increase its function. Also, the rate-limiting step of serotonin synthesis is catalyzed by tryptophan hydroxylase1 (Tph1) and has been shown to have higher expression in endothelial cells from lungs of IPAH patients. Importantly, $Tph1^{-/-}$ and $5HT_{2B}$ receptor knockout mice are less susceptible to hypoxic-induced PAH[147]. Serotonin has can inhibit voltage-gated K^+

channels in PASMC with a similar or higher efficacy than other K_v channel blockers endothelin-1, thromboxane A_2 analog U46619 and hypoxia[148]. Blocking K_v channels causes membrane depolarization leading to Ca^{2+} influx and cell contraction. Serotonin also leads to the downstream production of IP_3 though $G_{i/o}$. As previously discussed, IP_3 activates IP_3R and leads to Ca^{2+} release from the ER/SR, store depletion, and activation of SOCE, which all contribute to increased $[Ca^{2+}]_{cyt}$, PASMC contraction and proliferation, and PAH.

The PAH subgroup is comprised of a heterogeneous population of patients with a variety in disease etiology. Although arising from different origins, PAH patients share common pathological features such as: precapillary artery hypertension, slow clinical onset followed by progressive deterioration due to severe arteriopathy, increased thickness of the intima, media and adventitia of peripheral arteries and muscularization of the precapillary arterioles and capillaries [149,150]. Upon autopsy, vascular remodeling is apparent along with thrombotic lesions[151,152]. A hallmark of severe idiopathic pulmonary hypertension is the presence of plexiform lesions that can obstruct blood flow in arteries and arterioles but is only found in roughly 15% of PAH patients. Occlusion of the smaller blood vessels can arise from monoclonal proliferation of endothelial cells, smooth muscle cell proliferation, migration and hyperplasia with accumulation of circulating inflammatory, platelet and progenitor cells[153].

The pathogenesis of PAH can mainly be attributed to the combined effects of sustained vasoconstriction, arterial vessel remodeling, *in situ* thrombosis or obliteration

of arteries by plexiform lesions and arterial wall stiffening[154]. An initial event such as hypoxia can elicit transient vasoconstriction, which is important in order to optimize ventilation-perfusion matching[2]. The acute hypoxic-mediated vasoconstriction of pulmonary arteries is a normal response. However, chronic constriction in these airways is disparate from the hypoxic pulmonary vasoconstrictive response as it involves prolonged, rather than acute, vasoconstriction and excessive pulmonary vascular remodeling. Increased vascular wall non-compliance or stiffening has also been ascribed to breakdown of extracellular matrix and increased collagen accumulation around endothelial cells, smooth muscle cells and fibroblasts[155,156]. Interestingly, both the acute and chronic vasoconstriction require an increase in intracellular Ca^{2+} in PASMC.

Major pathological findings of IPAH include medial hypertrophy due to PASMC proliferation, muscularization of the arterial walls due to PASMC invasion of the intimal layer, endothelial cell proliferation, and concentric laminar fibrosis[157,158]. Pulmonary angiogram of IPAH patients shows diminished blood flow through pulmonary arteries with diameter less than 500 μm due to pulmonary vascular remodeling and vasoconstriction (Figure 9). Thus, IPAH is often referred to as 'small vessel disease' to distinguish it from obstructions in the main pulmonary artery that can cause PAH such as in chronic thromboembolic pulmonary hypertension (CTEPH). The intimal and medial hypertrophy, PASMC proliferation, remodeling, muscularization, concentric laminar fibrosis and sustained vasoconstriction that accompany PAH decrease vascular compliance and decrease the arterial lumen radius, thus increasing both PVR and PAP. An increase in PVR increases the stroke work of the right ventricle and thus exposes the

RV to pressure overload. Initially, adaptive hypertrophy of the RV overcomes the pressure overload but in time progresses to contractile dysfunction and decompensated right heart failure.

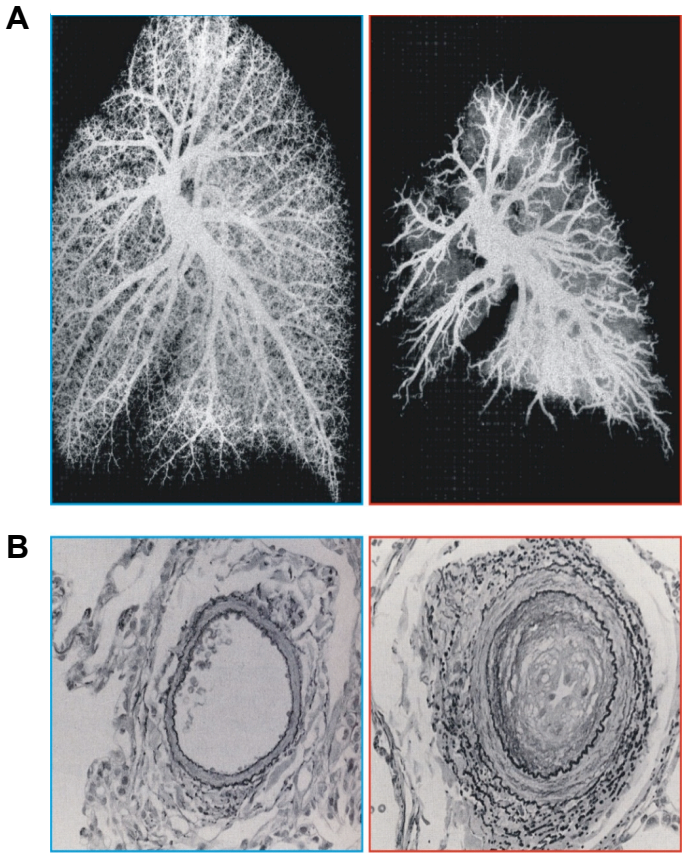

Figure 9: IPAH is a small vessel disease. A. Representative pulmonary angiograms from NPH-subject lung (left panel) and IPAH-patient lung (right panel). Blood flow is present in large, medium, and small size vessels in NPH-subject, but flow is absent in small size vessels in IPAH-patient lung. **B.** Elastic Van Gieson (EVG) staining of cross section of small pulmonary artery from NPH-subject (left panel) and IPAH-patient (right panel). IPAH-patient pulmonary artery shows intimal lesions, medial hypertrophy, adventitial thickening, which are all typical of IPAH-patient pulmonary arteries.

Chronic thromboembolic pulmonary hypertension (CTEPH) is a type of PAH, the initial cause of which is well defined. Initially, a thrombus from the peripheral venous circulation lodges in the PA where it fails to spontaneously resolve. The immediate rise in PAP caused by the blockage, however, is followed by a decline as ventricular hypertrophy compensates for the increased pressure load. Over time, however, cardiac output continues to decrease until pulmonary hypertension is fully developed. For many patients, CTEPH can be cured surgically with pulmonary thromboendarterectomy (PTE)[159] in which clot material is removed from the PA. Interestingly, surgically removed clot material is often a cast of the pulmonary arterial tree, indicating that the initial clot burden continued to grow after becoming lodged in the PA. Furthermore, clots are often recanalized, an additional indication of growth and abnormal cellular proliferation in CTEPH.

Certain patients who undergo PTE have poor post-operative outcomes (~15% of PTE patients), characterized by persistent pulmonary hypertension (often quoted as PVR > 500 dynes × s/cm^5). Post-operative mortality in these patients is much higher (~20-30%) than in patients who have a post-operative PVR <500 dynes × s/cm^5 (3-7%). Patients with high post-operative PVR are suspected to have underlying distal vessel PAH (*i.e.*, IPAH or other forms of PAH in addition to CTEPH) which is intractable to surgery. These patients would benefit tremendously from pre-operative treatment for underlying distal vessel disease before undergoing PTE. A genetic screen provides a noninvasive and inexpensive way to accomplish the goal of identifying people at high

risk for PAH to determine who, among CTEPH patients, should be treated for distal vessel PAH before undergoing PTE.

3.2 Treatment of Pulmonary Hypertension

Prior to drug developments of the last ten years, lung transplantation and Ca^{2+} channel blockers were the only treatments for IPAH. Nifedipine and diltiazem provided an early therapeutic approach but helped only a small percent of IPAH patients (<10-30%)[121,160]. The observation that three signaling pathways prostacyclin, endothelin, and nitric oxide are involved in PAH pathophysiology led to the development of three additional classes of drugs. Endothelin-1 is both an endogenous smooth muscle mitogen and vasoconstrictor and is upregulated in PA endothelial cells of PAH patiens [161]. Thus, endothelin receptor antagonists such as bosentan have proven effective at treating PAH by improving hemodynamics, exercise capacity and survival. Additionally, production of NO and prostacyclin (PGI_2), both potent vasodilators and inhibitors of SMC proliferation, are decreased in PAH patients. Prostacyclin analogues and phosphodiesterase-5 inhibitors such as sildenafil, which prolong the effects of NO, have also been found effective at treating IPAH. These drugs have both vasodilator and antiproliferative effects and have a variety of administrative routes, including inhalation, oral, and intravenous infusion by permanent indwelling catheter.

Drugs are commonly used in combinations determined on a per patient basis. For example, combination sildenafil and prostanoid treatment has been found to improve exercise capacity and pulmonary hemodynamics in patients with severe PAH[162], and inhaled iloprost, a prostacyclin analogue, when added to bosentan monotherapy regimens improves patients' exercise capacity and hemodynamics. However, some patients do not

respond to any pharmacological treatment or deteriorate after an initial beneficial period. These patients are placed on the lung transplant list.

Chapter 4. Materials and Methods

4.1 Isolation and Culture of Pulmonary Artery Smooth Muscle Cell

Sprague-Dawley rats (125-250 g) were decapitated; the right and left branches of the main pulmonary artery as well as the mesenteric artery and surrounding tissues were removed and placed in Hanks' solution (HBSS) comprised of Hanks' balanced salt (Irvine Scientific, Santa Ana, CA) supplemented with 14.98 mM N-2-hydroxyethylpiperazine-N'-2-ethanesulfonic acid (HEPES), 4.17 mM $NaHCO_3$, 0.4 mM $MgS0_4$ 10,000 U/ml penicillin, 10 mg/ml streptomycin, and 0.02 mM $CaCl_2$. Connective tissues were gently removed under a dissecting microscope using sterile conditions. The isolated PA or MA was incubated in 1 ml HBSS containing 1.5-2 mg collagenase (Worthington Biochemical, Freehold, NJ) for 20 min. The adventitia (plus a small amount of outer media) was carefully stripped off and the endothelium was scraped off with fine forceps. The resulting PA smooth muscle tissue was incubated at 37°C for 20-25 h in 10% fetal bovine serum culture medium (FBSCM), comprised of Dulbecco's modified Eagle's medium (DMEM, Sigma Chemical, St. Louis, MO) supplemented with 7 mM $NaHCO_3$, 10 mM HEPES at pH 7.2, and fortified with fetal bovine serum (10%, Irvine Scientific). The overnight incubation of the smooth muscle tissues in 10% FBSCM before enzymatic digestion improves the yield of the cells. The tissue was then incubated with 1.5-2 mg collagenase (Worthington), 0.5 mg elastase (Sigma), and 1 mg bovine serum albumin (Sigma) in 1 ml HBSS at 37°C for 40 min. After 15-20 min, the tissue was triturated three to five times with a fire polished Pasteur pipette to speed

digestion. The incubation mixtures were then diluted 20-fold by adding 20% FBSCM to stop digestion. The cell suspensions were centrifuged for 5 min at 1,500 rpm at room temperature, and the supernatant was removed. The resulting pellets were resuspended in 2-3 ml 10% FBSCM and triturated with fire-polished Pasteur pipettes to separate the cells. Aliquots (3-6 drops) of the cell suspensions were drawn off and placed on cover slips in Petri dishes with 2 ml of 10% FBSCM. Cells were fed twice weekly with 10% FBSCM and incubated in a humidified atmosphere of 5% CO_2, in air at 37°C for 3-7 days. Enzymatically dispersed VSM and cultured cells during this time were reported to retain morphological and functional properties of cells in vivo. After l0-20 days, the primary cultured cells had reached confluence on the cover slips. At this time, the cells were treated with trypsin (1 mg/ml, Sigma) in HBSS and then re-plated on cover slips in Petri dishes with the addition of 2 ml 10% FBSCM. Six to 12 hours later, the 10% FBSCM in the Petri dishes was replaced by fresh 10% FBSCM to remove dead and unattached cells.

The cells were then plated onto 25-mm coverslips and cultured in 10% FBS-DMEM in a humidified incubator (at 37°C with 5% CO_2). Cellular purity of cultures was determined using the smooth muscle α-actin monoclonal antibody and the nuclear acid stain, 4',6'-diamidino-2-phenylindole (DAPI, 5 μM). The DAPI-stained cells also cross-reacted with the smooth muscle cell α-actin antibody, indicating that the cultures were all smooth muscle cells.

Human PASMC

Pulmonary hypertensive human PASMC were isolated from IPAH patient lung. Two patients undergoing lobectomy for bronchogenic carcinoma, who had no evidence of pulmonary hypertension by physical examination, ECG, echocardiogram, or pathological examination of resected lung tissue, and 4 patients with obstructive disease, who had normal pulmonary arterial pressures, were the sources of tissue for normotensive control experiments. Lung tissue, removed from patients in the operating room, was immediately placed in cold (4°C) saline and taken to the laboratory for dissection. Muscular pulmonary arteries were incubated in Hanks' balanced salt solution (20 minutes) containing 2 mg/mL collagenase (Worthington Biochemical). The adventitia was stripped, and endothelium was removed. The remaining smooth muscle was digested with 2.0 mg/mL collagenase, 0.5 mg/mL elastase, and 1 mg/mL bovine albumin (Sigma Chemical Co) at 37°C to make a cell suspension of PASMC. The single PASMC was resuspended, plated onto 25-mm coverslips and incubated in a humidified atmosphere of 5% CO_2 in air at 37°C in 10% fetal bovine serum DMEM for 1 week. the cells were isolated from arteries of size at the range of 100–500 μm in diameter. Approval to use the human lung tissues and cells was granted by the University of California, San Diego (UCSD) Institutional Review Board. Control PASMC were purchased from Lonza and maintained in culture at low passage (<6) in SM growth medium (SmGM). The mean pulmonary arterial pressure of the IPAH patients was 52 mmHg.

All PASMC were cultured in M199 supplemented with 10% FCS, 100 µg/ml endothelial cell growth supplement (ECGS), 100 IU/ml penicillin, 100 µg/ml streptomycin, and 50 mg/l D-valine. Cells were plated on the coverslips coated with 2% gelatin. Approval to use the human lung tissues and cells was granted by the University of California, San Diego (UCSD) Institutional Review Board. The mean pulmonary arterial pressure of the IPAH patients was 52 mmHg.

All cells were incubated in a humidified environment at 37°C and 5% CO_2. Media was changed 24 hours after initial seeding and every 48 hours subsequently. When cells reached 80-90% confluency, cells were gently washed with phosphate buffered saline (PBS), incubated with 3mL of trypsin/EDTA solution until detachment (3-5 min), and then incubated with an equal amount of trypsin neutralizing solution. For PASMC, a 0.25% trypsin/EDTA solution (Lonza) was used. The cell suspension was then transferred to a sterile 15-ml round bottom tube, centrifuged at room temperature for 5 minutes at 200 G, and then resuspended in appropriate growth media and seeded. PASMC between passages 3 and 8 were used for experiments.

4.2 Transfection of PASMC

PASMC were transfected with siRNA against STIM2 (Santa Cruz sc-76589) or scramble siRNA as control using the Amaxa Nucleofector electroporation system. 16 μL of a 10 μM solution of siRNA was used per 2 x 10^5 cells in each reaction.

4.3 Immunoblot

PASMC were lysed (Lysate buffer: 0.5% sodium deoxycholate, 0.1% SDS, 1% triton-X, 0.1% protease inhibitor cocktail) and centrifuged at 16,000 g for 10 min at 4°C. Supernatants were used as a sample protein. Samples were separated through a SDS-polyacrylamide gel and transferred to nitrocellular membranes. Membranes were incubated with anti-STIM1, STIM2, Orai1, Orai2, and Orai3 antibodies (1:1,000), and followed by secondary antibody (1:4000) application. The immunoblots were detected with the ECL Western blotting detection reagents (Perkin-Elmer, Norton, OH). Band intensity quantified with ImageJ64, normalized to β-tubulin control, and expressed as arbitrary units.

4.4 Immunostaining

Cells were washed on ice three times with PBS. After fixing cells in 4% paraformaldehyde/PBS for 15 minutes at room temperature, coverslips were incubated in blocking solution (2% BSA, 2% FBS, 0.1% Triton X-100 in PBS) for 1 hour. Coverslips were then exposed to rabbit anti-$K_V1.5$ antibody (Alomone, 1:1000 in blocking solution) for 2 hours at room temperature. After washing cells with PBS, they were incubated with bovine anti-rabbit rhodamine-conjugated IgG antibody (Santa Cruz) for 45 minutes. Cells were also stained with DAPI (Invitrogen) to label nuclei. After washing again in PBS, coverslips were mounted onto glass slides using Fluoromount-G (Electron Microscopy Sciences) and visualized under appropriate fluorescent filters on an Olympus IX70 microscope. The SoftWoRx suite was used for deconvolution and image processing.

4.5 Measurement of Cytosolic Ca^{2+} Concentration

Cells on 25-mm cover slips were placed in a recording chamber on the stage of an inverted Nikon Eclipse/TE 200 microscope with the TE-FM epifluorescence attachment. Cytosolic Ca^{2+} concentration ($[Ca^{2+}]_{cyt}$) was measured in each cell using the membrane-permeable Ca^{2+}-sensitive fluorescent indicator, Fura-2-AM (Invitrogen). The cells were incubated at room temperature for 30 min in modified Krebs solution (MKS) containing 4 μM Fura-2-AM. The loaded cells were then washed with MKS for 30 min to remove excess extracellular dye and allow intracellular esterases to cleave cytosolic Fura-2-AM into active Fura-2. Fura-2 fluorescence was observed as 510-nm-wavelength light emission with excitation wavelengths of 340 and 380 nm by use of the digital fluorescence imaging system from Intracellular Imaging. In all experiments, multiple cells were imaged in a single field, and one arbitrarily chosen peripheral cytosolic area from each cell was spatially averaged. $[Ca^{2+}]_{cyt}$ was expressed as Fura-2 fluorescence emission ratio excited at 340 and 380 nm (F_{340}/F_{380}). Resting $[Ca^{2+}]_{cyt}$ was determined by the average F_{340}/F_{380} ratio during the initial MKS recording. The changes in $[Ca^{2+}]_{cyt}$ were calculated as the peak F_{340}/F_{380} minus the averaged steady state F_{340}/F_{380} ratio in the 20-sec preceding the initiation of the rise to peak. To ensure consistency all time periods in each condition were kept constant between experiments.

4.6 siRNA Mediated Knockdown of Orai and STIM

PASMC were transfected with siRNA against STIM2 (Santa Cruz sc-76589) or scramble siRNA (Santa cruz sc-37007) as control using the Amaxa Nucleofector electroporation system. 16 μL of a 10 μM solution of siRNA was used per 2 x 10^5 cells in each reaction. Transfected cells were cultured the following day and used for experiment after 48 hours.

4.7 Overexpression of Orai and STIM

Overexpression of STIM2 (pEX-CMV-SP-STIM2(15-746)) and Orai2 (pcDNA3.1 Orai2) was performed by the Amaxa Nucleofector electroporation system. The STIM2 and Orai2 plasmids was ordered from Addgene as provided by Dr. Meyer and Dr. Rao, respectively. pcDNA3.1 was used as the vector control. 48 hrs following transfection protein expression was examined or SOCE was measured or cell proliferation was determined by cell counting.

4.8 Chronic Hypoxic Treatement of Rat PASMC

Rat PASMC were isolated and cultured to passage one and then subjected to hypoxia. Hypoxia consisted of 48 hours of 3% O_2, 5% CO_2, and remainder N_2. Normoxia control consisted of room air supplemented with 5% CO_2.

Chapter 5. Results: Enhanced SOCE in IPAH Patient PASMC Increases $[Ca^{2+}]_{cyt}$ and Increases Proliferation.

5.1 IPAH patient PASMC have Enhanced SOCE Compared to NPH Control PASMC.

Increased cytosolic Ca^{2+} concentration has been shown to cause proliferation, migration, and contraction of PASMC, which are all believed to contribute to PAH phenotypes including hypoxia induced pulmonary hypertension and idiopathic pulmonary arterial hypertension[163,164]. Therefore the role of Ca^{2+} and the mechanisms that elevate Ca^{2+} concentration are of great importance to the study of the role of PASMC in IPAH. Previous research from our lab has shown that increased $[Ca^{2+}]_{cyt}$ and SOCE are important for contraction and proliferation of PASMC[32,62]. Furthermore, we found that IPAH-PASMC have higher resting $[Ca^{2+}]_{cyt}$ and enhanced SOCE compared to NPH-PASMC[165]. The first aim of this dissertation is to re-examine whether IPAH-PASMC have enhanced basal $[Ca^{2+}]_{cyt}$ and verify that these cells exhibit increased SOCE.

PASMC were isolated from IPAH lung transplant patient lung and secondary pulmonary hypertensive (SPH) patient lung or from normotensive (NPH) lung transplant patient as control. $[Ca^{2+}]_{cyt}$ was measured in IPAH patient PASMC and NPH patient PASMC using the Ca^{2+} binding dye fura-2. First we examined basal $[Ca^{2+}]_{cyt}$ in IPAH and control-PASMC. The control-PASMC (n = 18) and IPAH-PASMC (n = 7) were isolated from patients with similar mean pulmonary arterial pressures (48 ± 4 vs. 53 ± 4

mmHg, P = 0.30) and total vascular resistance (13.6 ± 3 vs. 11.2 ± 1.7 $mmHg^{-1}*min^{-1}$, P = 0.48). We observed that IPAH-PASMC had significantly higher resting or basal $[Ca^{2+}]_{cyt}$ compared to control cells (Figure 9, P < 0.01).

SOCE was determined by a store depletion, Ca^{2+} reintroduction protocol to measure both Ca^{2+} release from SR and Ca^{2+} influx through SOC. Change in $[Ca^{2+}]_{cyt}$ was measured as the ratio of F_{340}/F_{380} (F) and normalized to initial F_{340}/F_{380} ratio (F_0) measured in PASMC superfused with physiological salt solution (PSS). SOCE was induced by passive depletion of SR Ca^{2+} using 10 μM cyclopiazonic acid (CPA) in the absence of extracellular Ca^{2+} followed by re-addition of 1.8 mM extracellular Ca^{2+}. Consistent with our previously reported findings[166,167], IPAH-PASMC exhibited significantly larger (P=0.010) SOCE than NPH-PASMC (Figure 10).

The increased SOCE in IPAH-PASMC may be due to increased expression of serotonin in IPAH-PASMC. Serotonin (5-HT) activates serotonin receptor, which is a GPCR on the plasma membrane that when stimulated generates diacylglycerol and inositol triphosphate. DAG then opens ROC on the PM and mediates Ca^{2+} influx. IP_3 stimulates IP_3 receptor (IP_3R), which is a Ca^{2+} channel on the ER/SR membrane, to release Ca^{2+} from the ER/SR store. This leads to depletion of the ER/SR store and Ca^{2+} influx though SOC on the plasma membrane. In PASMC, 5-HT elicits oscillations in $[Ca^{2+}]_{cyt}$. Ca^{2+} oscillations are composed of Ca^{2+} release from the SR coupled with subsequent clearance of Ca^{2+} from the cytosol by reuptake (by SERCA) and extrusion (by PMCA). These oscillations generally have a set amplitude and frequency as the

expression level, activity, and sensitivity of the proteins and channels involved are fairly constant. 5-HT elicits Ca^{2+} oscillations in control or normal, PASMC within seconds of treatment, and the oscillations subside and $[Ca^{2+}]_{cyt}$ returns to baseline equally rapidly upon washout of 5-HT. In control or NPH-PASMC the amplitude of Ca^{2+} oscillations decrease over time (Figure 11). This indicates that the SR Ca^{2+} store is gradually becoming depleted due to an unmatched rate of filling compared to depletion. After the release phase some of the Ca^{2+} is extruded across the PM such that there is less Ca^{2+} in the cytosol for the re-uptake phase. Ideally, some measure of SOCE is activated by this transient store depletion and will refill the stores. However, 5-HT stimulation of NPH-PASMC overpowers the ability of SOCE to refill cytosolic Ca^{2+} in these cells (Figure 11).

The same dose of 5-HT also rapidly and reversibly elicited Ca^{2+} oscillations in IPAH-PAMSC. The Ca^{2+} oscillations have higher amplitude and increased frequency in IPAH-PASMC compared to control PASMC (Figure 11). Higher amplitude of Ca^{2+} release is indicative of increased $[Ca^{2+}]_{SR}$, and increased frequency of Ca^{2+} oscillations is indicative of increase expression, or activity, of IP_3R and SERCA. A larger number or increased activity of IP_3R and SERCA would enable increase rate of Ca^{2+} release and increased rate of Ca^{2+} re-uptake. While technically only one of which is necessary for increased frequency, the shape of the Ca^{2+} tracing would indicate that both are enhanced (Figure 11). The most important observation from 5-HT induced Ca^{2+} oscillations is that while control PASMC Ca^{2+} oscillations progressively decrease in amplitude, IPAH-PASMC Ca^{2+} oscillation amplitude is constant over a longer period of time (Figure 11). This, coupled with the observation that IPAH-PASMC have larger Ca^{2+} oscillations,

suggests that IPAH-PASMC have an increased capacity for SOCE. This increased capacity for SOCE may be due to enhanced sensitivity to store depletion and/or due to enhanced Ca^{2+} influx through SOC. Increase sensitivity to store depletion would be due to increase expression of STIM1/2 or increased activity of STIM1/2. Increased Ca^{2+} influx though SOC could be due to either enhanced expression of SOC (Orai or TRPC) or increased activity of SOC. In the following sections, we focus on whether the protein expression of STIM1/2 or Orai1/2/3 are increased in IPAH-PASMC. While whether the activity of STIM1/2 or Orai1/2/3 is enhanced in IPAH-PASMC is an interesting question, it is outside the focus of this dissertation. Albeit, discovery of a putative mutation in one of these genes that leads to increased activity and increased SOCE in IPAH-PASMC would be of landmark importance in diagnosis and potentially treatment of this disease.

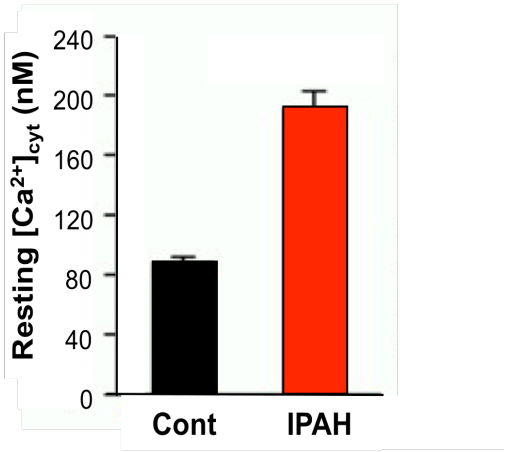

Figure 10: IPAH-patient PASMC have higher resting $[Ca^{2+}]_{cyt}$ than control PASMC (Cont). Summarized data showing resting $[Ca^{2+}]_{cyt}$ in PASMC from control patients (not pulmonary hypertensive, black bar) and IPAH-patients (red bar). Data are expressed as mean ± SE with the number of cells tested in parentheses. **P*<0.05, ****P*<0.001 vs. control PASMC as determined by Student's t-test.

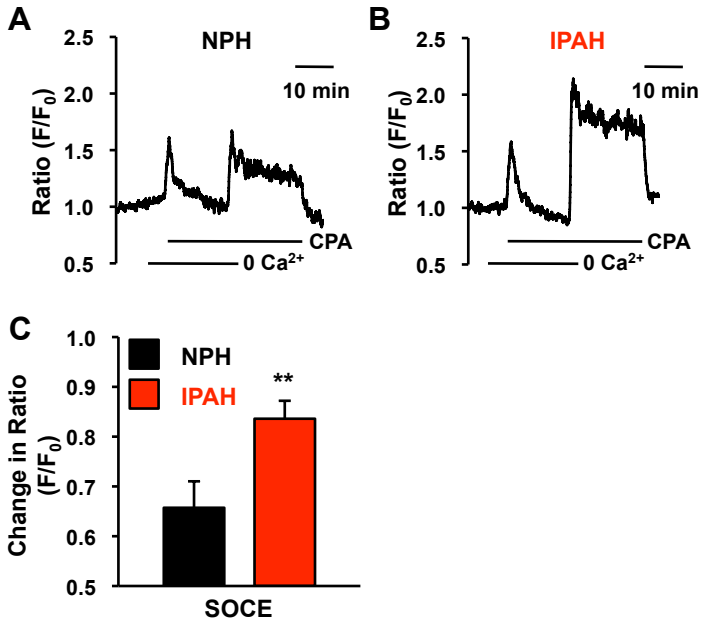

Figure 11: IPAH Patient PASMC exhibit Higher SOCE than NPH Patient PASMC. **A-B.** Representative records of $[Ca^{2+}]_{cyt}$ changes before, during and after application of 10 mM cyclopiazonic acid (CPA) in the absence or presence of external Ca^{2+} in normotensive NPH-PASMC (NPH, A), IPAH-PASMC (IPAH, B). **C.** Summary data (mean ± SE) showing the amplitude of CPA-induced SOCE in $[Ca^{2+}]_{cyt}$. ** $P < 0.01$ as determined by Student's t-test.

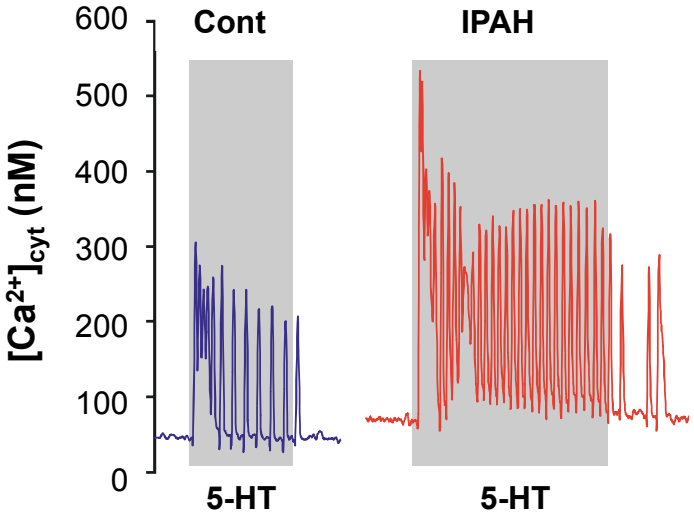

Figure 12: Serotonin elicits higher amplitude and frequency of Ca^{2+} oscillations in IPAH-PASMC compared to NPH-PASMC. Representative tracing showing effect of serotonin (5-HT) on $[Ca^{2+}]_{cyt}$ (nM) in IPAH patient PASMC and NPH subject PASMC (Cont). Serotonin causes Ca^{2+} oscillations, which are composed of cyclical Ca^{2+} release from the SR then Ca^{2+} re-uptake, in IPAH-PASMC and NPH-PASMC. However, in IPAH-PASMC 5-HT elicits greater amplitude and higher frequency of Ca^{2+} oscillations.

5.2 Inhibition of SOCE Decreases Proliferation and Contraction in PASMC.

Proliferation

In human PASMC chelation of extracellular Ca^{2+} and depletion of intracellular Ca^{2+} stores markedly inhibits cell proliferation in media containing serum and growth factors. Furthermore, basal $[Ca^{2+}]_{cyt}$ was significantly higher in proliferating cells than in growth-arrested cells[168]. As we have previously described, SOCE is a critical mechanism involved in maintaining $[Ca^{2+}]_{cyt}$ and $[Ca^{2+}]_{SR}$ through sustained Ca^{2+} influx and refilling of Ca^{2+} into the SR. Indeed, we observed that SOCE is significantly enhanced in proliferating PASMC compared to non-proliferating PASMC[63]. These results suggest that elevated $[Ca^{2+}]_{cyt}$ is necessary for human PASMC proliferation. Reduction of extracellular Ca^{2+} from 1.6 mM to 525 nM with the Ca^{2+} chelator EGTA significantly inhibits human and rat PASMC growth in media containing 10% FBS and growth factors. Furthermore, we found that Ni^{2+} a SOCE inhibitor decreases resting Ca^{2+} and proliferation of PASMC. Nifedipine, a non-selective Ca^{2+} channel inhibitor, together with Ni^{2+} had a slightly larger effect than Ni^{2+} alone in inhibiting resting Ca^{2+} and PASMC proliferation (Figure 13). These findings suggest that SOCE is mainly responsible for PASMC proliferation and that VDCE and ROCE play a smaller role. These data suggest that SOCE is the most important mechanism in elevating $[Ca^{2+}]_{cyt}$ and enhancing proliferation in PASMC.

In IPAH patient pulmonary arteries we observe increased thickness of the tunica media. Furthermore, intimal lesions in IPAH-PASMC are attributed in part to proliferation and migration of PASMC into the intima, which also leads to pulmonary hypertension. This increased thickness of the tunica media is due to pathologically enhanced proliferation of PASMC. Proliferation of control and IPAH patient PASMC was determined by counting cells at 0 hr (*i.e.*, two days after the cells are plated onto petri dishes) and 24, 48, and 72 hours later. At 0 hours, the control (NPH) PASMC group and IPAH-PASMC group had roughly the same number of cells (Figure 14A). After 72 hrs, the numbers of NPH-PASMC and IPAH-PASMC were both significantly increased (Figure 14A); however, the increase in IPAH-PASMC number was much greater than in NPH-PASMC (Figure 14B). Proliferation of PASMC is dependent on $[Ca^{2+}]_{cyt}$ and SOCE. And indeed IPAH patient PASMC exhibit elevated resting $[Ca^{2+}]_{cyt}$ (Figure 10), enhanced SOCE (Figure 11) and increase proliferation compared to NPH-PASMC (Figure 14).

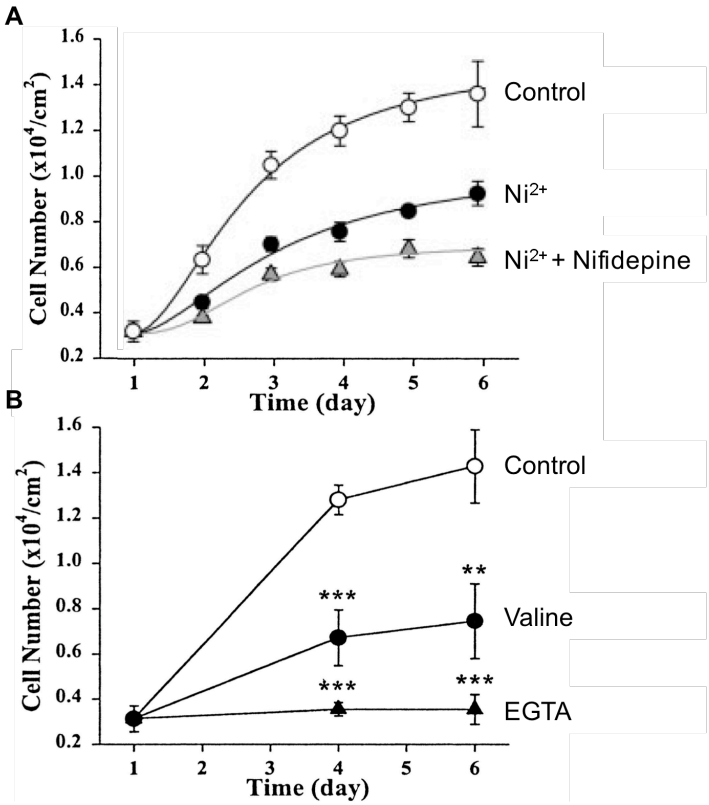

Figure 13: Inhibition of PASMC growth by chelation of extracellular Ca^{2+}. **A.** Cells were cultured in 10% FBS-DMEM in the absence (Control) and presence of 0.5 mM Ni^{2+} or 0.5 mM Ni^{2+} and 10 μM nifedipine. Viable cell numbers were determined every day for 6 days after cells were plated. **B.** Cells were cultured in 10% FBS-DMEM in the absence (Control) and presence of 2 mM EGTA or 100 mM valinomycin (Valine). Viable cell numbers were determined 1, 4, and 6 days after cells were plated. Data are means ± SE (n = 12 dishes of cells/group).

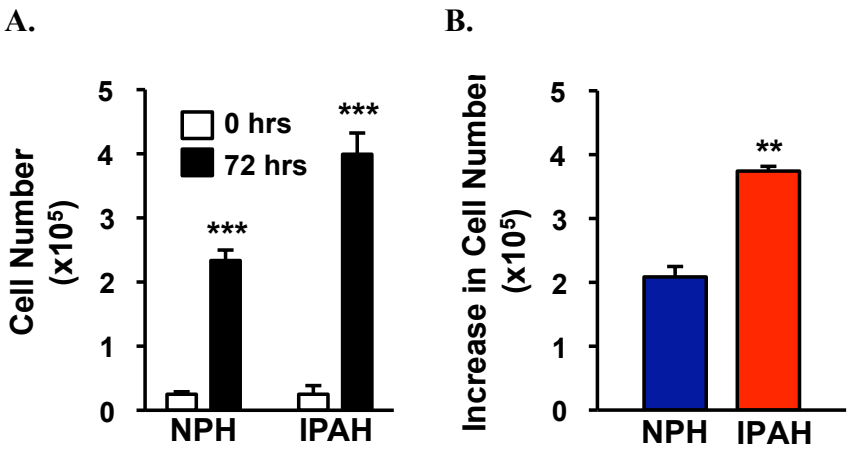

Figure 14: IPAH-patient PASMC have enhanced proliferation compared to NPH-PASMC. A. Summary data (mean ± SE) showing cell numbers for NPH-PASMC and IPAH-PASMC at 0 hours (0 hrs) and after 72 hrs of culture in growth media. *** $P<0.001$ vs. 0 hr. as determined by Student's t-test. **B.** Summary data showing the increase in cell numbers after 72 hrs in NPH-PASMC (blue) and IPAH-PASMC (red). ** $P<0.01$ vs. NPH as determined by Student's t-test. IPAH patient PASMC showed a significantly greater increase in cell number after 72 hours compared to NPH-PASMC.

Contraction

An increase in $[Ca^{2+}]_{cyt}$ in PASMC is a major trigger for pulmonary vasoconstriction. In isolated rat PA rings, removal of extracellular Ca^{2+} almost completely abolished the active tension induced by 40 mM K^+ or 2 mM Phenylepherine (PE) (Figure 15). Chelation of extracellular Ca^{2+} with 2 mM EGTA, which decreases free Ca^{2+} concentration to ~0.5 mM in MKS containing 1.8 mM $CaCl_2$ had the same inhibitory effects on contractions induced by 40 mM K^+ or PE (Figure 15). Furthermore, extracellular application of SOCE inhibitors Ni^{2+} or La^{3+} significantly inhibited prolonged PA constriction induced by PE[62]. This suggests that SOCE is an important mechanism in PA constriction.

An increase in $[Ca^{2+}]_{cyt}$ in PAEC stimulates nitric oxide (NO) synthesis and release, thereby causing PA relaxation[164]. Removal of the endothelium in isolated rat PA rings allows for the examination of the role of PASMC alone on PA vasoconstriction. Ni^{2+} and La^{3+} have been demonstrated to block SOC in many cell types. Indeed, extracellular application of Ni^{2+} (1 mM) or La^{3+} (50 mM) significantly and reversibly attenuated the SOCE-mediated PA contraction. These results indicate that Ca^{2+} release from the SR and influx though SOC both contribute to agonist mediated pulmonary vasoconstriction[62].

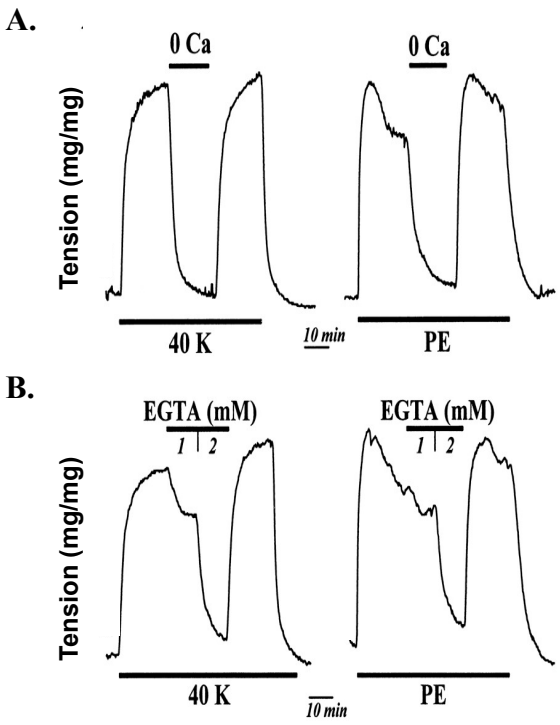

Figure 15: Extracellular Ca^{2+} is required for pulmonary vasoconstriction induced by 40 mM K^+ (40 K) and phenylephrine (PE). **A**. Representative tracings showing isolated pulmonary artery ring tension (tension in milligrams normalized to milligrams of tissue weight) induced by 40 K or 2 mM PE. Ca^{2+}-free solution was applied to the vessels when 40 mM K^+- or PE-mediated contraction reached a plateau. Extracellular Ca^{2+} is necessary for 40 K and PE induced PA vasoconstriction. **B**. Representative tracings showing isolated pulmonary artery ring tension (tension in milligrams normalized to milligrams of tissue weight) induced by 40 K or 2 mM PE. 1 or 2 mM EGTA was applied to the vessels when 40 mM K^+ or PE-mediated contraction, respectively, reached a plateau. Extracellular Ca^{2+} is necessary for 40 K and PE induced PA vasoconstriction.

5.3 Summary and Discussion

5.3.1 Summary

IPAH patient PASMC have higher resting $[Ca^{2+}]_{cyt}$ than control or NPH-PASMC. Higher resting $[Ca^{2+}]_{cyt}$ can be attributed to many mechanisms that regulate $[Ca^{2+}]_{cyt,}$ which include SOCE. IPAH patient PASMC exhibit enhanced SOCE compared to NPH-PASMC, therefore SOCE is likely an important mechanism in elevating $[Ca^{2+}]_{cyt}$ in IPAH-PASMC. IPAH-PASMC also exhibit pathogenically increased proliferation and contraction compared to NPH-PASMC, which leads to increased PA vasoconstriction and increased PVR and pulmonary hypertension. Ca^{2+} is necessary for both PASMC contraction and proliferation. And, Ca^{2+} is necessary for endothelium independent PA vasoconstriction, which is mediated by contraction of PASMC. $[Ca^{2+}]_{cyt}$ and enhanced SOCE are shown to be important for PASMC proliferation. And, SOCE can increase $[Ca^{2+}]_{cyt}$ independent of VDCC and ROC.

5.3.2 Discussion

Pathogenesis of IPAH is, at least in part, due to increased $[Ca^{2+}]_{cyt}$ in PASMC. Increased $[Ca^{2+}]_{cyt}$ in IPAH-PASMC causes increased proliferation and contraction of these cells, which leads to decreased radius of PA. This then increases the PVR and leads to PAH. Many mechanisms can increase the $[Ca^{2+}]_{cyt}$ in IPAH-PASMC, in this section we showed that SOCE is the most important mechanism in this regard. We showed that SOCE is significantly enhanced in IPAH-PASMC compared to NPH-PASMC. We also directly linked SOCE to PASMC proliferation and to PA contraction by demonstrating that inhibition of SOCE mitigated PASMC proliferation and mitigated vasoconstriction of endothelium free PA. Furthermore, inhibition of SOCE had a more significant effect on PASMC proliferation and PA vasoconstriction than other mechanism such as VDCE and ROCE. However, it is unclear how the molecular components that mediate SOCE, STIM and Orai, are involved in IPAH associated pathogenic increase in SOCE. We aim to explore this question in the following sections.

Chapter 5, in part, has been submitted for publication of the material as it may appear in Pulmonary Circulation, 2011, Song, MY; Makino, A, Yuan JX or in Antioxidants and Redox Signaling, 2011, Song, MY; Makino, A, Yuan JX. The dissertation author was the primary investigator and author of these papers.

Chapter 6. Results: STIM and Orai Protein Expression in PASMC from Chronic Hypoxia Treated Rat PASMC and IPAH-PASMC

6.1 All the Isoforms of STIM and Orai are Expressed in Human and Rat PASMC

Increased pulmonary vascular resistance, due to sustained vasoconstriction, vascular remodeling, *in situ* thrombosis and increased vascular wall stiffness, is the major cause for elevated pulmonary arterial pressure in patients with pulmonary arterial hypertension (PAH)[169,170]. Pulmonary angiograms show that patients with idiopathic pulmonary arterial hypertension (IPAH) and hypoxia-induced pulmonary hypertension (HPH) had significantly decreased blood flow to small and medium-sized pulmonary arteries. Decreased blood flow to small and medium-sized pulmonary arteries results mainly from a decrease in the diameter of the artery lumen as a result of sustained pulmonary vasoconstriction and vascular remodeling, two major causes for leading to increased pulmonary vascular resistance and pulmonary hypertension. HPH and IPAH share many pathological and histological traits such as concentric vascular remodeling and medial hypertrophy. In fact, rats subjected to chronic hypoxia are used as an *in vivo* model for studying pathogenic and therapeutic mechanisms of pulmonary arterial hypertension, and rat PASMC treated with hypoxia is a common *in vitro* model for studying cellular and molecular sequences of events involved in pulmonary vascular remodeling. Pulmonary vascular remodeling due to excessive proliferation of PASMC and vasoconstriction due to contraction of PASMC greatly contribute to the elevated pulmonary vascular resistance in patients and animals with IPAH and HPH.

An increase in cytosolic Ca^{2+} concentration ($[Ca^{2+}]_{cyt}$) in PASMC is a major trigger for pulmonary vasoconstriction and an important stimulus for cell proliferation and migration that contribute to the pulmonary vascular remodeling. Removal of extracellular Ca^{2+} or reduction of extracellular free $[Ca^{2+}]$ with the Ca^{2+} chelator (*e.g.*, EGTA and EDTA) not only significantly inhibits agonist-induced vasoconstriction in isolated pulmonary arterial rings, but also significantly attenuates PASMC proliferation when cultured in growth factor-including media[63]. Blockade of Ca^{2+} influx and depletion of intracellular Ca^{2+} stores in the sarcoplasmic reticulum or endoplasmic reticulum both attenuate PASMC contraction and proliferation[63]. Our preliminary studies show that the resting $[Ca^{2+}]_{cyt}$ is increased and agonist-induced rise in $[Ca^{2+}]_{cyt}$ are significantly enhanced in patients with IPAH in comparison to normotensive control subjects[149]. Furthermore, chronic hypoxia also increases $[Ca^{2+}]_{cyt}$ in PASMC[71,171]. Therefore, increased proliferation and contraction of PASMC in IPAH and HPH patients are likely related to the increase in $[Ca^{2+}]_{cyt}$ and enhancement of the mechanisms that mediate Ca^{2+} influx.

Store-operated Ca^{2+} entry (SOCE) is an important mechanism that mediates Ca^{2+} influx and raises $[Ca^{2+}]_{cyt}$ when intracellular stores are depleted by agonist- or ligand-induced Ca^{2+} mobilization[15,172]. Depletion of intracellular Ca^{2+} stores, predominantly the sarcoplasmic reticulum in PASMC, activates Ca^{2+} influx through store-operated Ca^{2+} channels expressed on the plasma membrane. STIM isoforms, which include two isoforms STIM1 and STIM2, are single transmembrane proteins that have been identified as the sensor of store depletion[114,173]. STIM1 and STIM2 are expressed on the SR

membrane and on the plasma membrane of PASMC. An EF-hand domain near the N-terminus of STIM1 and of STIM2 serves as the sensor of Ca^{2+} concentration in the SR lumen. STIM1 and STIM2 are locked in an inactive conformation when Ca^{2+} is bound to the EF-hand domain, but when Ca^{2+} is depleted in the SR the conformation of STIM1 and STIM2 changes to their active conformation[118,173]. The active STIM1 and STIM2 can oligomerize, translocate along the SR membrane to the pucta area close to the plasma membrane, activate store-operated Ca^{2+} channels, and elicit SOCE. In HEK cells, overexpression of STIM1 can reconstitute a robust inwardly rectifying Ca^{2+} current following store depletion[174]. Similar studies have shown that STIM2 can reconstitute SOCE in the absence of STIM1, though at a lower magnitude of Ca^{2+} influx[84,86]. While STIM2 has lower activity in activating Ca^{2+} channels (or store-operated Ca^{2+} channels) on the plasma membrane, it is more sensitive to small changes in Ca^{2+} concentration[175,176].

Preliminary data from our group and others indicate that receptor-operated and store-operated Ca^{2+} entry both play an important role in normal PASMC proliferation and migration[26,63]. Inhibition of SOCE with, for example, Ni^{2+}, 1-[β-[3-(4-methoxyphenyl)pro-poxy]-4-methoxyphenethyl]-1H-imidazole hydrochloride (SKF96365), or La^{3+} markedly attenuates PASMC proliferation[16,149,177,178]. Furthermore, CPA induced SOCE is significantly enhanced in IPAH-PASMC, and mRNA and protein expression of TRPC channels are upregulated in IPAH-PASMC in comparison to normotensive controls[72,167]. While we know that upregulated TRPC channels (*e.g.*, TRPC3 and TRPC6) contribute to the enhanced SOCE in IPAH-PASMC, it is unknown whether the recently discovered components of SOCE STIM1 and STIM2 and Orai1,

Orai2 and Orai3 are also involved in enhanced SOCE in IPAH-PASMC. Specifically, it is unclear which isoforms are expressed in human PASMC and whether protein expression level of the expressed isoforms is changed in IPAH patient PASMC compared to NPH-PASMC.

Western blot analysis was performed on lysed samples of human and rat PASMC. All isoforms of STIM and Orai were found to be expressed in human and rat PASMC (Figure 16). These data taken along with the fact the IPAH patient PASMC demonstrate higher SOCE suggest that some or all the isoforms of STIM and/or Orai are important in IPAH patient associated elevation of SOCE. Next we examined whether the protein expression level of STIM1/2 and/or Orai1/2/3 are changed in IPAH patient PASMC compared to NPH patient cells. And whether chronic hypoxia alters the protein expression level of STIM1/2 and/or Orai1/2/3 in rat PASMC.

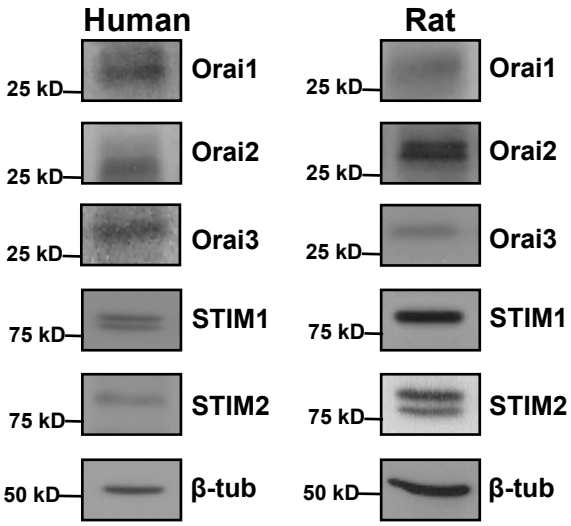

Figure 16: All Isoforms of STIM and Orai are Expressed in PASMC. Western blot analyses for Orai1, Orai2, Orai3, STIM1 and STIM2 in human and rat PASMC. β-tubulin (β-tub) was used as a loading control.

6.2 STIM1 Protein Expression Level in PASMC from Chronic Hypoxia Treated Rat PASMC and IPAH-PASMC

Chronic hypoxia causes pulmonary hypertension by increasing PASMC proliferation, migration and contraction through a Ca^{2+}-dependent mechanism[179,180]. Chronic hypoxia has been reported to inhibits K_V channels, causes membrane depolarization, opens voltage-gated Ca^{2+} channels and increase $[Ca^{2+}]_{cyt}$ in PASMC by increasing Ca^{2+} influx through voltage-gated Ca^{2+} channels[180]. Chronic hypoxia has also been shown to upregulate TRPC channels in rat PASMC and increase $[Ca^{2+}]_{cyt}$ via enhanced receptor-operated and store-operated Ca^{2+} influx[71,171,181-183]. As previously discussed STIM1 is known to mediate SOCE in a variety of cell types. To investigate whether upregulation of STIM1 is involved in hypoxia-mediated pulmonary vasoconstriction and vascular remodeling, we treated rat PASMC with hypoxia (P_{O2} = 22 mmHg for 48 hrs) and examined protein expression level of STIM1; in these experiments, we used β-tubulin as a loading control. Utilizing our *in vitro* rat model of PAH, we found that STIM1 was not increased following hypoxia (Figure 17). Therefore, enhanced SOCE in hypoxia treated rat PASMC was not due to increased protein expression of STIM1.

As previously described, PASMC from IPAH patients show enhanced SOCE compared to control PASMC[166,167,177,184]. However it is unknown whether the expression level of the proteins that mediate SOCE are altered in PASMC from IPAH patients. PASMC were isolated and cultured either from normotensive control subjects (NPH-

PASMC) or patients with IPAH (IPAH-PASMC). Protein levels of STIM1 were examined in IPAH-PASMC and NPH-PASMC whole cell lysate. In order to compare the protein expression levels of STIM1 between IPAH-PASMC and NPH-PASMC, we measured protein concentration in whole cell lysates and standardized protein loading with β-tubulin as a loading control. There was no significant morphological difference between NPH-PASMC and IPAH-PASMC. We found that IPAH-PASMC had significantly less protein expression levels of STIM1 compared to NPH-PASMC (Figure 18).

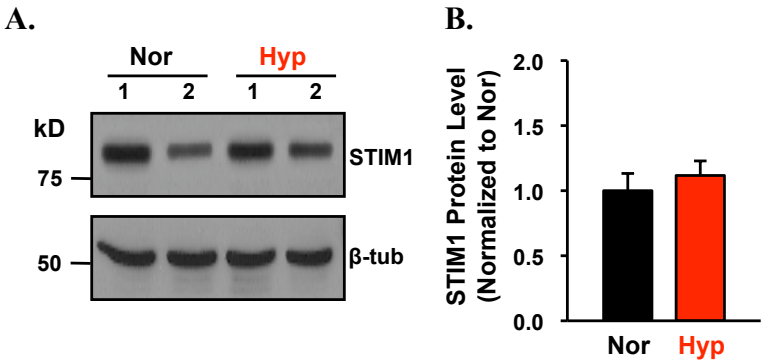

Figure 17: STIM1 protein expression is not increased in hypoxia treated PASMC. **A.** Representative western blot analyses for STIM1 protein in normoxia (room air supplemented with 5% CO_2) and hypoxia (3% O_2, 5% CO_2, balance N_2) treated PASMC. β-tubulin (β-tub) was used as a loading control. **B.** Averaged data comparing protein expression level of STIM1 between normoxia and hypoxia treatments. Values are normalized to average normoxia level. Hypoxia does not significantly alter protein expression of STIM1 in rat PASMC. Significance was calculated using Student's t-test.

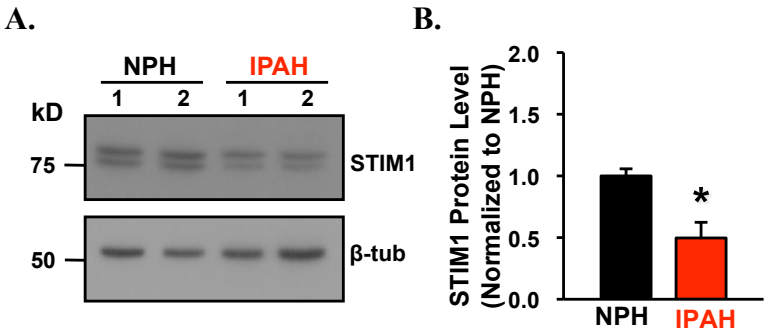

Figure 18: STIM1 protein expression is decreased in IPAH-patient PASMC. A: Representative western blot analyses for STIM1 protein in PASMC isolated from IPAH patient lung tissue or normotensive control patient lung tissue (NPH). β-tubulin (β-tub) was used as a loading control. **B:** Averaged data comparing protein expression level of STIM1 between IPAH and NPH PASMC. Values are normalized to average NPH level. * $P < 0.05$, ** $P < 0.01$, *** $P < 0.001$ vs. NPH. Significance was calculated using Student's t-test.

6.3 STIM2 Protein Expression Level in PASMC from Chronic Hypoxia Treated Rat PASMC and IPAH-PASMC

IPAH patient PASMC demonstrate significantly enhanced SOCE compared to NPH patient cells. And, all the isoforms of STIM and Orai, which are the protein component of SOCE, are expressed in IPAH and NPH patient PASMC. While much work has been done to link STIM1 with SOCE, STIM2 has also been shown to be able to reconstitute SOCE and to serve a similar purpose as STIM1[185]. Structurally STIM2 and STIM1 are very similar[186]. Therefore, we used western blot analysis to determine whether STIM2 protein expression level was increased in IPAH-PASMC over NPH-PASMC. PASMC were isolated and cultured either from normotensive control subjects or patients with IPAH. In order to compare protein expression level of STIM2 between IPAH-PASMC and NPH-PASMC, we measured protein concentration in whole cell lysates and standardized protein loading with β-tubulin as a loading control. Western blot analysis showed STIM2 was increased in IPAH-PASMC compared to NPH-PASMC (Figure 19). These data suggest that enhanced SOCE in IPAH patient PASMC may be due to increased protein expression of STIM2.

In order to investigate whether upregulation of STIM2 is also involved in hypoxia-mediated pulmonary vasoconstriction and vascular remodeling, we treated rat PASMC with hypoxia (P_{O2} = 22 mmHg for 48 hrs) and examined protein expression level of STIM2; in these experiments, we used β-tubulin as a loading control. Western blot analysis showed that STIM2 expression was increase in rat PASMC following

hypoxia (Figure 20). These data suggest that hypoxia enhanced SOCE in PASMC may be due to increased protein expression of STIM2.

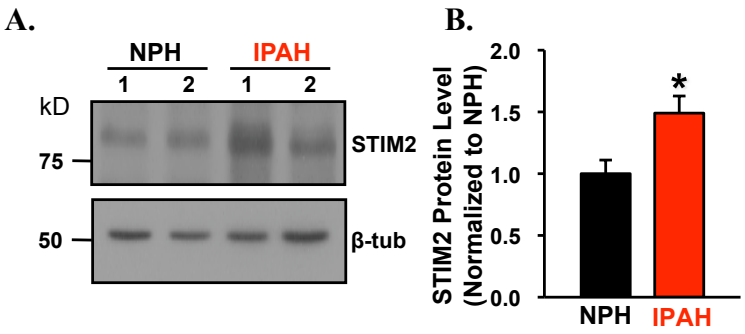

Figure 19: STIM2 protein expression is increased in IPAH patient PASMC. A. Representative western blot analyses for STIM2 protein in PASMC isolated from IPAH patient lung tissue or normotensive control patient lung tissue (NPH). β-tubulin (β-tub) was used as a loading control. **B.** Averaged data comparing protein expression level of STIM2 between IPAH and NPH PASMC. Values are normalized to average NPH level. * $P < 0.05$, ** $P < 0.01$, *** $P < 0.001$ vs. NPH. Significance was calculated using Student's t-test.

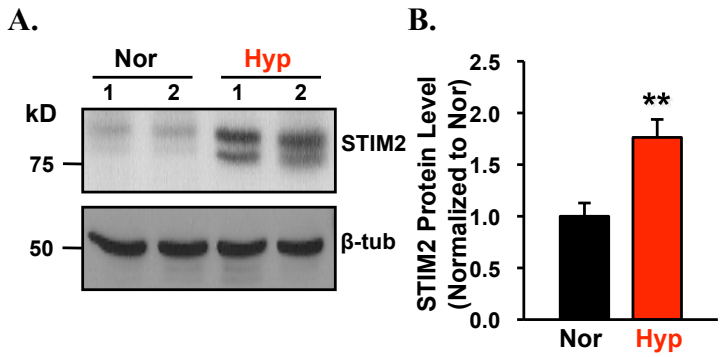

Figure 20: STIM2 protein expression is increased in hypoxia treated PASMC. A. Representative western blot analyses for STIM2 protein in normoxia (room air supplemented with 5% CO_2) and Hypoxia (3% O_2, 5% CO_2, balance N_2) treated PASMC. β-tubulin (β-tub) was used as a loading control. **B.** Averaged data comparing protein expression level of STIM2 between normoxia and hypoxia treatments. Values are normalized to average normoxia level. * $P < 0.05$, ** $P < 0.01$, *** $P < 0.001$ vs. Nor. Significance was calculated using Student's t-test.

6.4 Orai1 Protein Expression Level in PASMC from Chronic Hypoxia Treated Rat PASMC and IPAH-PASMC

IPAH patient PASMC demonstrate significantly enhance SOCE compared to NPH patient PASMC. And, all the isoforms of STIM and Orai, which are the protein component of SOCE, are expressed in PASMC. Much work has been done to link Orai1 with SOCE[82]. Tetramers of Orai1 form functional SOC[187]. We used western blot analysis to determine whether Orai1 protein expression level was different between IPAH patient PASMC and NPH patient PASMC. Western blot analysis showed that Orai1 protein expression level was not significantly different between IPAH and NPH patient PASMC (Figure 21). These data suggest that enhanced SOCE in IPAH patient PASMC are not due to increased protein expression of Orai1.

In order to investigate whether upregulation of Orai1 is involved in hypoxia-mediated pulmonary vasoconstriction and vascular remodeling, we treated rat PASMC with hypoxia (P_{O2} = 22 mmHg for 48 hrs) and examined protein expression level of STIM2; in these experiments, we used β-tubulin as a loading control. Western blot analysis showed that Orai1 expression was increased in rat PASMC following hypoxia (Figure 22). These data suggest that hypoxia enhanced SOCE in PASMC may be due to increased protein expression of Orai1.

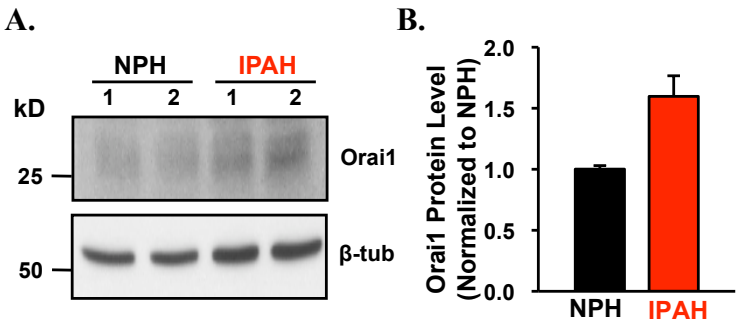

Figure 21: Orai1 protein expression is not increased in IPAH patient PASMC. A. Representative western blot analyses for Orai1 protein in PASMC isolated from IPAH patient lung tissue or normotensive control patient lung tissue (NPH). β-tubulin (β-tub) was used as a loading control. **B.** Averaged data comparing protein expression level of Orai1 between IPAH and NPH PASMC. Values are normalized to average NPH level. Hypoxia does not significantly alter protein expression of Orai1 in rat PASMC. Significance was calculated using Student's t-test.

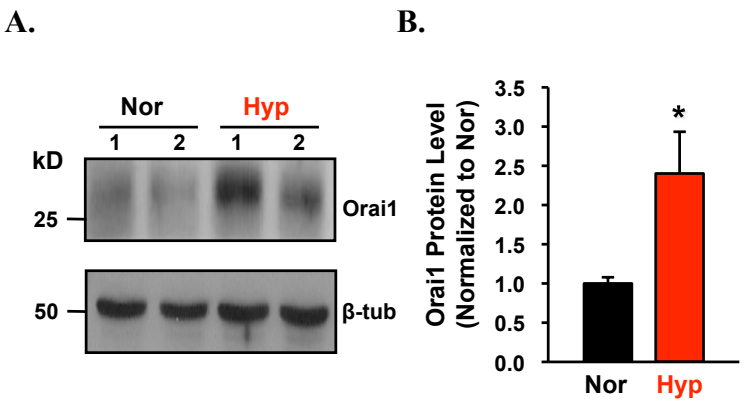

Figure 22: Orai1 protein expression is increased in hypoxia treated PASMC. A. Representative western blot analyses for Orai1 protein in normoxia (room air supplemented with 5% CO_2) and Hypoxia (3% O_2, 5% CO_2, balance N_2) treated PASMC. β-tubulin (β-tub) was used as a loading control. **B.** Averaged data comparing protein expression level of Orai1 between normoxia and hypoxia treatments. Values are normalized to average normoxia level. * $P < 0.05$, ** $P < 0.01$, *** $P < 0.001$ vs. Nor. Significance was calculated using Student's t-test.

6.5 Orai2 Protein Expression Level in PASMC from Chronic Hypoxia Treated Rat PASMC and IPAH-PASMC

IPAH patient PASMC demonstrate significantly enhance SOCE compared to NPH patient PASMC. And, all the isoforms of STIM and Orai, which are the protein component of SOCE, are expressed in PASMC. We used western blot analysis to determine whether Orai2 protein expression level was different between the IPAH patient PASMC and NPH patient PASMC. Western blot analysis showed that Orai2 protein expression level was significantly increased in IPAH-PASMC compared to NPH-PASMC (Figure 23). These data suggest that enhanced SOCE in IPAH-PASMC may be due to increased protein expression of Orai2.

To investigate whether upregulation of Orai2 is also involved in hypoxia-mediated pulmonary vasoconstriction and vascular remodeling, we treated rat PASMC with hypoxia (P_{O2} = 22 mmHg for 48 hrs) and examined protein expression level of Orai2; in these experiments, we used β-tubulin as a loading control. Western blot analysis showed that Orai2 expression was increased in rat PASMC following hypoxia (Figure 24). These data suggest that hypoxia enhanced SOCE in PASMC may be due to increased protein expression of Orai2.

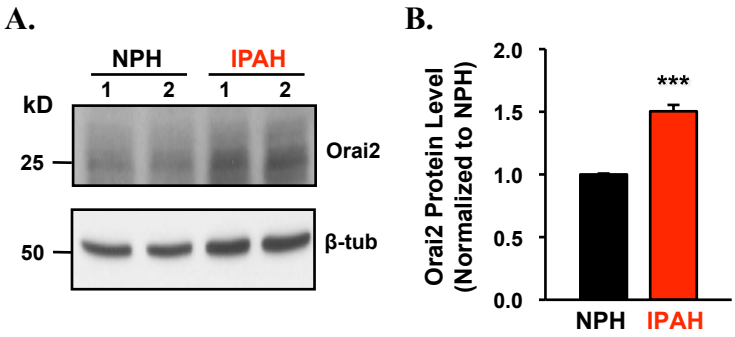

Figure 23: Orai2 protein expression is increased in IPAH patient PASMC. A. Representative western blot analyses for Orai2 protein in PASMC isolated from IPAH patient lung tissue or normotensive control patient lung tissue (NPH). β-tubulin (β-tub) was used as a loading control. **B.** Averaged data comparing protein expression level of Orai2 between IPAH and NPH PASMC. Values are normalized to average NPH level. * $P < 0.05$, ** $P < 0.01$, *** $P < 0.001$ vs. NPH. Significance was calculated using Student's t-test.

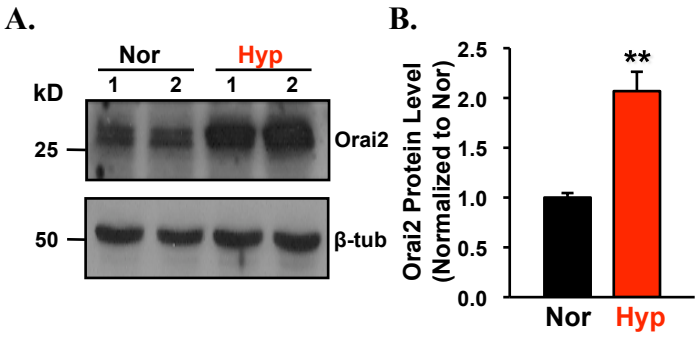

Figure 24: Orai2 protein expression is increased in hypoxia treated PASMC. A. Representative western blot analyses for Orai2 protein in normoxia (room air supplemented with 5% CO_2) and hypoxia (3% O_2, 5% CO_2, balance N_2) treated PASMC. β-tubulin (β-tub) was used as a loading control. **B.** Averaged data comparing protein expression level of Orai2 between normoxia and hypoxia treatments. Values are normalized to average normoxia level. * $P < 0.05$, ** $P < 0.01$, *** $P < 0.001$ vs. Nor. Significance was calculated using Student's t-test.

6.6 Orai3 Protein Expression Level in PASMC from Chronic Hypoxia Treated Rat PASMC and IPAH-PASMC

IPAH patient PASMC demonstrate significantly enhance SOCE compared to NPH patient PASMC. And, all the isoforms of STIM and Orai, which are the protein component of SOCE, are expressed in PASMC. We used western blot analysis to determine whether Orai3 protein expression level was different between IPAH patient PASMC and NPH patient PASMC. Western blot analysis showed that Orai3 protein expression level was not significantly different between IPAH and NPH patient PASMC (Figure 25). These data suggest that enhanced SOCE in IPAH patient PASMC is not due to increased protein expression of Orai3.

To investigate whether upregulation of Orai3 is also involved in hypoxia-mediated pulmonary vasoconstriction and vascular remodeling, we treated rat PASMC with hypoxia (P_{O2} = 22 mmHg for 48 hrs) and examined protein expression level of Orai3; in these experiments, we used β-tubulin as a loading control. Western blot analysis showed that Orai3 expression was not increase in rat PASMC following hypoxia (Figure 26). These data suggest that hypoxia enhanced SOCE in PASMC is not due to increased protein expression of Orai3.

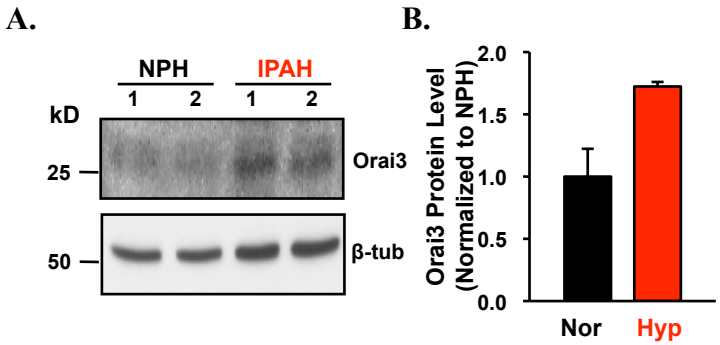

Figure 25: Orai3 protein expression is not increased in IPAH patient PASMC. A. Representative western blot analyses for Orai3 protein in PASMC isolated from IPAH patient lung tissue or normotensive control patient lung tissue (NPH). β-tubulin (β-tub) was used as a loading control. **B.** Averaged data comparing protein expression level of Orai3 between IPAH and NPH-PASMC. Values are normalized to average NPH level. * $P < 0.05$, ** $P < 0.01$, *** $P < 0.001$ vs. NPH. Significance was calculated using Student's t-test.

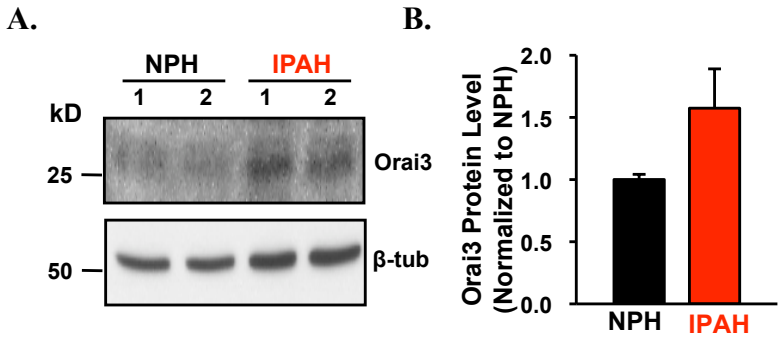

Figure 26: Orai3 protein expression is not increased in hypoxia treated PASMC. A. Representative western blot analyses for Orai3 protein in normoxia (room air supplemented with 5% CO_2) and Hypoxia (3% O_2, 5% CO_2, balance N_2) treated PASMC. β-tubulin (β-tub) was used as a loading control. **B.** Averaged data comparing protein expression level of Orai3 between normoxia and hypoxia treatments. Values are normalized to average normoxia level. * $P < 0.05$, ** $P < 0.01$, *** $P < 0.001$ vs. Nor. Significance was calculated using Student's t-test.

6.7 Summary and Discussion

6.7.1 Summary

Protein levels of STIM1, STIM2, Orai1, Orai2 and Orai3 were examined in IPAH-PASMC and NPH-PASMC whole cell lysate. In order to compare the protein expression level of these proteins between IPAH-PASMC and NPH-PASMC, we measured protein concentration in whole cell lysates and standardized protein loading with β-tubulin as a loading control. Surprisingly, STIM1 protein expression level was significantly decreased in IPAH-PASMC compared to NPH-PASMC. The protein expression level of STIM2, however, was significantly upregulated in IPAH-PASMC compared to NPH-PASMC. These data suggest that STIM2, rather than STIM1, may be important in enhancing SOCE in PASMC from IPAH patients. Neither Orai1 nor Orai3 were significantly upregulated in IPAH-PASMC. Orai2 protein expression level, however, was significantly increased in IPAH-PASMC compared to NPH-PASMC.

In order to investigate the effect of hypoxia on STIM1, STIM2, Orai1, Orai2 and Orai3 protein expression we treated rat PASMC with hypoxia (P_{O2} = 22 mmHg for 48 hrs) and examined the protein expression levels compared to normoxia treated rat PASMC. Corroborating to our findings in IPAH-PASMC, chronic hypoxia significantly upregulated Orai2 and STIM2 protein expression levels in rat PASMC. STIM1 and

Orai3 protein expression level was unchanged in PASMC subjected to hypoxia. Orai1 protein expression level was increased in PASMC subjected to hypoxia.

6.7.2 Discussion

In the literature there is much evidence that STIM1 serves as the predominant sensor of store depletion. Overexpression of STIM1 has been shown to enhance SOCE while knockdown of STIM1 decreases SOCE in several cell types[173]. We originally hypothesized that increased protein expression of STIM1 is responsible for elevated SOCE in IPAH patient PASMC and hypoxia enhanced SOCE in rat PASMC. However, western blot analysis showed that protein expression of STIM1 was not increased, but rather decreased, in either IPAH patient PASMC. Furthermore, we discovered that STIM2 and Orai2 protein expression levels were both increased in hypoxia treated rat PASMC.

Lu *et al*. also demonstrated the presence of SOCE and protein expression of STIM and Orai in PASMC[171]. These researchers measured intracellular Ca^{2+} and SOCE in primary cultures of rat PASMC using fluorescent microscopy and the Ca^{2+}-sensitive dye fura-2. They also found that hypoxia (4% O_2) and KCl (60 mM) increased $[Ca^{2+}]_{cyt}$. They then used cyclopiazonic acid to deplete Ca^{2+} stores in the SR and nifedipine to prevent Ca^{2+} entry through L-type voltage-operated Ca^{2+} channels. Under these conditions, the increase in $[Ca^{2+}]_{cyt}$ caused by restoration of extracellular Ca^{2+} and the decrease in fura-2 fluorescence caused by Mn^{2+} quenching were greater in distal PASMC, indicating greater SOCE in distal PA PASMC. Real-time quantitative polymerase chain reaction analysis of PASMC demonstrated expression of STIM1 and STIM2 and five of seven known TRPC isoforms (TRPC1 > TRPC6 > TRPC4 >> TRPC3 ≈ TRPC5). For both protein and mRNA, expression of STIM1, TRPC1, TRPC6, and TRPC4 was greater

in distal than proximal PASMC and PA. These results confirm our own findings that STIM1 and STIM2 are both expressed in PASMC. Furthermore, both STIM1 and STIM2 are expressed in distal PA, which are the arteries involved in vasoconstriction and in IPAH.

Our data suggests that STIM2 rather than STIM1 is the important isoform of STIM in IPAH-PASMC. Berna-Erro *et al*. assessed STIM abundance in mouse brain by Western blot analysis and obtained a clear signal for STIM2, whereas STIM1 was only weakly detectable[188]. Furthermore, immunocytochemical analysis revealed hardly any signal for STIM1 in cultured hippocampal neurons, whereas strong perinuclear staining was detected with antibodies directed against STIM2, consistent with its expected ER localization[188]. In contrast, in T cells the ratio of STIM1 to STIM2 abundance was reversed with STIM1 as the predominantly expressed isoform[189]. RT-PCR analysis of primary hippocampal neurons confirmed that STIM2 was the predominant member of the STIM family present[188]. STIM1 and Orai1 and Orai3 mRNA was weakly expressed in neurons, whereas Orai2 was strongly expressed in these cells[188]. These data demonstrate another cell type where STIM2 and Orai2, rather than STIM1 and Orai1, are the predominant mediators of SOCE.

These researchers tested the effect of STIM2 deficiency on neuronal Ca^{2+} homeostasis directly by performing Ca^{2+} imaging experiments in neuronal cultures extracted from cortical tissue[188]. They found that SOCE was reduced in *STIM2*$^{-/-}$ neurons, which are isolated for STIM2 knockout mice, compared to that in wild-type

controls. Furthermore, knockdown of STIM1 or Orai1 in $STIM2^{-/-}$ neurons did not decrease SOCE compared to control $STIM2^{-/-}$ neurons. Therefore, SOCE in mouse neurons is regulated by STIM2 and does not require STIM1 or Orai1. Furthermore, $STIM2^{-/-}$ neurons had lower basal $[Ca^{2+}]_{cyt}$ than did wild-type neurons, whereas no such difference was seen in $STIM1^{-/-}$ and $Orai1^{-/-}$ neurons[188]. This finding corroborates Brandman *et al.'s* theory, that based on the increased sensitivity of STIM2 over STIM1 to Ca^{2+}, STIM2's role is more important in the regulation of basal $[Ca^{2+}]_{cyt}$[190]. Berna-Erro *et al*. also found that the peak amplitude of Ca^{2+} release was decreased in $STIM2^{-/-}$ neurons compared to that in control, whereas the subsequent Ca^{2+} entry after re-addition of extracellular Ca^{2+} was indistinguishable[188]. This observation is consistent with the notion that STIM2 regulates store refilling, as well as the basal cytosolic Ca^{2+} concentration in neurons by sensing ER Ca^{2+} content and, if it is too low, activating SOCE. Consequently, ER Ca^{2+} content and the cytosolic Ca^{2+} concentration will be decreased in $STIM2^{-/-}$ neurons compared to wild-type neurons.

These data from Brandman *et al.* and Berna-Erro *et al*. coupled with our finding showing that STIM2 and Orai2 protein expression is increased in IPAH-PASMC and in rat PASMC subjected to chronic hypoxia suggest that STIM2 and Orai2 may be the functional isoforms in either PASMC in general or specifically in pathogenic PASMC from IPAH patients. Therefore, in the following section we aim to determine whether STIM2 and Orai2 are necessary for enhanced SOCE in IPAH-PASMC and if STIM2 and Orai2 are sufficient to enhance SOCE in NPH-PASMC.

Chapter 7. Results: Enhanced Protein Expression of STIM2 is Necessary for Enhanced SOCE in IPAH Patient PASMC.

7.1 siRNA Mediated Knockdown of STIM2 by Electroporation

Previously we observed enhanced protein expression of Orai2 and STIM2 in IPAH-PASMC and that hypoxia enhanced protein expression of Orai2 and STIM2 in rat PASMC. Surprisingly, neither STIM1 nor Orai1 protein expression levels were upregulated by hypoxia or IPAH in PASMC. Following these finding our goal is to examine whether the increased protein expression of STIM2 is 1) necessary for enhanced SOCE and proliferation in IPAH-PASMC and 2) sufficient to enhance SOCE and proliferation in NPH-PASMC. In order to answer these questions, we modulated the protein expression level of STIM2 in IPAH and NPH-PASMC and observed the effect on SOCE and proliferation.

Lipid based transfection methods such as Lipofectamine 2000 or Fugene 6 yielded low transfection efficiency in IPAH patient, NPH patient, and primary cultured rat PASMC. While such a low transfection efficiency could be overcome in patch clamp by co-transfecting with a fluorescent protein to select for transfected cells, such a co-transfection would interfere with our fura-2 based method of measuring SOCE. After much effort, we discovered that the Amaxa Nucleofector electroporation system was able to transfect our PASMC at a high efficiency and with acceptable levels of cell death. Primary cultured rat PASMC, which we found to be the most difficult to transfect with

lipid based methods, were transfected at 78.1% transfection efficiency as determined by FACS analysis of EGFP transfected cells (Figure 27).

A.

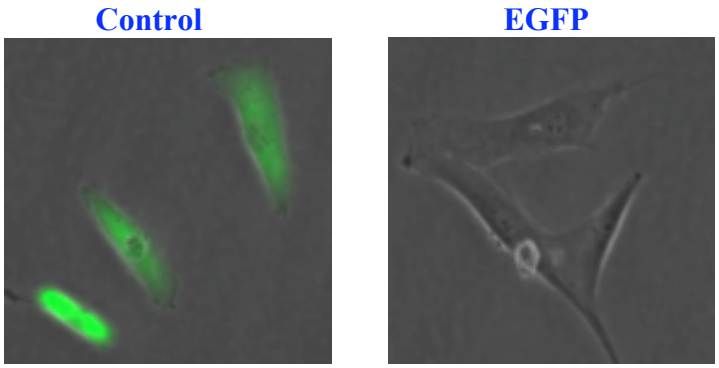

B.

	EGFP -	EGFP +
Control	94.9%	3.67%
EGFP	21.8%	78.1%

Figure 27: Transfection efficiency in PASMC. A. Representative images of PASMC taken 48 hours after transfection with either 2 μg vector (Control, *left panel*) or 2 μg EGFP (*right panel*) using the Amaxa Nucleofector system (program D-33). **B.** Flow cytometry analysis of Amaxa Nucleofector transfection of PASMC with EGFP (2 μg) showing 78.1% of PASMC were positive for EGFP 48 hours following nucleofection.

IPAH-PASMC and hypoxia treated primary cultured rat PASMC both had increased protein expression levels of STIM2. These data suggest whether increased protein expression of STIM2 is necessary for enhanced SOCE and enhanced proliferation in IPAH-PASMC. In order to answer this question we need to decrease the protein expression of STIM2 in IPAH-PASMC and compare SOCE and proliferation in these cells to in NPH-PASMC. Ideally, it would be best to decrease STIM2 protein expression level in IPAH patient PASMC to roughly match the expression level of STIM2 in NPH-PASMC. We electroporated IPAH-PASMC with differing amounts (4, 8, and 16 μL) of 10 μM siRNA against STIM2 (Santa Cruz sc- 76591) to decrease the protein concentration of STIM2 in IPAH-PASMC. We were able to decrease, or knockdown, STIM2 protein expression level of STIM2 in IPAH-PASMC in a dose dependent manner (Figure 28). And, for future experiments the 16 μL dose was used as it elicited a level of STIM2 protein expression comparable to NPH-PASMC. The same dose of siRNA targeting STIM2 did decrease protein expression level of STIM2 in rat PASMC cultured under normoxia, however was ineffective in decreasing protein expression level of STIM2 when the cells were treated with hypoxia (Figure 29). Due to this limitation, we did not pursue overexpression or knock down of STIM2 in rat PASMC.

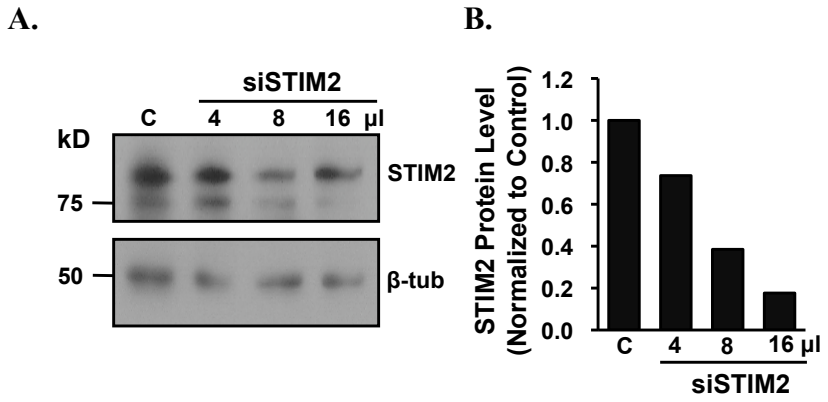

Figure 28: Dose-dependent knockdown of STIM2 in IPAH patient PASMC with siRNA. A. Representative Western blot image of STIM2 protein in IPAH-PASMC treated with siRNA against STIM2 (siSTIM2; with doses of 4, 8, and 16 µl) or control scrambled siRNA (indicated by "*C*"). β-tubulin (β-tub) was used as a loading control. **B**. Quantification of STIM2 protein expression level in IPAH-PASMC treated with control scrambled siRNA ("*C*") or 4, 8 and 16 µl of siRNA-STIM2. Values are normalized to the β-tub level at first and then normalized to the level of cells treated with control scrambled siRNA. STIM2 protein expression level in IPAH-PASMC was decreased in a dose-dependent manner by siRNA targeting STIM2.

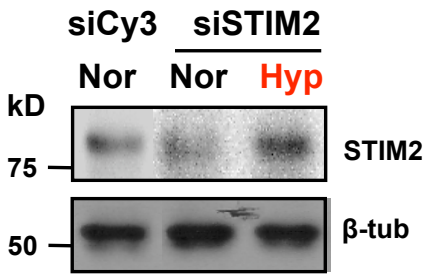

Figure 29: Hypoxia mitigates the effect of knockdown of STIM2 on STIM2 protein expression level in PASMC. Representative western blot analyses for STIM2 protein in Normoxia (Nor, room air supplemented with 5% CO_2) and Hypoxia (3% O_2, 5% CO_2, balance N_2) treated PASMC. Scramble siRNA (siCy3) was used as control for STIM2 siRNA (siSTIM2). β-tubulin (β-tub) was used as a loading control.

7.2 Knockdown of STIM2 in IPAH Patient PASMC Decreases SOCE

In order to determine the role of elevated protein expression of STIM2 in the enhancement of SOCE in IPAH patient PASMC compared to NPH-PASMC, we used an siRNA mediated knockdown strategy to determine the effect of STIM2 on SOCE. As previously determined, the dose of 16 μL of 10 μM siRNA against STIM2 was used to decrease protein expression of STIM2 in IPAH patient PASMC after 48 hours. 48 hours after transfection, we loaded the cells with Ca^{2+} dye fura-2 and utilized a store depletion, Ca^{2+} re-introduction protocol to measure both Ca^{2+} release from SR and Ca^{2+} influx through SOC.

Change in $[Ca^{2+}]_{cyt}$ was measured as the ratio of F_{340}/F_{380} (F) and normalized to initial F_{340}/F_{380} ratio (F_0) measured in PASMC superfused with physiological salt solution. SOCE was induced by passive depletion of SR Ca^{2+} using 10 μM cyclopiazonic acid (CPA) in the absence of extracellular Ca^{2+} followed by re-addition of 1.8 mM extracellular Ca^{2+}. Consistent with our previously reported findings[166,167], IPAH-PASMC exhibited significantly larger ($P = 0.010$) SOCE than NPH-PASMC (Figure 30). siRNA-mediated knockdown of STIM2 in IPAH-PASMC led to a significant decrease ($P = 0.023$) in the amplitude of SOCE (Figure 30). There was no significant difference in magnitude of SR Ca^{2+} release, or the rise in $[Ca^{2+}]_{cyt}$ due to Ca^{2+} leakage from the SR, in NPH-PASMC, IPAH-PASMC treated with scramble siRNA and IPAH-PASMC treated with siRNA-STIM2 (siSTIM2). Furthermore, there was no statistically significant difference ($P = 0.224$) in SOCE between NPH-PASMC and IPAH-PASMC treated with

siRNA-STIM2 (Figure 30). Western blot experiments also confirmed that the protein level of STIM2 is higher in IPAH-PASMC than in NPH-PASMC, and that siRNA-STIM2 effectively decreased protein expression level of STIM2 in IPAH-PASMC (Figure 30). These data suggest that increased protein expression level of STIM2 is necessary for the enhanced SOCE in IPAH-PASMC.

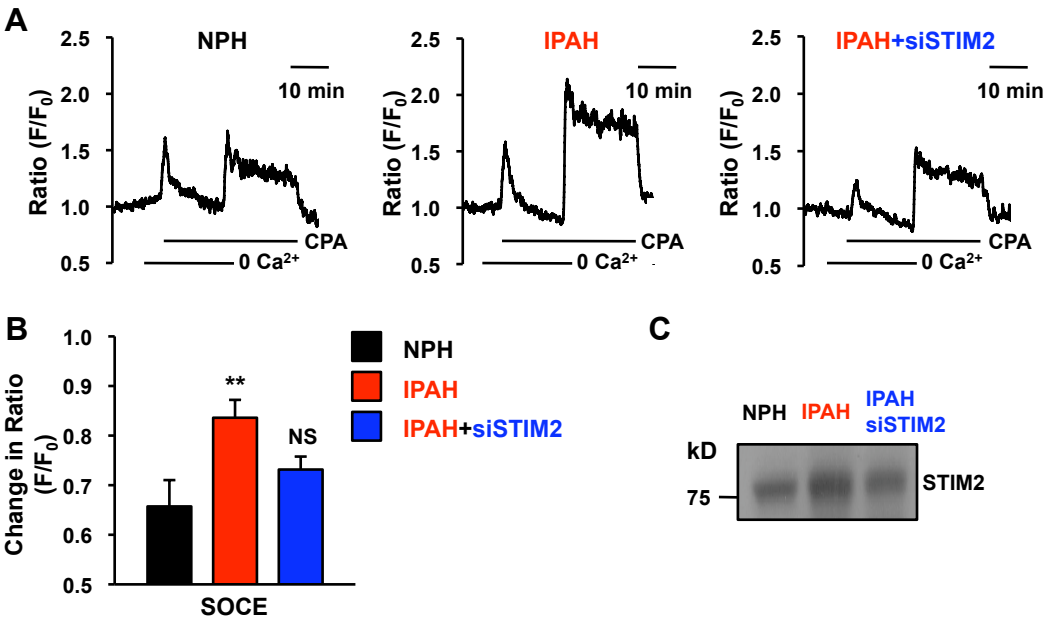

Figure 30: Increased protein expression of STIM2 is necessary for enhanced SOCE in IPAH patient PASMC. A. Representative records showing CPA-induced changes in $[Ca^{2+}]_{cyt}$ in the absence or presence of extracellular Ca^{2+} in NPH-PASMC (NPH, *left panel*), IPAH-PASMC (IPAH, *middle panel*) and IPAH-PASMC treated with siRNA targeting STIM2 (IPAH+siSTIM2, *right panel*). SOCE (indicated by the CPA-induced increase in $[Ca^{2+}]_{cyt}$ when extracellular Ca^{2+} is restored) was induced by passive depletion of SR Ca^{2+} using 10 μM CPA. NPH-PASMC *(left panel*) and IPAH-PASMC (*middle panel*) were treated with scrambled siRNA as a control. **B.** Summary data (mean ± SE) showing changes in CPA-induced increase in $[Ca^{2+}]_{cyt}$ immediately following re-addition of Ca^{2+} after store depletion (indicative of SOCE) in NPH-PASMC (black bar), IPAH-PASMC (red bar) and IPAH-PASMC treated with siRNA-STIM2 (blue bar). ** $P < 0.01$ (NS, not significant) vs. NPH. Significance was calculated using ANOVA. **C.** Western blot image of STIM2 protein expression in NPH-PASMC (NPH), IPAH-PASMC (IPAH) and IPAH-PASMC treated with siRNA-STIM2 (IPAH+siSTIM2). NPH-PASMC (black) and IPAH-PASMC (red) were treated with scrambled siRNA.

7.3 Knockdown of STIM2 in IPAH Patient PASMC Decreases Proliferation

Proliferation of PASMC was determined by counting cells at 0 hr (*i.e.*, two days after the cells are plated onto Petri dishes) and 24, 48, and 72 hrs later. At 0 hr, the control (NPH) PASMC group and IPAH-PASMC group had roughly the same number of cells (Figure 31A). After 72 hrs, the numbers of NPH-PASMC and IPAH-PASMC were both significantly increased (Figure 31A); however, the increase in IPAH-PASMC number was much greater that in NPH-PASMC (Figure 31B). Knockdown of STIM2 with siRNA had little effect on the change in NPH-PASMC number after 72 hrs (Figure 31C, *left panel*). However, knockdown of STIM2 with siRNA in IPAH-PASMC significantly decreased the increase in cell number after 72 hrs ($P < 0.001$) (Figure 31C, *right panel*, and D). The siRNA-STIM2-mediated knockdown of STIM2 appeared to attenuate IPAH-PASMC growth at early time (24 hrs) and last for at least 72 hrs (Figure 31D). These data indicate that upregulated STIM2 is necessary for the enhanced proliferation of IPAH-PASMC. Inhibition of STIM2 is an effective way to attenuate excessive proliferation of IPAH-PASMC; STIM2 may be a potential target for developing novel therapeutic approach for patients with IPAH.

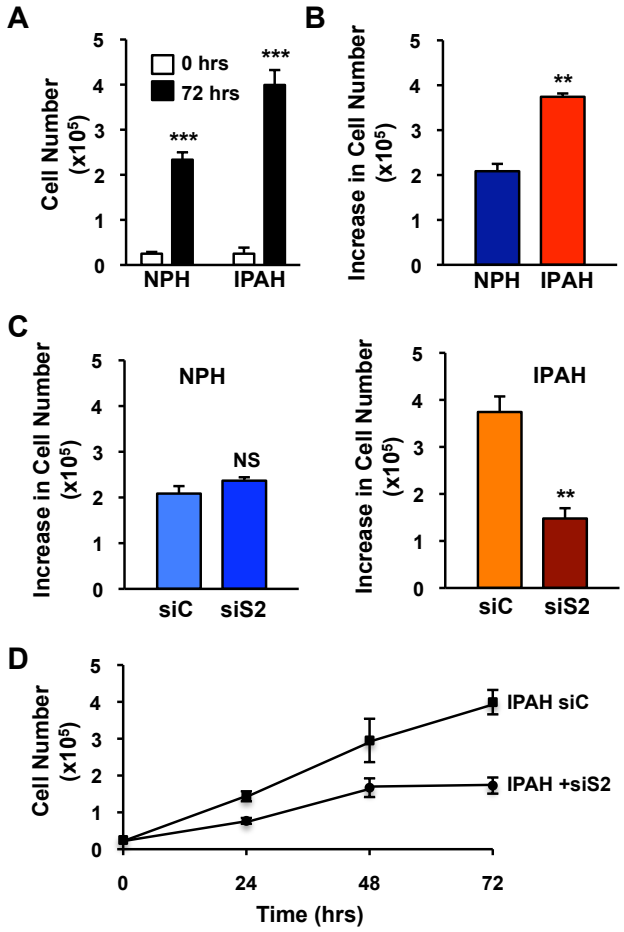

Figure 31: Knockdown of STIM2 mitigates enhanced proliferation in IPAH patient PASMC. A. Summary data (mean ± SE) showing cell numbers for NPH-PASMC and IPAH-PASMC before (0 hr) and after 72 hrs of culture in growth media. *** $P < 0.001$ vs. 0 hr. **B.** Summary data showing the increase in cell numbers after 72 hrs in NPH-PASMC (blue) and IPAH-PASMC (red). ** $P < 0.01$ vs. NPH. IPAH patient PASMC showed a significantly greater increase in cell number after 72 hours compared to NPH-PASMC. **C.** Summary data showing the increase in cell number after 72 hours in NPH-PASMC (*left panel*) and IPAH-PASMC (*right panel*) treated with either scrambled siRNA (siC) or siRNA against STIM2 (siS2). Decreasing the protein expression level of STIM2 did not affect the increase in cell number after 72 hrs in NPH-PASMC (*left panel*), but significantly inhibited the increase in cell number after 72 hrs in IPAH-PASMC (*right panel*). ** $P < 0.01$ vs. siC. **D.** Summary data showing total number of IPAH-PASMC cultured in growth media at 0, 24, 48 and 72 hrs. Cells were treated with scrambled siRNA (square symbols) or siRNA against STIM2 (circle symbols). IPAH-PASMC treated with siRNA-STIM2 had a slower rate of proliferation than IPAH-PASMC treated with scrambled siRNA. Significance was calculated using Student's t-test.

7.4 Overexpression of STIM2 in PASMC

In order to further examine the functional role of STIM2 in IPAH-PASMC, STIM2 was transiently transfected into NPH-PASMC to determine whether overexpression of STIM2 was sufficient to enhance SOCE and increase proliferation in NPH-PASMC. STIM2 was overexpressed in NPH-PASMC in a dose dependent manner (Figure 32). After 48 hours, 1 μg of STIM2-cDNA significantly enhanced protein expression of STIM2 in both HEK-293 cells (data not shown) and NPH-PASMC (Figure 32) and was used to overexpress STIM2 for the experiments described below.

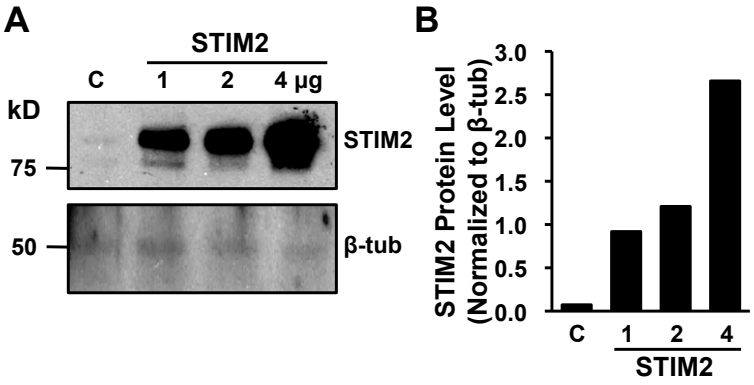

Figure 32: **Dose-dependent overexpression of STIM2 in NPH-PASMC. A.** Representative Western blot image of STIM2 protein in NPH-PASMC. STIM2 was overexpressed using 1, 2 or 4 µg of DNA. Vector DNA was used as a control ("*C*"). β-tubulin (β-tub) was used as a loading control. **B.** Quantification of STIM2 protein expression level in NPH-PASMC transfected with vector DNA ("C") and 1, 2, or 4 µg of STIM2-DNA. Values are normalized to β-tubulin. STIM2 protein expression level was increased in a dose dependent manner in NPH-PASMC transfected with STIM2.

7.5 Overexpression of STIM2 is Not Sufficient to Enhance SOCE in Normal PASMC.

Change in $[Ca^{2+}]_{cyt}$ was measured as the ratio of F_{340}/F_{380} (F) and normalized to initial F_{340}/F_{380} ratio (F_0) as described above. SOCE was induced by passive depletion of SR Ca^{2+} with 10 μM CPA in NPH-PASMC superfused with Ca^{2+}-free solution followed by restoration of extracellular Ca^{2+} (1.8 mM). Overexpression of STIM2 in NPH-PASMC (48 hrs after STIM2 transfection) had no significant effect on either the amplitude of the rise in $[Ca^{2+}]_{cyt}$ due to Ca^{2+} release from the SR (Figure 33 B, *left panel*) or the amplitude of SOCE (Figure 33B, *right panel*) in comparison to NPH-PASMC transfected with control vector. In fact, overexpression of STIM2 caused a slight (but not statistically significant) decrease in the peak amplitude of SOCE (Figure 33B, *right panel*). These data suggest that overexpression of STIM2 is not sufficient to enhance SOCE in normal PASMC.

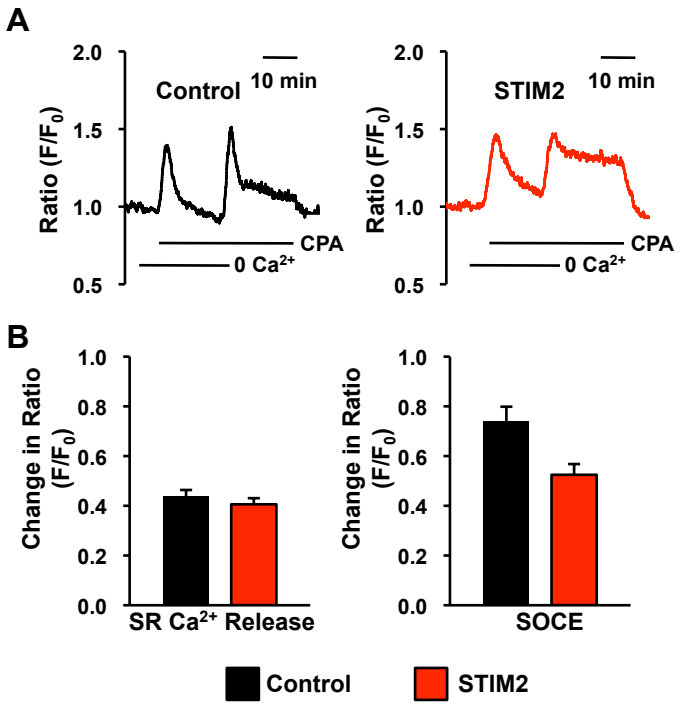

Figure 33: Overexpression of STIM2 is not sufficient to enhance SOCE in normal PASMC. **A.** Representative records showing changes in $[Ca^{2+}]_{cyt}$ before, during and after application of CPA (10 μM) in the absence or presence of extracellular Ca^{2+} in vector control (*left panel*) and STIM2-transfected (*right panel*) NPH-PASMC. SOCE was induced by passive depletion of SR Ca^{2+} using CPA. **B.** Summary data (mean ± SE) showing changes in $[Ca^{2+}]_{cyt}$ immediately following addition of CPA in the absence of extracellular Ca^{2+}, which reflects SR Ca^{2+} release (SR Ca^{2+} Release, *left panel*), in control (black) and STIM2-transfected (red) NPH-PASMC. There was no difference in magnitude of SR Ca^{2+} release between the two groups. Summary data (mean ± SE) showing changes in $[Ca^{2+}]_{cyt}$ immediately following re-addition of Ca^{2+} after CPA-induced store depletion (indicative of SOCE, *right panel*) in control (black) and STIM2-overexpressing PASMC (red). There was no difference in magnitude of SOCE between the two groups. Significance was calculated using Student's t-test.

7.6 Overexpression of STIM2 does Not Increase Proliferation in Normal PASMC.

In order to examine whether overexpression of STIM2 in normal PASMC would enhance cell proliferation, we measured and compared cell number in NPH-PASMC transfected with a control vector and NPH-PASMC transfected with STIM2. As shown in Figure 34, overexpression of STIM2 failed to enhance proliferation in NPH-PASMC. In these experiments, proliferation of PASMC was determined by counting cells at time 0 and 72 hrs. Transfection of PASMC with either STIM2 cDNA or control vector was performed 48 hrs prior to time 0. At time 0, PASMC transfected with STIM2 or control vector had the same number of cells to start with. After 72 hrs, both control vector- and STIM2-transfected PASMC proliferated, but the increase in cell number was similar between NPH-PASMC transfected with a control vector and STIM2 (Figure 34). These data suggest that overexpression of STIM2 is not sufficient to enhance proliferation in NPH-PASMC.

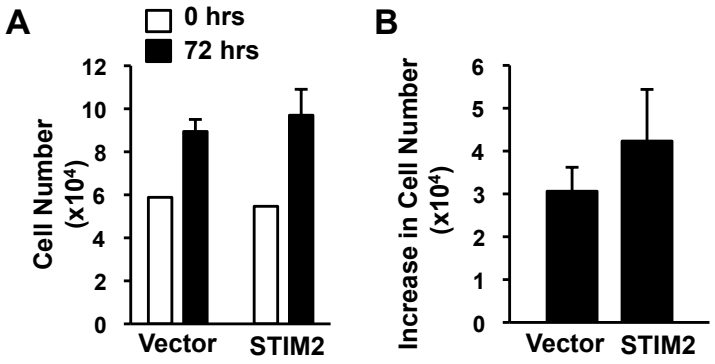

Figure 34: Overexpression of STIM2 does not increase NPH-PASMC proliferation. **A.** Summary data for NPH-PASMC proliferation after 72 hrs. Cell number was counted at time zero (0 hrs: white bar) and 72 hrs (72 hrs: black bar) and shown as the multiple of 10^4. After 72 hrs, both vector control and STIM2-overexpressing NPH-PASMC increased in cell number. **B.** Summary data (mean ± SE) showing the increase in cell number after 72 hrs in NPH-PASMC. STIM2-overexpressing PASMC (STIM2) did not show a greater increase in cell number after 72 hrs compared to control (Vector). Cell counts were repeated four times (n = 4). Significance was calculated using Student's t-test.

7.7 Role of Orai2 in SOCE in PASMC from IPAH Patients

We have previously demonstrated that Orai2 protein expression level in increased in IPAH-PASMC compared to NPH-PASMC and is also increased in rat PASMC subjected to chronic hypoxia (Chapter 6.5). Furthermore, while STIM2 is necessary for enhanced SOCE in IPAH-PASMC, STIM2 alone is not sufficient to enhance SOCE in NPH-PASMC (Chapter 7.2 and 7.5). These findings suggest that Orai2 may also be necessary for enhanced SOCE in IPAH-PASMC and that Orai2 and STIM2 co-overexpression in NPH-PASMC is sufficient to enhance SOCE in NPH-PASMC. In order to test whether Orai2 is necessary for enhanced SOCE in IPAH-PASMC, we attempted to decrease the protein expression level of Orai2 in IPAH-PASMC using siRNA that targets Orai2. We tried siRNA purchased from two different companies, at several different dosages and examined protein expression after 48 and 72 hours. Unfortunately, we were unable to significantly decrease the protein expression level of Orai2 in IPAH-PASMC (data not shown).

Next we overexpressed Orai2 in order to test whether Orai2 alone could enhance SOCE in NPH-PASMC. Orai2 was successfully overexpressed in HEK293 cells and in NPH-PASMC (Figure 35). However, increased protein expression of Orai2 did not enhance SOCE compared to vector control in NPH-PASMC cells (Figure 36). These data suggest that Orai2 alone is not sufficient to enhance SOCE in IPAH-PASMC. The effect of overexpression of Orai2 on proliferation in NPH-PASMC was not examined, because overexpression of Orai2 had no effect on SOCE in these cells. The fact that

Orai2 alone and STIM2 alone are insufficient to enhance SOCE in NPH-PASMC, suggests the question of whether increased protein expression of both STIM2 and Orai2 will be sufficient to enhance SOCE in NPH-PASMC.

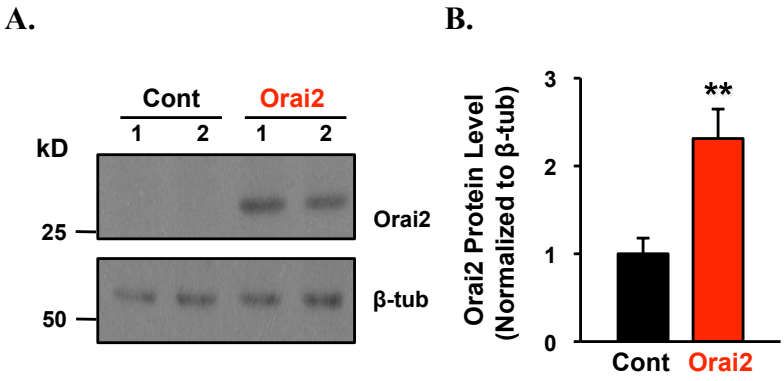

Figure 35: **Overexpression of Orai2 in NPH-PASMC. A.** Representative Western blot image of oOai2 protein in NPH-PASMC. STIM2 was overexpressed using 2 μg of DNA. Vector DNA was used as a control ("Cont"). β-tubulin (β-tub) was used as a loading control. **B.** Quantification of Orai2 protein expression level in NPH-PASMC transfected with vector DNA ("Cont") and 2 μg of Orai2-DNA. Values are normalized to β-tubulin. * $P < 0.05$, ** $P < 0.01$, *** $P < 0.001$ vs. Cont. Significance was calculated using Student's t-test.

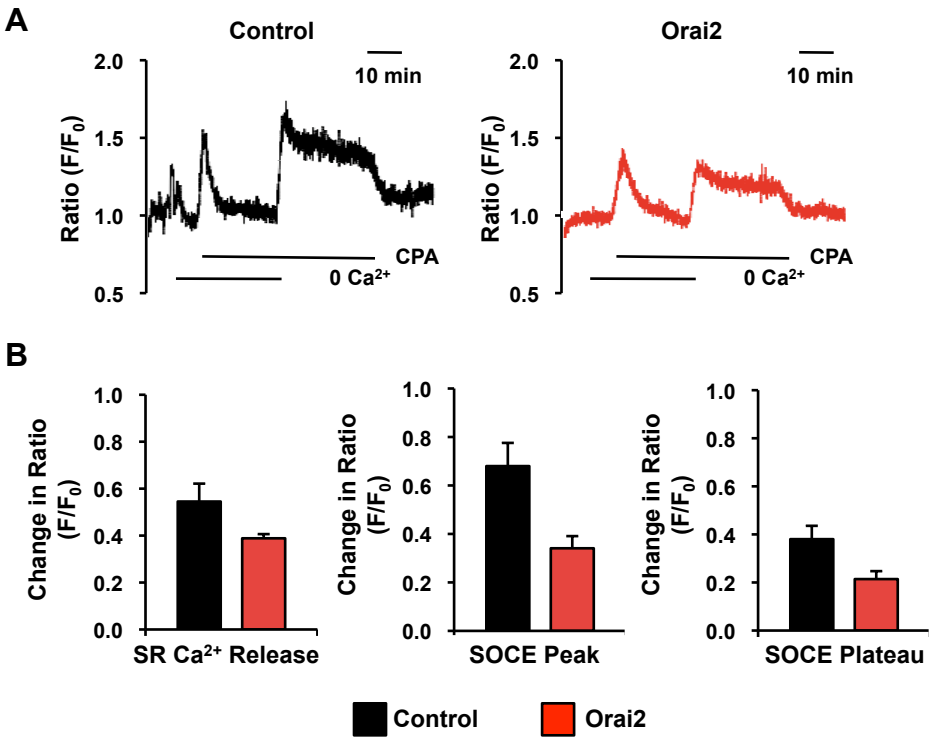

Figure 36: Overexpression of Orai2 alone is not sufficient to enhance SOCE in normal PASMC. A. Representative records showing changes in $[Ca^{2+}]_{cyt}$ before, during and after application of CPA (10 μM) in the absence or presence of extracellular Ca^{2+} in vector control (*left panel*) and Orai2-transfected (*right panel*) NPH-PASMC. SOCE was induced by passive depletion of SR Ca^{2+} using CPA. **B.** Summary data (mean ± SE) showing changes in $[Ca^{2+}]_{cyt}$ immediately following addition of CPA in the absence of extracellular Ca^{2+}, which reflects SR Ca^{2+} release (SR Ca^{2+} Release, *left panel*), in control (black) and Orai2-transfected (red) NPH-PASMC. There was no difference in magnitude of SR Ca^{2+} release between the two groups. Summary data (mean ± SE) showing changes in $[Ca^{2+}]_{cyt}$ immediately following re-addition of Ca^{2+} after CPA-induced store depletion (indicative of Peak SOCE, *middle panel*) in control (black) and Orai2-overexpressing PASMC (red). There was no difference in magnitude of Peak SOCE between the two groups. Summary data (mean ± SE) showing changes in $[Ca^{2+}]_{cyt}$ before withdrawal of CPA (indicative of Plateau SOCE, *right panel*) in control (black) and Orai2-overexpressing PASMC (red). There was no difference in magnitude of Plateau SOCE between the two groups. Significance was calculated using Student's t-test.

7.8 Overexpression of Both STIM2 and Orai2 in PASMC

In order to determine whether Orai2 and STIM2 co-overexpression in NPH-PASMC is sufficient to enhance SOCE we co-expressed Orai2 and STIM2 in HEK293 and in NPH-PASMC and measured protein expression of Orai2/STIM2 and SOCE after 48 hours. In HEK293 cells and in NPH-PASMC, 2 μg of Orai2 and 2 μg of STIM2 when transfected separately were both able to elicit increased protein expression levels of Orai2 and STIM2, respectively. Furthermore, overexpression of Orai2 alone had no effect on STIM2 protein expression level, and overexpression of STIM2 alone had no effect on Orai2 protein expression level in HEK293 and in human PASMC. Overexpression of Orai2 and STIM2 together in HEK293 cells did not enhance SOCE compared to vector control (Figure 38). In fact, overexpression of STIM2 and Orai2 had no effect on ER Ca^{2+} release, peak SOCE, or on the plateau phase of SOCE in HEK293 cells (Figure 38). These results corroborate finding from other researchers that strongly suggest STIM1 and Orai1 are the functionally significant isoforms in HEK293 cells[114,191]. Overexpressed Orai2 and STIM2 together in NPH-PASMC significantly enhanced protein expression of Orai2 and STIM2 in these cells after 48 hours (Figure 37). When we overexpressed Orai2 and STIM2 together in NPH-PASMC, SOCE and SR Ca^{2+} release were unchanged after 48 hours. However, 72 hours after co-overexpression SR calcium release and peak SOCE were increased (Figure 39). Furthermore, baseline resting $[Ca^{2+}]_{cyt}$ was increased (data not shown). Taken together these data show that overexpression of Orai2 and STIM2 together in HEK293 does not enhance SOCE in these cells, but does in fact

enhance SOCE in PASMC. Therefore, overexpression of STIM2 and Orai2 together is sufficient to enhance SOCE and basal $[Ca^{2+}]_{cyt}$ in PASMC. Furthermore, these data suggest that in PASMC STIM2 and Orai2 are pathogenically increased in IPAH patients.

Chapter 7 in part, has been submitted for publication of the material as it may appear in Pulmonary Circulation, 2011, Song, MY; Makino, A, Yuan JX or in Antioxidants and Redox Signaling, 2011, Song, MY; Makino, A, Yuan JX. The dissertation author was the primary investigator and author of these papers.

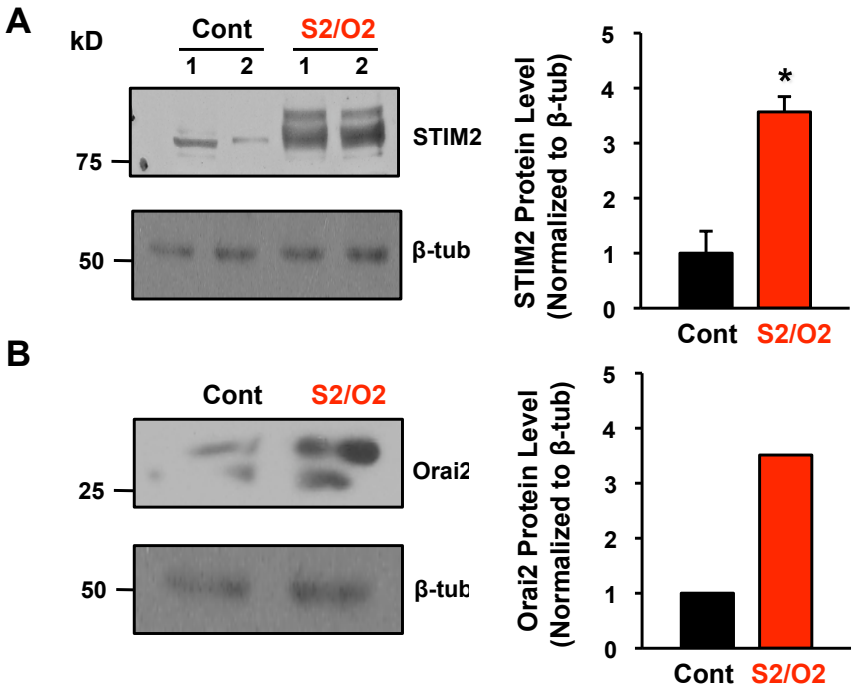

Figure 37: **Overexpression of Orai2 and STIM2 in PASMC. A.** Representative Western blot image (*left panel*) for STIM2 protein in NPH-PASMC transfected with either 2 μg vector control (Cont) or co-transfected with 2 μg STIM2 and 2 μg Orai2 (S2/O2). β-tubulin (β-tub) was used as a loading control. Quantification of STIM2 protein expression level in NPH-PASMC transfected with either Cont or S2/O2 (*right panel*). Values are normalized to β-tubulin and average Cont level. * $P < 0.05$, ** $P < 0.01$, *** $P < 0.001$ vs. Cont. **B.** Representative Western blot image (*left panel*) for Orai2 protein in NPH-PASMC transfected with either 2 μg vector control (Cont) or co-transfected with 2 μg STIM2 and 2 μg Orai2 (S2/O2). β-tubulin (β-tub) was used as a loading control. Quantification of STIM2 protein expression level in NPH-PASMC transfected with either Cont or S2/O2 (*right panel*). Values are normalized to β-tubulin and average Cont level. Significance was calculated using Student's t-test.

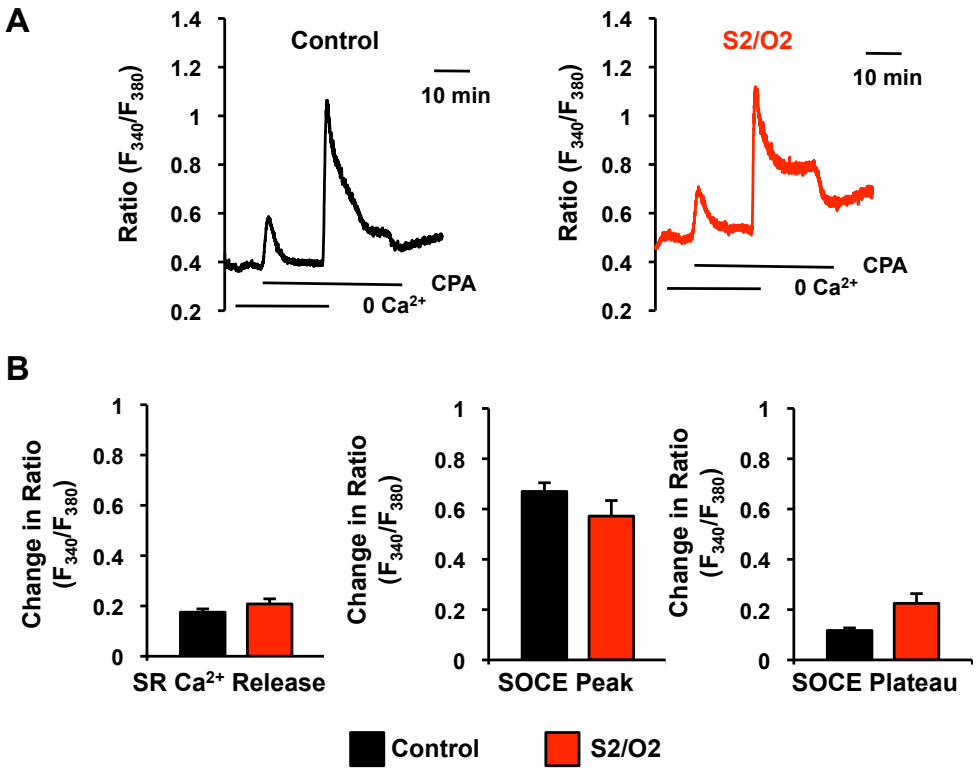

Figure 38: Overexpression of Orai2 and STIM2 does not enhance SOCE in HEK293 cells. A. Representative records showing changes in $[Ca^{2+}]_{cyt}$ before, during and after application of CPA (10 μM) in the absence or presence of extracellular Ca^{2+} in vector control (*left panel*) and STIM2-transfected (*right panel*) HEK293 cells. SOCE was induced by passive depletion of SR Ca^{2+} using CPA. **B.** Summary data (mean ± SE) showing changes in $[Ca^{2+}]_{cyt}$ immediately following addition of CPA in the absence of extracellular Ca^{2+}, which reflects ER Ca^{2+} release (ER Ca^{2+} Release, *left panel*), in control (black) and STIM2/Orai2-transfected (red) HEK293 cells. There was no difference in magnitude of ER Ca^{2+} release between the two groups. Summary data (mean ± SE) showing changes in $[Ca^{2+}]_{cyt}$ immediately following re-addition of Ca^{2+} after CPA-induced store depletion (indicative of SOCE Peak, *middle panel*) in control (black) and STIM2/Orai2-overexpressing HEK293 cells (red). Peak SOCE (*middle panel*) and Plateau SOCE (*right panel*) were unchanged by STIM2/Orai2 overexpression. Significance was calculated using Student's t-test.

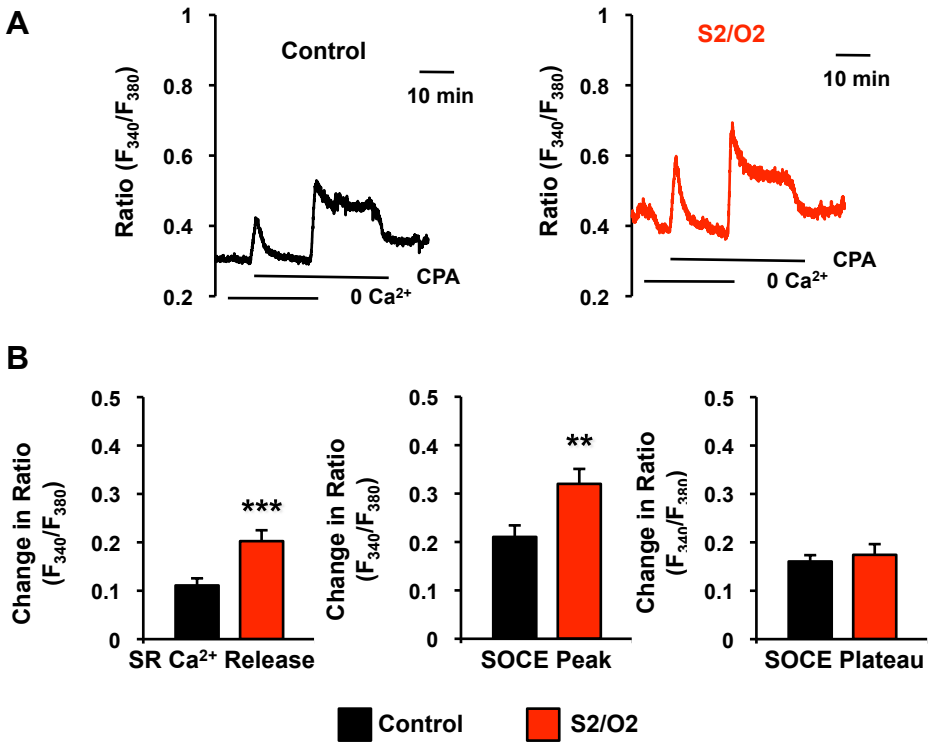

Figure 39: Overexpression of Orai2 and STIM2 does enhance SOCE in PASMC. A. Representative records showing changes in $[Ca^{2+}]_{cyt}$ before, during and after application of CPA (10 μM) in the absence or presence of extracellular Ca^{2+} in vector control (*left panel*) and STIM2-transfected (*right panel*) NPH-PASMC. SOCE was induced by passive depletion of SR Ca^{2+} using CPA. **B.** Summary data (mean ± SE) showing changes in $[Ca^{2+}]_{cyt}$ immediately following addition of CPA in the absence of extracellular Ca^{2+}, which reflects SR Ca^{2+} release (SR Ca^{2+} Release, *left panel*), in control (black) and STIM2/Orai2-transfected (red) NPH-PASMC. Summary data (mean ± SE) showing changes in $[Ca^{2+}]_{cyt}$ immediately following re-addition of Ca^{2+} after CPA-induced store depletion (indicative of SOCE Peak, *middle panel*) in control (black) and STIM2/Orai2-overexpressing PASMC (red). Peak SOCE was enhanced by STIM2/Orai2 overexpression. Plateau SOCE (*right panel*) was unchanged by STIM2/Orai2 overexpression. Significance was calculated using Student's t-test.

Chapter 8. Conclusion

8.1 Summary of All Results.

We previously reported that SOCE was significantly enhanced in PASMC from IPAH patients compared to PASMC from normotensive control subjects. And, enhanced SOCE plays an important role in the pathophysiological changes in PASMC associated with pulmonary arterial hypertension such as enhanced proliferation, migration and contraction of PASMC. Therefore, we examine whether the expression levels of STIM1, STIM2, Orai1, Orai2 and Orai3 are altered in IPAH-PASMC compared to control PASMC, and whether these putative changes in expression level are responsible for the enhanced SOCE and proliferation in IPAH-PASMC. Compared to the control PASMC, the protein expression level of STIM2 was significantly increased in IPAH-PASMC, whereas STIM1 protein expression was decreased. Similarly, hypoxia enhanced the protein expression level of STIM2, but not STIM1, in rat PASMC after 48 hours. In IPAH-PASMC, the small interfering RNA (siRNA)-mediated knockdown of STIM2 decreased SOCE and proliferation, while knockdown of STIM2 in control PASMC had no effect on either SOCE or proliferation. Overexpression of STIM2 in the control PASMC failed to enhance SOCE or proliferation. These data indicate that enhanced protein expression of STIM2 alone is necessary, but not sufficient, for enhanced SOCE and proliferation of IPAH-PASMC.

Orai2 protein expression level was increased in IPAH-PASMC compared to NPH-PASMC. Orai1 and Orai3 protein expression levels also seemed to increase, however these differences were not statistically significant. The lack of statistical significance is likely due to the difficulty in obtaining patient samples and some natural variation between patients. 48 hours of hypoxia significantly increased protein expression of Orai1 and Orai2, but not Orai3. These data suggest that Orai2 may be important in IPAH-PASMC. Overexperssion of Orai2 alone in NPH-PASMC did not enhance SOCE or proliferation.

Since neither STIM2 alone nor Orai2 alone are sufficient to enhance SOCE in PASMC, we co-overexpressed Orai2 along with STIM2 and examined SOCE. Co-overexpression of Orai2 and STIM2 was performed in both HEK293 and PASMC. Protein expression was elevated in both cell types after 48 hours. In HEK298 cells SOCE was not affected after 48 hours. In PASMC, SOCE and basal $[Ca^{2+}]_{cyt}$ was increased after 72 hours. These data suggest that increased protein expression level of both Orai2 and STIM2 is sufficient to enhance SOCE in PASMC.

8.2 Discussion

A rise in $[Ca^{2+}]_{cyt}$ is a major trigger for pulmonary vasoconstriction and is an important stimulus for PASMC proliferation which leads to pulmonary vascular remodeling[32,127]. Human PASMC functionally express many signal transduction proteins and kinases (*e.g.*, calmodulin, CaMK, MAPK and calcineurin) and transcription factors (*e.g.*, CREB, c-Fos/c-Jun, c-Myc, NFAT, NF-κB) that are sensitive to changes in $[Ca^{2+}]_{cyt}$ or Ca^{2+}-calmodulin[36]. An increase in $[Ca^{2+}]_{cyt}$ can rapidly increase $[Ca^{2+}]$ in nuclei[15,192-194] and stimulates nuclear events that are related to cell proliferation. In the cell cycle, it has been well demonstrated that there are at least four steps that are regulated by Ca^{2+} or Ca^{2+}/CaM: the transition from G_0 to G_1 phase, the transition from G_1 to S phase, the transition from S to M phase, and the whole process in M phase[195]. In isolated pulmonary arterial rings, removal of extracellular Ca^{2+} abolished high K^+-mediated pulmonary vasoconstriction and significantly inhibited agonist-mediated pulmonary vasoconstriction[32,100,196]. In cultured PASMC, reduction of free Ca^{2+} concentration in the culture medium significantly inhibited cell proliferation in the presence of growth factors, while depletion of intracellularly stored Ca^{2+} in the sarcoplasmic reticulum also significantly attenuated smooth muscle cell proliferation[197-199]. In addition, Ca^{2+} is an important signal in initiating and guiding cell migration[200-205]. These observations indicate that intracellular Ca^{2+} signaling, regulated by Ca^{2+} influx through Ca^{2+}-permeable channels and Ca^{2+} extrusion via Ca^{2+}-Mg^{2+} ATPase (Ca^{2+} pumps) in the plasma membrane, Ca^{2+} release through IP_3/ryanadine receptors and Ca^{2+} uptake via the Ca^{2+}-Mg^{2+} ATPase on the SR/ER membrane, plays an important role in the regulation of

smooth muscle cell contraction, migration and proliferation. Upregulated expression of Ca^{2+}-permeable channels and enhanced Ca^{2+} influx therefore causes sustained vasoconstriction, stimulates smooth muscle cell migration and proliferation, and ultimately cause vascular wall thickening.

IPAH-PASMC demonstrated significantly enhanced SOCE and proliferated faster compared to NPH-PASMC[166,167,206]. Many studies have shown that STIM1 can enhance SOCE when overexpressed in a variety of cell types[84,114,118,207,208]. This led us to hypothesize that STIM1 protein expression would be upregulated in IPAH-PASMC. Surprisingly STIM2, but not STIM1, protein expression was increased in IPAH-PASMC compared to NPH-PASMC. These findings were consistent with the observations showing that protein expression of STIM2 is upregulated in rat PASMC subjected to hypoxia (48 hrs). These data suggest that STIM2 may be the important isoform for pathophysiological increase in SOCE in PASMC from IPAH patients. Interestingly, STIM1 protein expression level was decreased compared to NPH-PASMC. Perhaps, a decrease in STIM1 along with an increase in STIM2 protein expression levels can influence SOCE. Brandman *et al.* demonstrated that knockdown of STIM1 while over expressing STIM2 did not affect SOCE compared to overexpression of STIM2 alone in HEK293 cells[190]. Furthermore, knockdown of STIM1 did not affect the increase in basal $[Ca^{2+}]_{cyt}$ caused by overexpression of STIM2[190]. While these data were not obtained from PASMC, they still strongly suggest that the decrease in STIM1 protein expression level is not relevant to the role of STIM2 on SOCE in PASMC.

Further examination showed that STIM2 plays an important functional role in both augmented SOCE and enhanced proliferation in IPAH-PASMC. Using siRNA mediated knockdown of STIM2 protein expression level in IPAH-PASMC, we found that increased protein expression of STIM2 in IPAH-PASMC was necessary for increased SOCE. When STIM2 protein expression level in IPAH-PASMC was decreased to the level similar to NPH-PASMC, IPAH-PASMC no longer exhibited enhanced SOCE or enhanced proliferation. However, overexpression of STIM2 alone could not enhance SOCE or proliferation in NPH-PASMC, suggesting that STIM2 does not act alone in eliciting the pathophysiological changes in PASMC associated with IPAH. Taken together, these findings suggest that STIM2 is necessary, but not sufficient, for the enhanced proliferation and SOCE found in IPAH-PASMC. Functional interaction of STIM2 with Orai channels may also be important.

Many researchers have singled out Orai1 as the predominant isoform mainly because overexpression of Orai1 along with STIM1 yields a larger SOCE than Orai2 or Orai3 with STIM1 in HEK293 cells[86]. Our data, however, shows that in IPAH-PASMC the protein expression level of Orai2, rather than Orai1 or Orai3, is significantly increased compared to NPH-PASMC. Orai1 and Orai3 do seem to be increased, however not at a statistically significant level. The power of these studies is limited by the number of IPAH patients from which we can collect PASMC (n = 4). Perhaps with more patient samples we could clarify whether Orai1 and Orai3 are statistically significantly increased in IPAH-PASMC. However, without access to more patient sample, we used chronic hypoxia as a model of IPAH in order to examine protein the effect of hypoxia on protein

expression levels of STIM and Orai in rat PASMC. We found that Orai1 and Orai2 protein expression levels were significantly increased, while Orai3 protein expression level was unchanged. These data corroborate our IPAH-PASMC findings and suggest that Orai2 and STIM2 are the relevant isoforms in IPAH-PASMC. Overexpression of Orai2 in PASMC did not enhance SOCE or proliferation compared to vector control. These data suggest that Orai2 is insufficient to enhance SOCE in PASMC. Furthermore, overexpression of STIM2 and Orai2 together also did not enhance SOCE in PASMC. These data taken together with our studies showing that increase protein expression of STIM2 in sufficient to enhance SOCE in IPAH-PASMC suggest that increase expression of Orai2 may not play an important role in IPAH-PASMC.

As mentioned earlier, STIM2 overexpression had no effect on SOCE and proliferation in NPH-PASMC, while knockdown of STIM2 in IPAH-PASMC decreased both SOCE and proliferation. Therefore, it seems that STIM2 is functionally active only in IPAH-PASMC and has no or little function in NPH-PASMC. Several explanations could explain how STIM2 is "turned on" in IPAH but not in NPH-PASMC. STIM2 could be activated by phosphorylation or another form of post-translational modification. It is widely accepted that Rho/ROCK signaling is involved in Ca^{2+} sensitization, proliferation, contraction, and migration in PASMC[209]. Researchers have demonstrated that Rho/ROCK signaling pathway plays a significant role in the pathogenesis of different experimental models of PAH as well as PAH in patients[210]. Perhaps the pathogenesis of IPAH involves RhoA/ROCK signaling though STIM2.

A second explanation for how STIM2 is only active in IPAH-PASMC but not NPH-PASMC involves store-operated channels (SOC) on the plasma membrane. Strong evidence suggests that Orai1 interacts with STIM1 and functions as a SOC. Orai1 was discovered through genome wide RNAi screening. A mutation in Orai1 in patients with severe combined immune deficiency eliminates the Ca^{2+} release-activated Ca^{2+} currents (I_{CRAC}), which can then be reconstituted by expressing wild-type Orai1[82,83]. Orai1 spans the plasma membrane four times with both the C- and N- terminus in the cytoplasm. Co-expression of STIM1 with Orai1 in HEK293 cells resulted in large increases in SOCE and I_{CRAC} compared to vector control cells[85,86]. Co-immunoprecipitation data showed that STIM1 and Orai1 interact and store depletion significantly increases the amount to interaction[119]. Furthermore, other isoforms of Orai (*e.g.*, Orai2 and Orai3) are also believed to play a role in SOCE[83]. Our lab has previously demonstrated that TRPC channels also function as SOC and are important in PASMC physiology and pathophysiology[33,166,167,184,211]. TRPC channels are important in the regulation of vascular tone since they regulate the Ca^{2+} influx required for agonist-induced vasoconstriction and mitogen-mediated smooth muscle cell proliferation. And, the ability of TRPC channels to alter $[Ca^{2+}]_{cyt}$ without a change in membrane potential lends them the ability to modulate vasoconstriction and vasorelaxation through a voltage-independent mechanism. Agonist- and hypoxia-induced pulmonary vasoconstriction is believed to be, at least in part, mediated though Ca^{2+} influx through TRPC1 and TRPC6 channels[184,212]. Upregulated TRPC channel expression, enhanced SOCE, and increased $[Ca^{2+}]_{cyt}$ are associated with enhanced proliferation of PASMC isolated from IPAH patients[73,167]. Therefore, increasing SOCE and proliferation in PASMC may be a

function of both increasing protein expression of STIM2 and increasing protein expression of SOC such as TRPC in the plasma membrane.

Our data supports this idea that both increased protein expression of STIM2 and another protein, in this case Orai2, is necessary to enhance SOCE. Overexpression of both STIM2 and Orai2 together increased SOCE in PASMC, but not in HEK293 cells. These data not only demonstrate an important role for STIM2 and Orai2 in PASMC, but also suggest that this role for STIM2 and Orai2 is unique to PASMC. Many researchers have studied the role of STIM2 and Orai2 in a variety of cell types. With the exception of neurons, in each case these researchers have concluded that STIM2 and Orai2 play a secondary role to STIM1 and Orai1.

8.3 Future Directions and Clinical Implications

Since upregulated protein expression of STIM2 is necessary for augmented SOCE and enhanced proliferation in PASMC from IPAH patients, downregulation of STIM2 protein expression and/or inhibition of STIM2 protein function in PASMC may be an important target for developing therapeutic approaches for IPAH. In theory, if we were able to decrease the protein expression or the function of STIM2 in PASMC we could change the couse of IPAH by mitigating pulmonary vascular remodeling and decreasing vasoconstriction. In practice, however, specifically decreasing STIM2 activity or expression level in PASMC *in vivo* is a difficult task. This is mainly due to the localization of STIM2 on the SR membrane of PASMC. Potential drugs would have to cross the endothelial layer from the blood and then cross the plasma membrane in order to directly interact with STIM2 protein or mRNA. While it is a technically difficult task to target STIM2 in PASMC, the finding I have previously presented demonstate that it is worth exploring. Current literature suggests that STIM2 is functionally not as important as STIM1 in a majority of cell types. The two notable exceptions being in neurons and in PASMC from IPAH patients. Furthermore, knockdown of STIM2 did not significantly affect either proliferation or calcium handling in normal or healthy PASMC, but our results demonstrated that knockdown of STIM2 preferentially decreases SOCE and proliferation in diseased or IPAH patient PASMC. These data suggest that knockdown of STIM2 in IPAH patients will not lead to significant toxicity or adverse affects in other cell types.

Further experiments are needed in order to investigate whether STIM2 inhibition is feasible as a potential IPAH therapy. First and foremost, we should further explore the localization of STIM2 in PASMC from both normal subjects and IPAH patients. We should verify that when overexpressed in PASMC, STIM2 does in fact localize on the SR membrane, which would suggest that STIM2 is functionally overexpressed. We should also verify that knockdown of STIM2 in IPAH-PASMC decreases the expression of STIM2 on the SR membrane. Next it is important to determine the degree that STIM2 interacts with STIM1, Orai1, Orai2 and Orai3 in normal PASMC and in IPAH patient PASMC. Furthermore, we should examine whether STIM2 and the TRPC's interact in PASMC. After answering these questions, we will have a better understanding of the role of STIM2 in the physiology and pathophysiology of PASMC.

In this research project, I directly decreased or increased STIM2 protein expression with siRNA or cDNA, respectively. While this is a feasible technique *in vitro*, gene therapy or knockdown of STIM2 with siRNA *in vivo* is technically difficult. Specifically targeted knockdown or overexpression of STIM2 in PASMC *in vivo* is likely impossible given current technology. Instead, we should pursue pharmacological methods of inhibiting STIM2 expression in PASMC. This includes targeting cell surface receptors that lead to the downstream production of transcription factors responsible for the expression of STIM2. Transcription factors that facilitate expression of STIM2 as opposed to STIM1 are Egr-3, CUTL1, Egr-2, Egr-1, Pbx1a, c-Rel, POU2F1, HSF1 (long), IRF-1 and TFIID. More work is needed to elucidate which of these transcription factors can be targeted both specifically in PASMC and without significant toxicity.

References

1. Yuan JX, Rubin LJ. Pathophysiology of pulmonary hypertension. In: Scharf SM, Pinksy MR, Magder S, eds. Respiratory-Circulatory Interactions in Health and Disease. New York: Marcel Dekker, Inc.; 2001:447-77.

2. Ward JP, McMurtry IF. Mechanisms of hypoxic pulmonary vasoconstriction and their roles in pulmonary hypertension: new findings for an old problem. Curr Opin Pharmacol 2009;9:287-96.

3. Cornfield DN, Stevens T, McMurtry IF, Abman SH, Rodman DM. Acute hypoxia increases cytosolic calcium in fetal pulmonary artery smooth muscle cells. Am J Physiol 1993;265:L53-L6.

4. Cornfield DN, Stevens T, McMurtry IF, Abman SH, Rodman DM. Acute hypoxia causes membrane depolarization and calcium influx in fetal pulmonary artery smooth muscle cells. Am J Physiol 1994;266:L469-L75.

5. Bergofsky EH, Holtzman S. A study of the mechanisms involved in the pulmonary arterial pressor response to hypoxia. Circ Res 1967;20:506-19.

6. Brij SO, Peacock AJ. Cellular responses to hypoxia in the pulmonary circulation. Thorax 1998;53:1075-9.

7. Adnot S, Raffestin B, Eddahibi S, Braquet P, Chabrier P-E. Loss of endothelium-dependent relaxant activity in the pulmonary circulation of rats exposed to chronic hypoxia. J Clin Invest 1991;87:155-62.

8. Abe Y, Tomita T. Cable properties of smooth muscle. J Physiol 1968;196:87-100.

9. Somlyo AV, Somlyo AP. Electromechanical and pharmacomechanical coupling in vascular smooth muscle. J Pharmacol Exp Ther 1968;159:129-45.

10. Blatter LA, Hüser J, Ríos E. Sarcoplasmic reticulum Ca^{2+} release flux underlying Ca^{2+} sparks in cardiac muscle. Proc Natl Acad Sci USA 1997;94:4176-81.

11. Noble D, Tsien RW. The kinetics and rectifier properties of the slow potassium current in cardiac Purkinje fibres. J Physiol 1968;195:185-214.

12. Somlyo AP, Somlyo AV. Vascular smooth muscle. II. Pharmacology of normal and hypotensive vessels. Pharmacol Rev 1970;22:249-53.

13. Somlyo AP. Vascular smooth muscle contraction. In: Price TR, Nelson E, eds. Cerebrovascular Diseases. New York, NY: Raven Press; 1979:273-81.

14. Goodenough DA, Paul DL. Beyond the gap: functions of unpaired connexon channels. Nat Rev Mol Cell Biol 2003;4:285-94.

15. Berridge M, Bootman M, Roderick H. Calcium signalling: dynamics, homeostasis and remodelling. Nat Rev Mol Cell Biol 2003;4:517.

16. Firth AL, Remillard CV, Yuan JX. TRP channels in hypertension. Biochim Biophys Acta 2007;1772:895-906.

17. Gerthoffer WT. Mechanisms of vascular smooth muscle cell migration. Circ Res 2007;100:607-21.

18. Rao JN, Liu SV, Zou T, et al. Rac1 promotes intestinal epithelial restitution by increasing Ca2+ influx through interaction with phospholipase C-(gamma)1 after wounding. Am J Physiol Cell Physiol 2008;295:C1499-509.

19. Roderick HL, Cook SJ. Ca2+ signalling checkpoints in cancer: remodelling Ca2+ for cancer cell proliferation and survival. Nat Rev Cancer 2008;8:361-75.

20. Landsberg JW, Yuan JX. Calcium and TRP channels in pulmonary vascular smooth muscle cell proliferation. News Physiol Sci 2004;19:44-50.

21. Gill DL, Spassova MA, Soboloff J. Signal transduction. Calcium entry signals--trickles and torrents. Science 2006;313:183-4.

22. Benham CD, Tsien RW. Calcium-permeable channels in vascular smooth muscle: voltage-activated, receptor-operated, and leak channels. Soc Gen Physiol Ser 1987.

23. Parekh AB, Penner R. Store depletion and calcium influx. Physiol Rev 1997;77:901-30.

24. Echevarria W, Leite MF, Guerra MT, Zipfel WR, Nathanson MH. Regulation of calcium signals in the nucleus by a nucleoplasmic reticulum. Nat Cell Biol 2003;5:440-6.

25. Hughes AD. Calcium channels in vascular smooth muscle cells. J Vasc Res 1995;32:353-70.

26. Sweeney M, McDaniel SS, Platoshyn O, et al. Role of capacitative Ca^{2+} entry in bronchial contraction and remodeling. J Appl Physiol 2002;92:1594-602.

27. Somlyo AP, Somlyo AV. Smooth muscle: excitation-contraction coupling, contractile regulation, and the cross-bridge cycle. Alcohol Clin Exp Res 1994;18:138-43.

28. Sheng M, McFadden G, Greenberg ME. Membrane depolarization and calcium induce c-fos transcription via phosphorylation of transcription factor CREB. Neuron 1990;4:571-82.

29. Morales S, Diez A, Puyet A, et al. Calcium controls smooth muscle TRPC gene transcription via the CaMK/calcineurin-dependent pathways. Am J Physiol Cell Physiol 2006:00096.2006.

30. Planas-Silva MD, Means AR. Expression of a constitutive form of calcium/calmodulin dependent protein kinase II leads to arrest of the cell cycle in G_2. EMBO J 1992;11:507-17.

31. Lu KP, Means AR. Regulation of the cell cycle by calcium and calmodulin. Endocr Rev 1993;14:40-58.

32. Golovina VA, Platoshyn O, Bailey CL, et al. Upregulated *TRP* and enhanced capacitative Ca^{2+} entry in human pulmonary artery myocytes during proliferation. Am J Physiol Heart Circ Physiol 2001;280:H746-H55.

33. Golovina VA, Platoshyn O, Bailey CL, et al. Upregulated *TRP* and enhanced capacitative Ca^{2+} entry in human pulmonary artery myocytes during proliferation. Am J Physiol Heart Circ Physiol 2001;280:H746-55.

34. Putney J. Muscarinic, alpha-adrenergic and peptide receptors regulate the same calcium influx sites in the parotid gland. J Physiol 1977;268:139.

35. Tessier-Lavigne M, Goodman C. The molecular biology of axon guidance. Science 1996;274:1123.

36. Berridge MJ. Calcium signalling and cell proliferation. BioEssays 1995;17:491-500.

37. Clapham DE. TRP channels as cellular sensors. Nature 2003;426:517-24.

38. Clapham DE, Montell C, Schultz G, Julius D. International Union of Pharmacology. XLIII. Compendium of voltage-gated ion channels: transient receptor potential channels. Pharmacol Rev 2003;55:591-6.

39. Montell C, Birnbaumer L, Flockerzi V. The TRP channels, a remarkably functional family. Cell 2002;108:595-8.

40. Montell C, Birnbaumer L, Flockerzi V, et al. A unified nomenclature for the superfamily of TRP cation channels. Mol Cell 2002;9:229-31.

41. Nilius B, Sage SO. TRP channels: novel gating properties and physiological functions. J Physiol 2005;567:33-4.

42. Nilius B, Talavera K, Owsianik G, Prenen J, Droogmans G, Voets T. Gating of TRP channels: a voltage connection? J Physiol 2005;567:35-44.

43. Clapham DE, Julius D, Montell C, Schultz G. International Union of Pharmacology. XLIX. Nomenclature and Structure-Function Relationships of Transient Receptor Potential Channels10.1124/pr.57.4.6. Pharmacol Rev 2005;57:427-50.

44. Song MY, Yuan JX. Introduction to TRP channels: structure, function, and regulation. Adv Exp Med Biol 2010;661:99-108.

45. Anbanandam A, Bieber Urbauer RJ, Bartlett RK, Smallwood HS, Squier TC, Urbauer JL. Mediating molecular recognition by methionine oxidation: conformational switching by oxidation of methionine in the carboxyl-terminal domain of calmodulin. Biochemistry 2005;44:9486-96.

46. Ramsey IS, Delling M, Clapham DE. An introduction to TRP channels. Annu Rev Physiol 2006;68:619-47.

47. Song MY, Makino A, Yuan JX. Role of Reactive Oxygen Species and Redox in Regulating the Function of Transient Receptor Potential Channels. Antioxid Redox Signal 2011.

48. Voets T, Prenen J, Fleig A, et al. CaT1 and the calcium release-activated calcium channel manifest distinct pore properties. J Biol Chem 2001;276:47767-70.

49. Peier A, Moqrich A, Hergarden A, Reeve A, Andersson D. A TRP channel that senses cold stimuli and menthol. Cell 2002;108:705.

50. Zhu M. Multiple roles of calmodulin and other Ca^{2+} binding proteins in the functional regulation of TRP channels. Pflugers Arch 2005;451:105.

51. Berridge MJ, Bootman MD, Roderick HL. Calcium signalling: dynamics, homeostasis and remodelling. Nat Rev Mol Cell Biol 2003;4:517-29.

52. Pedersen SF, Owsianik G, Nilius B. TRP channels: An overview. Cell Calcium 2005;38:233-52.

53. Wes PD, Chevesich J, Jeromin A, Rosenberg C, Stetten G, Montell C. TRPC1, a human homolog of a *Drosophila* store-operated channel. PNAS 1995;92:9652-6.

54. Plant T, Schaefer M. Receptor-operated cation channels formed by TRPC4 and TRPC5. Naunyn Schmiedebergs Arch Pharmacol 2005;371:266.
55. Hofmann T, Obukhov AG, Schaefer M, Harteneck C, Gudermann T, Schultz G. Direct activation of human TRPC6 and TRPC3 channels by diacylglycerol. Nature 1999;397:259-63.

56. Dietrich A, Mederos y Schnitzler M, Emmel J, Kalwa H, Hofmann T, Gudermann T. N-linked protein glycosylation is a major determinant for basal TRPC3 and TRPC6 channel activity. J Biol Chem 2003;278:47842-52.

57. Kwan H, Huang Y, Yao X. Regulation of canonical transient receptor potential isoform 3 (TRPC3) channel by protein kinase G. Proc Natl Acad Sci USA 2004;101:2625.

58. Vazquez G, Wedel BJ, Aziz O, Trebak M, Putney JW, Jr. The mammalian TRPC cation channels. Biochim Biophys Acta 2004;1742:21-36.

59. Vannier B, Peyton M, Boulay G, Brown D, Qin N. Mouse trp2, the homologue of the human trpc2 pseudogene, encodes mTrp2, a store depletion-activated capacitative Ca2+ entry channel. Proc Natl Acad Sci USA 1999;96:2060.

60. Lucas P, Ukhanov K, Leinders-Zufall T, Zufall F. A diacylglycerol-gated cation channel in vomeronasal neuron dendrites is impaired in TRPC2 mutant mice: mechanism of pheromone transduction. Neuron 2003;40:551.

61. Xu S-Z, Beech DJ. TRPC1 is a membrane-spanning subunit of store-operated Ca^{2+} channels in native vascular smooth muscle cells. Circ Res 2001;88:84-7.

62. Kunichika N, Yu Y, Remillard CV, Platoshyn O, Zhang S, Yuan JX. Overexpression of *TRPC1* enhances pulmonary vasoconstriction induced by capacitative Ca^{2+} entry. Am J Physiol Lung Cell Mol Physiol 2004;287:L962-L9.

63. Yu Y, Sweeney M, Zhang S, et al. PDGF stimulates pulmonary vascular smooth muscle cell proliferation by upregulating TRPC6 expression. Am J Physiol Cell Physiol 2003;284:C316-30.

64. Weissmann N, Sommer N, Schermuly RT, Ghofrani HA, Seeger W, Grimminger F. Oxygen sensors in hypoxic pulmonary vasoconstriction. Cardiovascular Research 2006;71:620-9.

65. Birnbaumer L. TRPC4 knockout mice The coming of age of TRP channels as gates of calcium entry responsible for cellular responses. Circ Res 2002;91:1-3.

66. Tiruppathi C, Freichel M, Vogel SM, et al. Impairment of store-operated Ca^{2+} entry in $TRPC4^{-/-}$ mice interferes with increase in lung microvascular permeability. Circ Res 2002;91:70-6.

67. Schaefer M, Plant T, Obukhov A, Hofmann T, Gudermann T, Schultz G. Receptor-mediated regulation of the nonselective cation channels TRPC4 and TRPC5. J Biol Chem 2000;275:17517.

68. Ordaz B, Tang J, Xiao R, et al. Calmodulin and calcium interplay in the modulation of TRPC5 channel activity: identification of a novel C-terminal domain for calcium/calmodulin-mediated facilitation. J Biol Chem 2005;280:30788-96.

69. Lievremont J-P, Bird G, St.J., Putney JW, Jr. Canonical transient receptor potential TRPC7 can function as both a receptor- and store-operated channel in HEK-293 cells. Am J Physiol Cell Physiol 2004;287:C1709-C16.

70. Wang J, Weigand L, Lu W, Sylvester JT, Semenza GL, Shimoda LA. Hypoxia inducible factor 1 mediates hypoxia-induced TRPC expression and elevated intracellular Ca^{2+} in pulmonary arterial smooth muscle cells. Circ Res 2006;98:1528-37.

71. Lu W, Wang J, Shimoda LA, Sylvester JT. Differences in STIM1 and TRPC expression in proximal and distal pulmonary arterial smooth muscle are associated with differences in Ca^{2+} responses to hypoxia. Am J Physiol Lung Cell Mol Physiol 2008;295:L104-13.

72. Yu Y, Fantozzi I, Remillard CV, et al. Enhanced expression of transient receptor potential channels in idiopathic pulmonary arterial hypertension. Proc Natl Acad Sci USA 2004;101:13861-6.

73. Yu Y, Platoshyn O, Yuan JX. Correlation of ion channel activity with gene expression using single-cell RT-PCR and patch clamp techniques. In: Yuan JX, ed. Ion Channels in the Pulmonary Vasculature. New York, NY: Marcel Dekker; 2004:in press.

74. Groschner K, Rosker C, Lukas M. Role of TRP channels in oxidative stress. Novartis Found Symp 2004;258:222-30; discussion 31-5, 63-6.

75. Groschner K, Hingel S, Lintschinger B, et al. Trp proteins form store-operated cation channels in human vascular endothelial cells. FEBS Lett 1998;437:101-6.

76. Poteser M, Graziani A, Rosker C, et al. TRPC3 and TRPC4 associate to form a redox-sensitive cation channel: evidence for expression of native TRPC3-TRPC4 heteromeric channels in endothelial cells. J Biol Chem 2006;281:13588-95.

77. Xu SZ, Sukumar P, Zeng F, et al. TRPC channel activation by extracellular thioredoxin. Nature 2008;451:69-72.

78. Xu Y, Liu B, Zweier JL, He G. Formation of hydrogen peroxide and reduction of peroxynitrite via dismutation of superoxide at reperfusion enhances myocardial blood flow and oxygen consumption in postischemic mouse heart. J Pharmacol Exp Ther 2008;327:402-10.

79. Takahashi S, Lin H, Geshi N, et al. Nitric oxide-cGMP-protein kinase G pathway negatively regulates vascular transient receptor potential channel TRPC6. J Physiol 2008;586:4209-23.

80. Yoshida T, Inoue R, Morii T, et al. Nitric oxide activates TRP channels by cysteine S-nitrosylation. Nat Chem Biol 2006;2:596-607.

81. Foster MW, Hess DT, Stamler JS. S-nitrosylation TRiPs a calcium switch. Nat Chem Biol 2006;2:570-1.

82. Feske S, Gwack Y, Prakriya M, et al. A mutation in Orai1 causes immune deficiency by abrogating CRAC channel function. Nature 2006;441:179-85.

83. Mercer JC, Dehaven WI, Smyth JT, et al. Large store-operated calcium selective currents due to co-expression of Orai1 or Orai2 with the intracellular calcium sensor, Stim1. J Biol Chem 2006;281:24979-90.

84. Soboloff J, Spassova MA, Dziadek MA, Gill DL. Calcium signals mediated by STIM and Orai proteins--a new paradigm in inter-organelle communication. Biochim Biophys Acta 2006;1763:1161-8.

85. Soboloff J, Spassova MA, Hewavitharana T, et al. STIM2 is an inhibitor of STIM1-mediated store-operated Ca^{2+} entry. Curr Biol 2006;16:1465-70.

86. Soboloff J, Spassova MA, Tang XD, Hewavitharana T, Xu W, Gill DL. Orai1 and STIM reconstitute store-operated calcium channel function. J Biol Chem 2006;281:20661-5.

87. Yeromin AV, Zhang SL, Jiang W, Yu Y, Safrina O, Cahalan MD. Molecular identification of the CRAC channel by altered ion selectivity in a mutant of Orai. Nature 2006;443:226-9.

88. De Waard M, Gurnett CA, Campbell KP. Structural and functional diversity of voltage-activated calcium channels. Ion Channels 1996;4:41-87.

89. Miller RJ. Voltage-sensitive Ca^{2+} channels. J Biol Chem 1992;267:1403-6.

90. Moreno Davila H. Molecular and functional diversity of voltage-gated calcium channels. Ann NY Acad Sci 1999;868:102-17.

91. Brueggemann LI, Markun DR, Henderson KK, Cribbs LL, Byron KL. Pharmacological and electrophysiological characterization of store-operated currents and capacitative Ca^{2+} entry in vascular smooth muscle cells. J Pharmacol Exp Ther 2006;317:488-99.

92. Tombler E, Cabanilla NJ, Carman P, et al. G Protein-induced trafficking of voltage-dependent calcium channels. J Biol Chem 2006;281:1827-39.

93. Wijetunge S, Lymn JS, Hughes AD. Effects of protein tyrosine kinase inhibitors on voltage-operated calcium channel currents in vascular smooth muscle cells and pp60(c-src) kinase activity. Br J Pharmacol 2000;129:1347-54.

94. Yuan JX. Oxygen-sensitive K^+ channel(s): where and what? Am J Physiol Lung Cell Mol Physiol 2001;281:L1345-L9.

95. Yuan JX, Aldinger AM, Juhaszova M, et al. Dysfunctional voltage-gated K^+ channels in pulmonary artery smooth muscle cells of patients with primary pulmonary hypertension. Circulation 1998;98:1400-6.

96. Burg ED, Remillard CV, Yuan JX. K^+ channels in apoptosis. J Membr Biol 2006;209:3-20.

97. Wible BA, Wang L, Kuryshev YA, Basu A, Haldar S, Brown AM. Increased K^+ efflux and apoptosis induced by the potassium channel modulatory protein KChAP/PIAS3β in prostate cancer cells. J Biol Chem 2003;277:17852-62.

98. Yuan XJ. Voltage-gated K^+ currents regulate resting membrane potential and $[Ca^{2+}]_i$ in pulmonary arterial myocytes. Circ Res 1995;77:370-8.

99. Yuan XJ, Tod ML, Rubin LJ, Blaustein MP. NO hyperpolarizes pulmonary artery smooth muscle cells and decreases the intracellular Ca^{2+} concentration by activating voltage-gated K^+ channels. Proc Natl Acad Sci USA 1996;93:10489-94.

100. Platoshyn O, Golovina VA, Bailey CL, et al. Sustained membrane depolarization and pulmonary artery smooth muscle cell proliferation. Am J Physiol Cell Physiol 2000;279:C1540-9.

101. Platoshyn O, Yu Y, Golovina VA, et al. Chronic hypoxia decreases K_V channel expression and function in pulmonary artery myocytes. Am J Physiol Lung Cell Mol Physiol 2001;280:L801-L12.

102. Archer SL, London B, Hampl V, et al. Impairment of hypoxic pulmonary vasoconstriction in mice lacking the voltage-gated potassium channel Kv1.5. FASEB J 2001;15:1801-3.

103. Nelson MT, Cheng H, Rubart M, et al. Relaxation of arterial smooth muscle by calcium sparks. Science 1995;270:633-7.
104. Nelson MT, Patlak JB, Worley JF, Standen NB. Calcium channels, potassium channels, and voltage dependence of arterial smooth muscle tone. Am J Physiol 1990;259:C3-C18.

105. Nelson MT, Huang Y, Brayden JE, Hescheler J, Standen NB. Arterial dilations in response to calcitonin gene-related peptide involve activation of K^+ channels. Nature 1990;344:770-3.

106. Yuan XJ, Tod ML, Rubin LJ, Blaustein MP. Hypoxic and metabolic regulation of voltage-gated K^+ channels in rat pulmonary artery smooth muscle cells. Exp Physiol 1995;80:803-13.

107. Fleischmann BK, Murray RK, Kotlikoff MI. Voltage window for sustained elevation of cytosolic calcium in smooth muscle cells. Proc Natl Acad Sci USA 1994;91:11914-8.

108. Gutman GA, Chandy KG, Grissmer S, et al. International Union of Pharmacology. LIII. Nomenclature and molecular relationships of voltage-gated potassium channels. Pharmacol Rev 2005;57:473-508.

109. Coetzee WA, Amarillo Y, Chiu J, et al. Molecular diversity of K^+ channels. Ann NY Acad Sci 1999;868:233-85.

110. Rudy B. Diversity and ubiquity of K channels. Neuroscience 1988;25:729-49.

111. Archer SL, Souil E, Dinh-Xuan AT, et al. Molecular identification of the role of voltage-gated K^+ channels, Kv1.5 and Kv1.2, in hypoxic pulmonary vasoconstriction and control of resting membrane potential in rat pulmonary artery myocytes. J Clin Invest 1998;101:2319-30.

112. Roos J, DiGregorio PJ, Yeromin AV, et al. STIM1, an essential and conserved component of store-operated Ca^{2+} channel function. J Cell Biol 2005;169:435-45.

113. Zhang SL, Yeromin AV, Zhang XH, et al. Genome-wide RNAi screen of Ca^{2+} influx identifies genes that regulate Ca^{2+} release-activated Ca^{2+} channel activity. Proc Natl Acad Sci U S A 2006;103:9357-62.

114. Abdullaev IF, Bisaillon JM, Potier M, Gonzalez JC, Motiani RK, Trebak M. Stim1 and Orai1 mediate CRAC currents and store-operated calcium entry important for endothelial cell Proliferation. Circ Res 2008;23:1289-99.

115. Muik M, Frischauf I, Derler I, et al. Dynamic coupling of the putative coiled-coil domain of ORAI1 with STIM1 mediates ORAI1 channel activation. J Biol Chem 2008;283:8014-22.
116. Manji SSM, Parker NJ, Williams RT, et al. STIM1: a novel phosphoprotein located at the cell surface. Biochim Biophys Acta 2000;1481:147-55.

117. Roos J, DiGregorio PJ, Yeromin AV, et al. STIM1, an essential and conserved component of store-operated Ca^{2+} channel function. J Cell Biol 2005;169:435-45.

118. Luik RM, Wang B, Prakriya M, Wu MM, Lewis RS. Oligomerization of STIM1 couples ER calcium depletion to CRAC channel activation. Nature 2008;454:538-42.

119. Yeromin AV, Zhang SL, Jiang W, Yu Y, Safrina O, Cahalan MD. Molecular identification of the CRAC channel by altered ion selectivity in a mutant of Orai. Nature 2006;443:226-9.

120. Rubin LJ. Pulmonary arterial hypertension. Proc Am Thorac Soc 2006;3:111-5.

121. Rubin LJ, Rich S. Primary Pulmonary Hypertension. New York, NY: Marcel Dekker Inc.; 1997.

122. Rubin LJ. Primary pulmonary hypertension. N Engl J Med 1997;336:111-7.

123. Simonneau G, Galiè N, Rubin LJ, et al. Clinical classification of pulmonary hypertension. J Am Coll Cardiol 2004;43:S5-S12.

124. Simonneau G, Robbins IM, Beghetti M, et al. Updated clinical classification of pulmonary hypertension. J Am Coll Cardiol 2009;54:S43-54.

125. Badesch DB, Champion HC, Sanchez MA, et al. Diagnosis and assessment of pulmonary arterial hypertension. J Am Coll Cardiol 2009;54:S55-66.

126. Rosenkranz S. Pulmonary hypertension: current diagnosis and treatment. Clin Res Cardiol 2007;96:527-41.

127. Mandegar M, Fung Y-CB, Huang W, Remillard CV, Rubin LJ, Yuan JX. Cellular and molecular mechanisms of pulmonary vascular remodeling: role in the development of pulmonary hypertension. Microvasc Res 2004;68:75-103.

128. Lane KB, Machado RD, Pauciulo MW, et al. Heterozygous germline mutations in *BMPR2*, encoding a TGF-β receptor, cause familial primary pulmonary hypertension. Nat Genet 2000;26:81-4.

129. Beppu H, Ichinose F, Kawai N, et al. *BMPR-II* heterozygous mice have mild pulmonary hypertension and an impaired pulmonary vascular remodeling response to prolonged hypoxia. Am J Physiol Lung Cell Mol Physiol 2004;287:L1241-L7.

130. Long L, Crosby A, Yang X, et al. Altered bone morphogenetic protein and transforming growth factor-beta signaling in rat models of pulmonary hypertension: potential for activin receptor-like kinase-5 inhibition in prevention and progression of disease. Circulation 2009;119:566-76.

131. Fantozzi I, Platoshyn O, Wong AH, et al. Bone morphogenetic protein-2 upregulates expression and function of voltage-gated K^+ channels in human pulmonary artery smooth muscle cells. Am J Physiol Lung Cell Mol Physiol 2006;291:L993-L1004.

132. Deng Z, Morse JH, Slager SL, et al. Familial primary pulmonary hypertension (gene *PPH1*) is caused by mutations in the bone morphogenetic protein receptor II-gene. Am J Cardiol 2000;67:737-44.

133. Itoh S, Itoh F, Goumans M-J, ten Dijke P. Signaling of transforming growth factor-β family members through Smad proteins. Eur J Biochem 2000;267:6954-67.

134. Nohe A, Keating E, Knaus P, Petersen NO. Signal transduction of bone morphogenetic protein receptors. Cell Signal 2004;16:291-9.

135. Zhang S, Fantozzi I, Tigno DD, et al. Bone morphogenetic proteins induce apoptosis in human pulmonary vascular smooth muscle cells. Am J Physiol Lung Cell Mol Physiol 2003;285:L740-54.

136. Lagna G, Nguyen PH, Ni W, Hata A. BMP-dependent activation of caspase-9 and caspase-8 mediates apoptosis in pulmonary artery smooth muscle cells. Am J Physiol Lung Cell Mol Physiol 2006;291:L1059-67.

137. Nishihara A, Watabe T, Imamura T, Miyazono K. Functional heterogeneity of bone morphogenetic protein receptor-II mutants found in patients with primary pulmonary hypertension. Mol Cell Biol 2002;13:3055-63.

138. Machado RD, Rudarakanchana N, Atkinson C, et al. Functional interaction between BMPR-II and Tctex-1, a light chain of dynein, is isoform-specific and disrupted by mutations underlying primary pulmonary hypertension. Hum Mol Genet 2003;12:3277-86.

139. Machado RD, Pauciulo MW, Thomson JR, et al. *BMPR2* haploinsufficiency as the inherited mechanism for primary pulmonary hypertension. Am J Hum Gen 2001;68:92-102.

140. Young KA, Ivester C, West J, Carr M, Rodman DM. BMP signaling controls PASMC K_V channel expression *in vitro* and *in vivo*. Am J Physiol Lung Cell Mol Physiol 2006;290:L841-L8.
141. Zhang S, Fantozzi I, Tigno DD, et al. Bone morphogenetic proteins induce apoptosis in human pulmonary vascular smooth muscle cells. Am J Physiol Lung Cell Mol Physiol 2003;285:L740-L54.

142. Morrell NW, Yang X, Upton PD, et al. Altered growth responses of pulmonary artery smooth muscle cells from patients with primary pulmonary hypertension to transforming growth factor-β_1 and bone morphogenetic proteins. Circulation 2001;104:790-5.

143. Eddahibi S, Humbert M, Fadel E, et al. Serotonin transporter overexpression is responsible for pulmonary artery smooth muscle hyperplasia in primary pulmonary hypertension. J Clin Invest 2001;108:1141-50.

144. Blanpain C, Le Poul E, Parma J, et al. Serotonin 5-HT_{2B} receptor loss of function mutation in a patient with fenfluramine-associated primary pulmonary hypertension. Cardiovasc Res 2003;60:518-28.

145. MacLean MR. Pulmonary hypertension and the serotonin hypothesis: where are we now? Int J Clin Pract Suppl 2007:27-31.

146. MacLean MR, Herve P, Eddahibi S, Adnot S. 5-Hydroxytryptamine and the pulmonary circulation: receptors, transporters and relevance to pulmonary arterial hypertension. Br J Pharmacol 2000;131:161-8.

147. Morecroft I, Dempsie Y, Bader M, et al. Effect of tryptophan hydroxylase 1 deficiency on the development of hypoxia-induced pulmonary hypertension. Hypertension 2007;49:232-6.

148. Cogolludo A, Frazziano G, Cobeno L, et al. Role of reactive oxygen species in Kv channel inhibition and vasoconstriction induced by TP receptor activation in rat pulmonary arteries. Ann N Y Acad Sci 2006;1091:41-51.

149. Firth AL, Mandel J, Yuan JX. Idiopathic pulmonary arterial hypertension. Dis Model Mech 2010;3:268-73.

150. Stenmark KR, McMurtry IF. Vascular remodeling versus vasoconstriction in chronic hypoxic pulmonary hypertension: a time for reappraisal? Circ Res 2005;97:95-8.

151. Tuder RM, Marecki JC, Richter A, Fijalkowska I, Flores S. Pathology of pulmonary hypertension. Clin Chest Med 2007;28:23-42, vii.

152. Johnson SR, Granton JT, Mehta S. Thrombotic arteriopathy and anticoagulation in pulmonary hypertension. Chest 2006;130:545-52.
153. Firth AL, Yau J, White A, et al. Chronic exposure to fibrin and fibrinogen differentially regulates intracellular Ca2+ in human pulmonary arterial smooth muscle and endothelial cells. Am J Physiol Lung Cell Mol Physiol 2009;296:L979-86.

154. Yuan XJ, Zhao L, Deng X-X, Cai Y-N. Changes of pulmonary artery pressure induced by infusion of diamide in rat breathing low oxygen gas mixture. Chinese Journal of Physiological Sciences 1990;6:286-9.

155. Runo JR, Loyd JE. Primary pulmonary hypertension. Lancet 2003;361:1533-44.

156. Ooi CY, Wang Z, Tabima DM, Eickhoff JC, Chesler NC. The role of collagen in extralobar pulmonary artery stiffening in response to hypoxia-induced pulmonary hypertension. Am J Physiol Heart Circ Physiol;299:H1823-31.

157. Mandegar M, Thistlethwaite PA, Yuan JX. Molecular biology of primary pulmonary hypertension. Cardiol Clin 2004;22:417-29.

158. Runo JR, Loyd JE. Primary pulmonary hypertension. Lancet 2003;361:1533-44.

159. Jamieson SW, Kapelanski DP, Sakakibara N, et al. Pulmonary endarterectomy: experience and lessons learned in 1500 cases. Ann Thorac Surg 2003;76:1457-62.

160. Chin KM, Rubin LJ. Pulmonary arterial hypertension. J Am Coll Cardiol 2008;51:1527-38.

161. Giaid A, Yanagisawa M, Langleben D, et al. Expression of endothelin-1 in the lungs of patients with pulmonary hypertension. N Engl J Med 1993;328:1732-9.

162. Ghofrani HA, Rose F, Schermuly RT, et al. Oral sildenafil as long-term adjunct therapy to inhaled iloprost in severe pulmonary arterial hypertension. J Am Coll Cardiol 2003;42:158-64.

163. Yuan JX. Hypoxic Pulmonary Vasoconstriction: Cellular and Molecular Mechanisms. Boston, MA: Kluwer Academic Publishers; 2004.

164. Yuan JX. Ion Channels in the Pulmonary Vasculature. New York, NY: Taylor & Francis; 2005.

165. Zhang S, Patel HH, Murray F, et al. Pulmonary artery smooth muscle cells from normal subjects and IPAH patients show divergent cAMP-mediated effects on TRPC expression and capacitative Ca^{2+} entry. Am J Physiol Lung Cell Mol Physiol 2007;292:L1202-L10.

166. Brevnova EE, Platoshyn O, Zhang S, Yuan JX. Overexpression of human *KCNA5* increases $I_{K(V)}$ and enhances apoptosis. Am J Physiol Cell Physiol 2004;287:C715-C22.
167. Yu Y, Keller SH, Remillard CV, et al. A functional single-nucleotide polymorphism in the TRPC6 gene promoter associated with idiopathic pulmonary arterial hypertension. Circulation 2009;119:2313-22.

168. Landsberg JW, Yuan JX-J. Calcium and TRP channels in pulmonary vascular smooth muscle cell proliferation. News Physiol Sci 2004;19:47-52.

169. Morrell NW, Adnot S, Archer SL, et al. Cellular and molecular basis of pulmonary arterial hypertension. J Am Coll Cardiol 2009;54:S20-31.

170. Hassoun PM, Mouthon L, Barbera JA, et al. Inflammation, growth factors, and pulmonary vascular remodeling. J Am Coll Cardiol 2009;54:S10-9.

171. Lu W, Wang J, Peng G, Shimoda LA, Sylvester JT. Knockdown of stromal interaction molecule 1 attenuates store-operated Ca^{2+} entry and Ca^{2+} responses to acute hypoxia in pulmonary arterial smooth muscle. Am J Physiol Lung Cell Mol Physiol 2009;297:L17-25.

172. Cahalan MD. STIMulating store-operated Ca^{2+} entry. Nat Cell Biol 2009;11:669-77.

173. Zhang SL, Yu Y, Roos J, et al. STIM1 is a Ca^{2+} sensor that activates CRAC channels and migrates from the Ca^{2+} store to the plasma membrane. Nature 2005;437:902-5.

174. Ross PE, Cahalan MD. Ca^{2+} influx pathways mediated by swelling or stores depletion in mouse thymocytes. J Gen Physiol 1995;106:415-44.

175. Darbellay B, Arnaudeau S, Konig S, et al. STIM1- and Orai1-dependent store-operated calcium entry regulates human myoblast differentiation. J Biol Chem 2009;284:5370-80.

176. El Boustany C, Katsogiannou M, Delcourt P, et al. Differential roles of STIM1, STIM2 and Orai1 in the control of cell proliferation and SOCE amplitude in HEK293 cells. Cell Calcium 2010;47:350-9.

177. Cahalan MD, Zhang SL, Yeromin AV, Ohlsen K, Roos J, Stauderman KA. Molecular basis of the CRAC channel. Cell Calcium 2007;42:133-44.

178. Burg ED, Remillard CV, Yuan JX-J. K^+ channels in apoptosis. J Membr Biol 2006;209:3-20.

179. Yuan JX, Rubin LJ. Pathogenesis of pulmonary arterial hypertension: The need for multiple hits. Circulation 2005;111:534-8.
180. Sweeney M, Yuan JX. Hypoxic pulmonary vasoconstriction: role of voltage-gated potassium channels. Respir Res 2000;1:40-8.

181. Peng J-B, Brown EM, Hediger MA. Epithelial Ca^{2+} entry channels: transcellular Ca^{2+} transport and beyond. J Physiol 2003;551:729-40.

182. Shimoda LA, Wang J, Sylvester J. Ca^{2+} channels and chronic hypoxia. Microcirculation 2006;13:657-70.

183. Lin MJ, Leung GP, Zhang WM, et al. Chronic hypoxia-induced upregulation of store-operated and receptor-operated Ca^{2+} channels in pulmonary arterial smooth muscle cells: a novel mechanism of hypoxic pulmonary hypertension. Circ Res 2004;95:496-505.

184. Krick S, Platoshyn O, Sweeney M, et al. Nitric oxide induces apoptosis by activating K^+ channels in pulmonary vascular smooth muscle cells. Am J Physiol Heart Circ Physiol 2002;282:H184-H93.

185. Darbellay B, Arnaudeau S, Ceroni D, Bader CR, Konig S, Bernheim L. Human muscle economy myoblast differentiation and excitation-contraction coupling use the same molecular partners, STIM1 and STIM2. J Biol Chem 2010;285:22437-47.

186. Stathopulos PB, Zheng L, Ikura M. Stromal interaction molecule (STIM) 1 and STIM2 calcium sensing regions exhibit distinct unfolding and oligomerization kinetics. J Biol Chem 2009;284:728-32.

187. Vig M, Beck A, Billingsley JM, et al. CRACM1 multimers form the ion-selective pore of the CRAC channel. Curr Biol 2006;In Press.

188. Berna-Erro A, Braun A, Kraft R, et al. STIM2 regulates capacitive Ca2+ entry in neurons and plays a key role in hypoxic neuronal cell death. Sci Signal 2009;2:ra67.

189. Gilio K, van Kruchten R, Braun A, et al. Roles of platelet STIM1 and Orai1 in glycoprotein VI- and thrombin-dependent procoagulant activity and thrombus formation. J Biol Chem 2010;285:23629-38.

190. Brandman O, Liou J, Park WS, Meyer T. STIM2 is a feedback regulator that stabilizes basal cytosolic and endoplasmic reticulum Ca^{2+} levels. Cell 2007;131:1327-39.

191. Zhang SL, Yu Y, Roos J, et al. STIM1 is a Ca^{2+} sensor that activates CRAC channels and migrates from the Ca^{2+} store to the plasma membrane. Nature 2005;437:902-5.

192. Allbritton NL, Oancea E, Kuhn MA, Meyer T. Source of nuclear calcium signals. Proc Natl Acad Sci USA 1994;91:12458-62.
193. Wu G, Xie X, Lu ZH, Ledeen RW. Sodium-calcium exchanger complexed with GM1 ganglioside in nuclear membrane transfers calcium from nucleoplasm to endoplasmic reticulum. Proc Natl Acad Sci U S A 2009;106:10829-34.

194. Faury G, Usson Y, Robert-Nicoud M, Robert L, Verdetti J. Nuclear and cytoplasmic free calcium level changes induced by elastin peptides in human endothelial cells. Proc Natl Acad Sci U S A 1998;95:2967-72.

195. Baran I. Calcium and cell cycle progression: possible effects of external perturbations on cell proliferation. Biophys J 1996;70:1198-213.

196. McDaniel SS, Platoshyn O, Wang J, et al. Capacitative Ca^{2+} entry in agonist-induced pulmonary vasoconstriction. Am J Physiol Lung Cell Mol Physiol 2001;280:L870-L80.

197. Waldron RT, Short AD, Gill DL. Thapsigargin-resistant intracellular calcium pumps. J Biol Chem 1995;270:11955-61.

198. Ufret-Vincenty CA, Short AD, Alfonso A, Gill DL. A novel Ca^{2+} entry mechanism is turned on during growth arrest induced by Ca^{2+} pool depletion. J Biol Chem 1995;270:26790-3.

199. Waldron RT, Short AD, Gill DL. Thapsigargin-resistant intracellular calcium pumps. Role in calcium pool function and growth of thapsigargin-resistant cells. J Biol Chem 1995;270:11955-61.

200. Wei Z, Manevich Y, Al-Mehdi AB, Chatterjee S, Fisher AB. Ca^{2+} flux through voltage-gated channels with flow cessation in pulmonary microvascular endothelial cells. Microcirculation 2004;11:517-26.

201. Wei C, Wang X, Chen M, Ouyang K, Song LS, Cheng H. Calcium flickers steer cell migration. Nature 2009;457:901-5.

202. Pfleiderer PJ, Lu KK, Crow MT, Keller RS, Singer HA. Modulation of vascular smooth muscle cell migration by calcium/ calmodulin-dependent protein kinase II-delta 2. Am J Physiol Cell Physiol 2004;286:C1238-45.

203. Lundberg MS, Curto KA, Bilato C, Monticone RE, Crow MT. Regulation of vascular smooth muscle migration by mitogen-activated protein kinase and calcium/calmodulin-dependent protein kinase II signaling pathways. J Mol Cell Cardiol 1998;30:2377-89.

204. Bilato C, Curto KA, Monticone RE, Pauly RR, White AJ, Crow MT. The inhibition of vascular smooth muscle cell migration by peptide and antibody antagonists of the alphavbeta3 integrin complex is reversed by activated calcium/calmodulin-dependent protein kinase II. J Clin Invest 1997;100:693-704.

205. Pauly RR, Bilato C, Sollott SJ, et al. Role of calcium/calmodulin-dependent protein kinase II in the regulation of vascular smooth muscle cell migration. Circulation 1995;91:1107-15.

206. Zhang S, Patel HH, Murray F, et al. Pulmonary artery smooth muscle cells from normal subjects and IPAH patients show divergent cAMP-mediated effects on TRPC expression and capacitative Ca^{2+} entry. Am J Physiol Lung Cell Mol Physiol 2007;292:L1202-10.

207. Burg ED, Remillard CV, Yuan JX. Potassium channels in the regulation of pulmonary artery smooth muscle cell proliferation and apoptosis: pharmacotherapeutic implications. Br J Pharmacol 2008;153 Suppl 1:S99-S111.

208. Potier M, Gonzalez JC, Motiani RK, et al. Evidence for STIM1- and Orai1-dependent store-operated calcium influx through I_{CRAC} in vascular smooth muscle cells: role in proliferation and migration. Faseb J 2009;23:2425-37.

209. Wirth A. Rho kinase and hypertension. Biochim Biophys Acta 2010;1802:1276-84.

210. Wang Y, Liang D, Wang S, et al. Role of the G-protein and tyrosine kinase--Rho/ROK pathways in 15-hydroxyeicosatetraenoic acid induced pulmonary vasoconstriction in hypoxic rats. J Biochem 2010;147:751-64.

211. Du L, Sullivan CC, Chu D, et al. Signaling molecules in nonfamilial pulmonary hypertension. N Engl J Med 2003;348:500-9.

212. Kunichika N, Landsberg JW, Yu Y, et al. Bosentan inhibits transient receptor potential channel expression in pulmonary vascular myocytes. Am J Respir Crit Care Med 2004;170:1101-7.